PNWD-3496
WTP-RPT-110 Rev. 0

# Test Results for Pulse Jet Mixers in Prototypic Ultrafiltration Feed Process and High-Level Waste Lag Storage Vessels

J. M. Bates
J.W. Brothers
J.M. Alzheimer
D.E. Wallace
P.A. Meyer

August 2004

Prepared for Bechtel National, Inc.
under Contract 24590-101-TSA-W000-0004

## LEGAL NOTICE

# Test Results for Pulse Jet Mixers in Prototypic Ultrafiltration Feed Process and High-Level Waste Lag Storage Vessels

J. M. Bates
J.W. Brothers
J.M. Alzheimer
D.E. Wallace
P.A. Meyer

August 2004

8/17/04
for W. Tamosaitis
ACCEPTED FOR PROJECT USE

Prepared for Bechtel National, Inc.
under Contract 24590-101-TSA-W000-0004

Test specification: 24590-WTP-TSP-RT-03-008 Rev 0
Test plan: TP-RPP-WTP-296
Test exceptions: 24590-WTP-TEF-RT-03-060, -081
R&T focus area: Pretreatment
Test Scoping Statement(s): B-100

Battelle - Pacific Northwest Division
Richland, Washington 99352

# Completeness of Testing

*This report describes the results of work and testing specified by TP-RPP-WTP-296. The work and any associated testing followed the quality assurance requirements outlined in the Test Specification/Plan. The descriptions provided in this test report are an accurate account of both the conduct of the work and the data collected. Test plan results are reported. Also reported are any unusual or anomalous occurrences that are different from expected results. The test results and this report have been reviewed and verified.*

Approved:

Gordon H. Beeman, Manager
WTP R&T Support Project

8/12/04
Date

# Summary

Battelle – Pacific Northwest Division (PNWD) was contracted to provide Bechtel National Inc. (BNI) with results of simulant tests using the scaled prototypic ultrafiltration process (UFP) and lag storage (LS) vessels and associated pulse jet mixer (PJM) equipment for the Waste Treatment Plant (WTP) Project. The UFP vessel, the LS vessel, and the concentrate receipt vessel (CRV) are to be used in the WTP for mixing radioactive waste from the underground Hanford storage tanks (note: the CRV tank was deleted from the baseline design of the WTP after the Phase I testing was completed). BNI, through its subcontract with PNWD, is testing a PJM-fitted mixing vessel at multiple scales to experimentally verify dimensional scaling effects in PJM systems. The scaling methodologies of the mixing system for a generic 4-PJM vessel will be validated by tests conducted at three scales: large-scale (nearly full-scale at the 336 Building), ~1/4 scale (at the Applied Process Engineering Laboratory) (APEL) in Richland, and small scale [~1/8 tests at Savannah River Technology Center (SRTC)]. The LS and UFP scaled prototypes are located in the high-bay area of the APEL facility. The CRV scaled prototype was tested at SRTC. This report documents the prototype scaled testing at the APEL.

## Objectives

The overall objective of this work is to provide mixing performance information on the operating parameters critical for the uniform movement (total mobilization) of the tank contents. The specific objective of the testing is to provide data on the mobilization of non-Newtonian simulants for the assessment of PJM mixing configurations for the UFP and LS vessels. PJM configurations include 1) baseline designs as provided by BNI and 2) enhanced configurations and/or operational parameters that are demonstrated to provide acceptable mobilization/mixing performance. The non-Newtonian simulant is to possess target rheological characteristics that are similar to those predicted for WTP waste streams.

The final results of this test effort will eventually be used to generate the engineering and bounding parametric correlations that will help ensure that the WTP Project has functional fluidic mixing systems for the UFP and LS non-Newtonian vessels. The objectives in the applicable test specifications were met.

| Test Objective | Objective Met (Y/N) | Discussion |
|---|---|---|
| 1. Provide design information on operating parameters | Y | Multiple PJM operational and geometric parameters exercised |
| 2. Conduct tests in 1/4 scale vessel | Y | UFP vessel was scale factor of 1/4.94, LS was 1/4.29 |

## Test Exceptions

| List Test Exceptions | Describe Test Exceptions |
|---|---|
| 1. 24590-WTP-TEF-RT-03-060 | Revised test matrix |
| 2. 24590-WTP-TEF-RT-03-081 | Revised test matrix for final 'best' mixing configurations |

## Results and Performance Against Success Criteria

| List Success Criteria | How the Tests Did or Did Not Meet the Success Criteria |
|---|---|
| Demonstrate a combination of PJM operating conditions and physical arrangements that provide full mobilization of the UFP and LS vessels. | PJM geometrical and operational conditions were identified that provided complete tank mobilization (types III and IV mobilization states). |

Each test was conducted by first configuring the PJMs in the desired geometric array and then placing them within the acrylic test tank with the nozzle at a specified offset from the dish-shaped tank bottom. The geometric array included adjustments to the desired circular radius and offset relative to one another. Tests were conducted to determine the effectiveness of various configurations and operating parameters. The more promising test results are summarized in Tables 4.2 for the LS and 4.4 for the UFP. The full complement of tests (both LS and UFP) are also presented in the report. Early tests indicated the need to classify mixing effectiveness in terms that had not previously been used. The WTP PJM Steering Committee designated the classification scheme shown in Figure S.1.

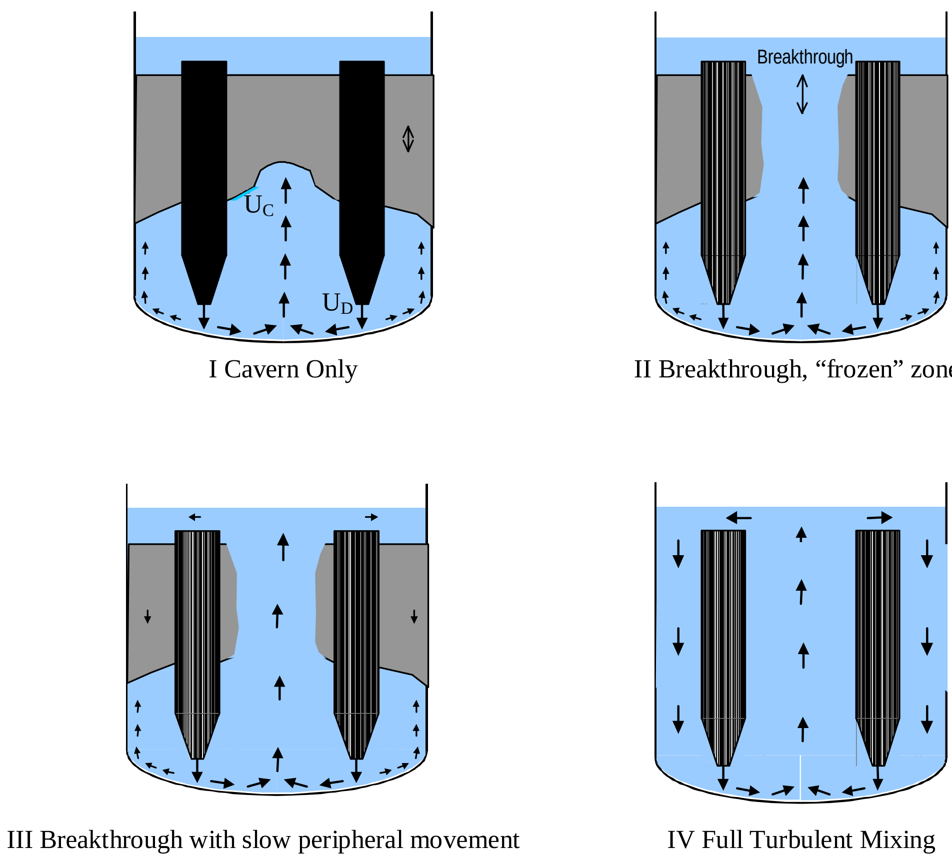


**Figure S.1**. Definition of PJM Mobilization States

## Quality Requirements

PNWD implemented the RPP-WTP quality assurance requirements by performing work in accordance with the quality assurance project plan (QAPjP) approved by the RPP-WTP Quality Assurance (QA) organization. This QAPjP conforms to the quality requirements of NQA-1-1989 and NQA-2a-1990, Part 2.7, as instituted through PNWD's Waste Treatment Plant Support Project (WTPSP) Quality Assurance Requirements and Description Manual.

PNWD addressed verification activities by conducting an independent technical review of this final data report in accordance with procedure QA-RPP-WTP-604. This review verified that the reported results were traceable and that inferences and conclusions were soundly based. This review procedure is part of PNWD's *WTPSP Quality Assurance Requirements and Description Manual.*

## R&T Test Conditions

This report summarizes the test configurations and individual test parameters and results. As-built dimensions of test configurations are reported at a level consistent with the usefulness of the results. That is, tests that were essentially screening or scoping tests do not have an equivalent level of rigor to the as-built configurations as those that were deemed most important or successful by the WTP Steering Committee.[a] All testing reported was performed at approximately one quarter scale. Proof of scaling relationships and correlations is presented under separate cover. Test equipment and materials provided prior to the start of testing included:

- scaled acrylic tanks
- spun steel, scaled dished bottom
- data acquisition and control system including computer and input/output hardware and software
- level measurement devices for the interior of each PJM
- control manifold for compressed air, vacuum, and vent including pressure measurement for the manifold
- steel PJMs for candidate testing
- Laponite® simulant prepared to 100 Pa shear strength
- Kaolin-bentonite clay mixture prepared with 80% kaolin and 20% bentonite clay with ~100 Pa yield strength.

| R&T Test Conditions | Were Test Conditions Followed? |
|---|---|
| Prepare test plan to implement the test specification | Test plan prepared and approved by WTP R&T |
| Test units to be provided by BNI | UFP and LS test vessels and initial PJM units supplied by BNI |
| Test conditions specified in test matrix supplied in the test specification | Test matrix supplied (and superceded by subsequent updates via test exceptions) |

(a) WTP-RPT-113, "Technical Basis for Scaling of Pulse Jet Mixer Performance with Non-Newtonian Slurries."

## Simulant Use

The rheological characteristics of the simulants are compared with actual waste rheology in Poloski et al. (2004). Mixing tests with actual waste are neither planned nor within the scope of the current efforts due to the difficulty of obtaining and working with actual waste samples. Should new or extended insight into actual waste properties become available, careful comparison with the properties of the simulants used in the current tests is recommended, and the potential impacts on PJM performance should be investigated.

Two simulants were used in the course of the Phase I testing. Initial testing used optically transparent Laponite, a thixotropic colloidal synthetic clay, and later tests used a kaolin/bentonite clay mixture exhibiting a Bingham plastic rheology that closely represented the rheology of actual waste slurries.

## Discrepancies and Follow-on Tests

There were no design or operations issues associated with the testing and/or the results presented in this report. However, care must be exercised in using the data presented in this report in drawing broad conclusions regarding the PJM performance in vessels with significantly larger dimensions than the test vessels. Scaling issues are addressed specifically in a separate report.[a] The reader is encouraged to thoroughly understand the contents of the scaling technical basis report prior to application or extrapolation of the results presented here. Casual extrapolation of these results to actual waste behavior is also not recommended. Should actual waste properties be found to differ significantly from those used to develop the simulant materials employed in the current testing, additional PJM performance testing is strongly suggested.

## Reference

Poloski AP, PA Meyer, LK Jagoda, and PR Hrma. August 2004. *Non-Newtonian Slurry Simulant Development and Selection for Pulse Jet Mixer Testing.* WTP-RPT-111, Battelle – Pacific Northwest Division, Richland, WA.

(a) WTP-RPT-113, “Technical Basis for Scaling of Pulse Jet Mixer Performance with Non-Newtonian Slurries.”

# Acronyms and Abbreviations

| | |
|---|---|
| APEL | Applied Process Engineering Laboratory |
| BNI | Bechtel National Inc. |
| CFD | computational fluid dynamics |
| CRV | concentrate receipt vessel |
| DACS | data acquisition and control software |
| DOE | U.S. Department of Energy |
| FUA | Facility Use Agreement |
| GR&R | gas retention and release |
| H | tank fill height |
| H/D | height to diameter ratio |
| HLW | high-level waste |
| $H_c$ | cavern height |
| $H_c(t)$ | cavern height as a function of time |
| Hz | frequency (1/sec) |
| ICH | inner core height |
| ID | inside diameter |
| L | length of PJMs |
| LS | lag storage |
| OCH | outer core height |
| OD | outer diameter |
| PCD | pitch circle diameter |
| PSD | particle size distribution |
| PIT | passive integrated transponder |
| PJM | pulse jet mixer |
| PNWD | Battelle – Pacific Northwest Division |
| PVC | polyvinyl chloride |
| QAPjP | quality assurance project plan |
| QA | quality assurance |
| R&T | Research and Technology (group) |
| RF | radio frequency (tags) |
| RFD | reverse flow diverter |
| RH | ram's head (extensions to PJM nozzles) |
| RPP | River Protection Project |
| RPP-WTP | River Protection Project – Waste Treatment Plant |
| SSR | solid state relay |
| TBD | to be determined |
| UMAX | discharge velocity from PJM at maximum available drive pressure for system |
| UMIN | discharge velocity from PJM for minimum detectable cavern above dished bottom |
| UFP | ultrafiltration process |
| WTP | Waste Treatment Plant |
| WTPSP | Waste Treatment Plant Support Project |

## DACS Related Definitions, Acronyms, and Abbreviations

**component:** one of the parts that make up a *system*. A component may be hardware or software and may be subdivided into other units or components [IEEE Std 610.12-1990]. For this report, component refers to a single piece of hardware instead of the terms "part" and "unit." The term "module" will be used to refer to a group of components composing a subsystem.

**DACS**---Data Acquisition & Control System

**extendibility:** the ease with which a system or component can be modified to increase its storage or functional capacity [IEEE Std 610.12-1990] (synonyms: extensibility; expandability).

**functional requirement:** function that a system or component must be able to perform [IEEE Std 610.12-1990]. In this requirements specification, functional requirements specify how inputs to the software will be transformed into outputs [IEEE Std 830-1984].

**interface requirement:** external item with which a system or component must interact or that sets constraints on format, timing, or other factors caused by such an interaction [IEEE Std 610.12-1990].

**module:** a group of components composing a subsystem; see *component.*

**performance:** the speed, accuracy, or memory use by which a system or component accomplishes its designated functions within given constraints [IEEE Std 610.12-1990] (contrast with *reliability*).

**performance requirement:** condition imposed on a functional requirement, specifying, for example, the speed, accuracy, or memory use with which a given function must be performed [IEEE Std 610.12-1990] or a static numerical requirement such as the number of simultaneous users to be supported or the number of files and records to be handled [IEEE Std 830-1984].

**product:** a system or component, along with any necessary data and documentation, for which requirements are specified in a *requirements specification.*

**requirement:** (1) a condition or capability needed to solve a problem or achieve an objective; (2) a condition or capability that must be met or possessed by a *system* or *component* to satisfy a contract, standard, *specification*, or other formally imposed document; (3) a documented representation of a condition or capability as in (1) or (2) [adapted from IEEE Std 610.12-1990].

**requirements specification (RS):** a document of essential *requirements* (functions, performance, design constraints, and attributes) of the software and/or hardware and their external interfaces [adapted from IEEE Std 610.12-1990].

**software:** computer program that applies to all data acquisition, process control, data analysis processes, data presentation/plotting, and archival storage.

**system:** a collection of *components* related in such a way as to produce a result greater than what their parts, separately, could produce.

**unit:** see *component.*

**usability:** the ease with which a user can learn to operate, prepare inputs for, and interpret outputs of a system or component [IEEE Std 610.12-1990].

## Units

| | |
|---|---|
| °C | degrees centigrade |
| CFM | cubic feet per minute |
| cm | centimeter |
| cP | centipoise |
| D | diameter |
| deg | degree |
| ft | feet |
| g | gram |
| gal | gallon |
| gpm | gallons per minute |
| H | height |
| hr | hour |
| in. | inch |
| L | liter |
| lb | pound |
| µm | micrometer |
| m | meter |
| mA | milliamp |
| min | minute |
| Pa | Pascal |
| psi | pounds per square inch |
| psia | pounds per square inch, absolute |
| psig | pounds per square inch, gauge |
| s or sec | second |
| SP GR | specific gravity |
| wt% | weight percent |

# Acknowledgments

The authors would like to thank Tom Loftus, Richard Ehlers and Don Cravens, Frank Felix, Rod Bechtol, Mike Longaker, Mark Sweeney, Karen Mercer, Bill Combs, Dennis Mullen, Mike Johnson, Bill Buchmiller, Theresa Claphan, Renee Russell, Lynette Jagoda, Judith Bamberger, Ron Myers, Jim Fort, Soto Yokuda, Richard Brown, Dan Tano, Jackie Newell, and Kate Deters for all their help with the test system configuration, simulant preparation, and assistance during all phases of the testing. Thanks also to Mike McKinnon for the technical review and to Sheila Bennett for technical editing efforts on this document.

# Contents

# Figures

# Tables

# 1.0 Introduction

## 1.1 Background

The Hanford Site has 177 single- and double-shell tanks containing radioactive waste. The U.S. Department of Energy (DOE) Office of River Protection's Waste Treatment Plant (WTP) is being designed and built to pretreat and then vitrify a large portion of these wastes. The WTP consists of three primary facilities: a pretreatment facility, a low-activity waste (LAW) vitrification facility, and a high-level waste (HLW) vitrification facility. The pretreatment facility receives waste feed from the Hanford tank farms and separates it into 1) a high-volume, low-activity, liquid process stream stripped of most solids and radioisotopes and 2) a much smaller-volume HLW slurry containing most of the solids and most of the radioactivity. In the pretreatment facility, solids and radioisotopes are removed from the waste by precipitation, filtration, and ion exchange processes to produce the LAW streams. The slurry of filtered solids is blended with two ion exchange eluate streams containing soluble radioisotopes to produce the HLW stream. The HLW and LAW vitrification facilities convert these process streams into glass, which is poured directly into stainless steel canisters. The major unit operations of the WTP are shown on the process flowsheet presented in Figure 1.1.

The process stream significant to this report is identified on the diagram as "HLW pretreated sludge." Several vessels through which the HLW pretreated sludge stream will be processed will be mixed using pulse jet mixer (PJM) technology. This technology has been selected for use in so called "black cell" regions of the WTP. Within these regions of the plant, maintenance capability will not be available for the operating life of the WTP. PJM technology was selected for use in these regions because of the lack of moving mechanical parts that require maintenance.

The concept behind PJM mixing technology involves a pulse tube coupled with a jet nozzle. One end of the tube is immersed in the tank, while periodic vacuum, vent, and pressurized air are supplied to the opposite end. This creates various operating modes for the pulse tube, including the drive cycle (pressure), where the contents of the PJM tube are discharged at high velocity through the nozzle; the refill mode (vacuum), where the tank contents refill the pulse tube; and an equilibration mode (vent), where the pulse tube and tank fill levels approach the same level. The PJM system uses these operating modes to produce a sequence of drive cycles that provide mixing in the vessel. PJM operating parameters, velocity, nozzle diameter, and drive time, along with the rheological properties of the fluid being mixed, all contribute to the effectiveness of mixing within the vessel.

Many of the waste slurries to be received and processed in the Waste Treatment Plant exhibit non-Newtonian behavior. In particular, when stationary, they can develop gel-like properties and behave like very weak solids. When an applied force exceeds their shear strength, they act like a fluid and begin to flow. The majority of available knowledge for mixing non-Newtonian fluids is associated with the use of mechanical agitators. The subject of jet mixing in non-Newtonian fluids is a relatively new and developing field, with some theoretical analysis and applied research being pursued in industry and academia. The field of non-steady jet mixing in non-Newtonian fluids is essentially in its infancy.

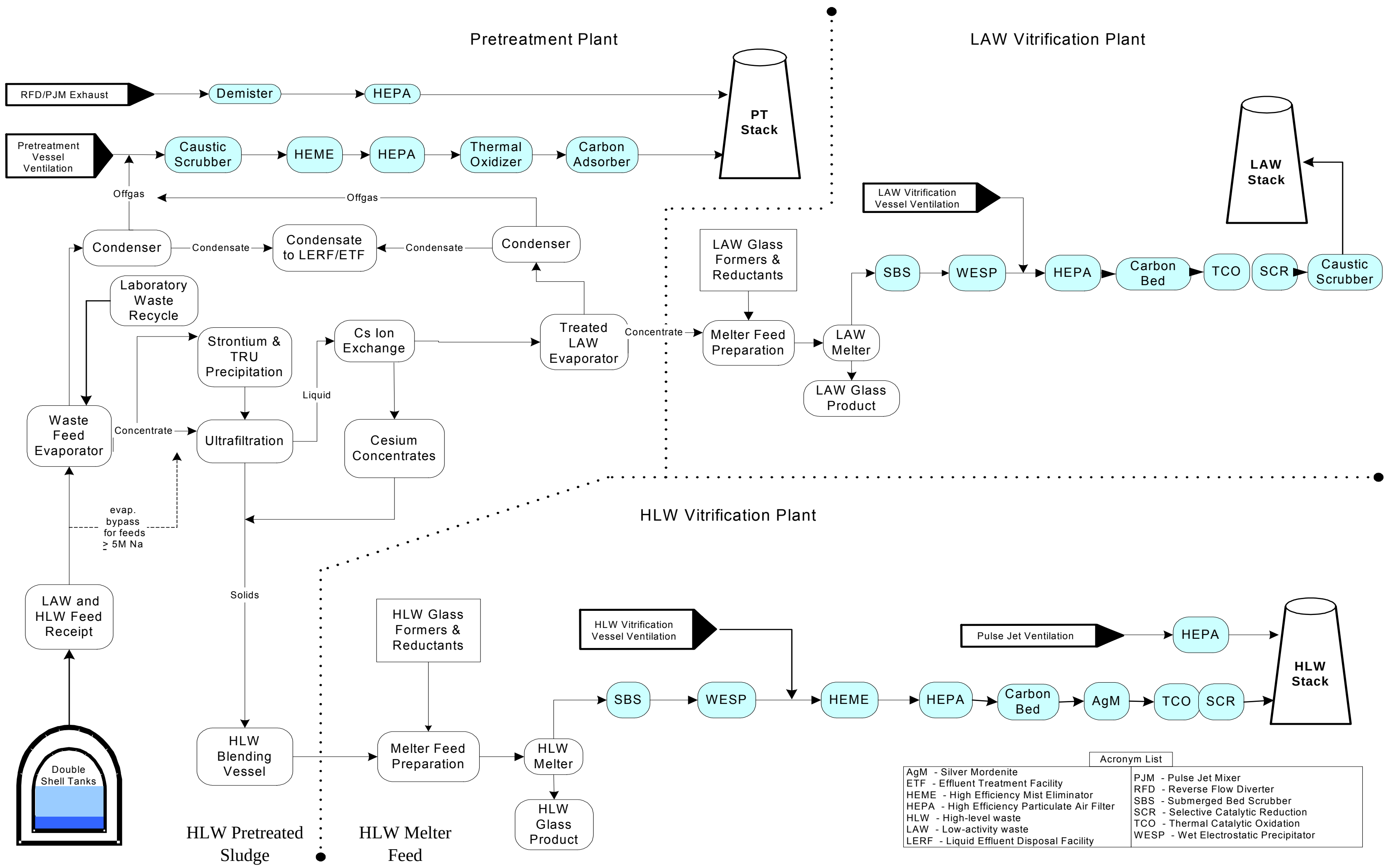


**Figure 1.1**. RPP-WTP Basic Process Flowsheet

One essential phenomenon observed in mixing of Non-Newtonian fluids is the formation of a cavern, illustrated in Figure 1.2. A cavern is essentially an enclosed region near the mixing jet that is highly agitated and turbulent. The cavern is surrounded by material that is essentially stationary, and the transition between the two regions can be very abrupt. The reason for the cavern formation is as follows: Fluid motion created by the jet discharge decreases with distance away from the jet. At some point, fluid velocities are low enough that resulting fluid stresses are no longer able to overcome the shear strength of the non-Newtonian material. Hence a force balance occurs that is stable. As the jet discharge increases, fluid velocities increase and the cavern grows. As the strength of the non-Newtonian material increases, the cavern is smaller.

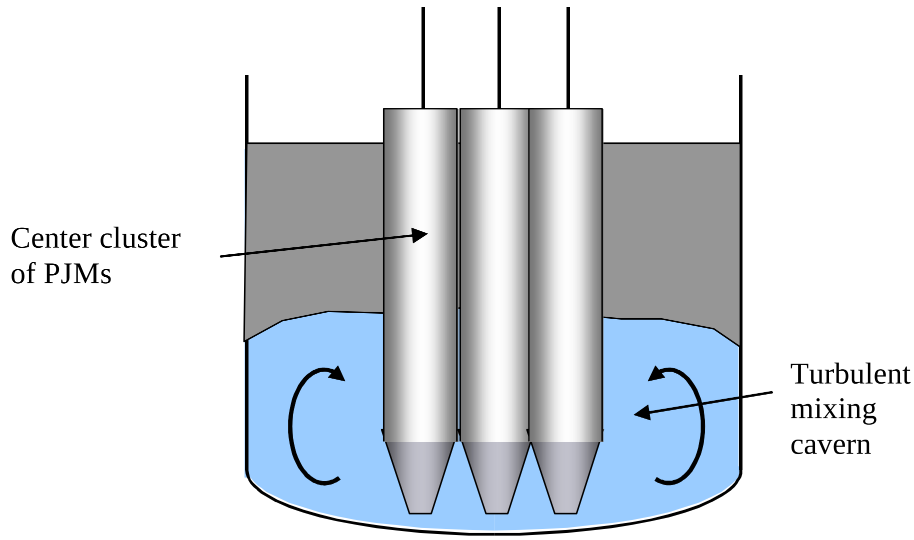


**Figure 1.2**. Example of Cavern Formation in Non-Newtonian Waste

A successful mixing system design involves placement of jets so there are no regions of stationary material in the mixing vessel. However, given the absence of established design guidelines for PJM operation in non-Newtonian fluids, validation of adequate mixing system performance is required.

Confirmation of adequate PJM performance in WTP vessels has been accomplished normally using computational fluid dynamics (CFD) analysis. This approach has worked well for the large portion of vessels that contain Newtonian fluids. The approach has not worked for the vessels that contain non-Newtonian fluids because of difficulties in demonstrating that the CFD approach accurately reflects actual fluid behavior. Continuing with the CFD approach involves the prospect of significant risk, requiring the development of new computational models, benchmark testing, and protracted analyses.

On the basis of recommendations from the research and technology (R&T) peer group, DuPont mixing consultant Art Etchells, and the fluidics contractor AEA, it was agreed to shift the design validation approach to testing of non-Newtonian vessels as a more efficient solution in terms of cost, schedule, and assurance of closure. Accordingly, a less analytical, more empirical strategy, with dimensionally scaled and full-scale testing included, has been developed.

## 1.2 Scaled Test Strategy

The PJM Task Team (R&T, Engineering, R&D, and mixing consultants) developed an integrated strategy for scaled testing to validate PJM mixing in WTP vessels containing non-Newtonian fluids in June 2003. This methodology is a well-accepted (but limited) method for rating fluid mixing systems experimentally. (For WTP applications, these Phase 1 experiments are recognized as limited in that they do not account for differences between simulants and actual wastes or for radiolytic/thermolytic gases generated with actual wastes.) Scaled testing will meet the project requirements for rating the design of the fluidic mixing systems of non-Newtonian vessels and will have only minimal impacts on schedule. Scaled testing is generally a technically sound and defensible approach to rating a mixing design and is applicable within limitations to the WTP PJM mixing processes.

The goals of the scaled PJM mixing tests were as follows:

- to assess mixing performance of AEA baseline PJM designs in non-Newtonian slurries.
- to provide information on the operating parameters critical for the uniform movement (total mobilization) of these non-Newtonian slurries.
- to identify PJM configuration options that would result in the uniform movement (total mobilization) of these non-Newtonian slurries.

To achieve these goals, the scaled test strategy consisted of the following major components:

**Simulant Development**. The mixing performance in the PJM test vessels needed to be assessed for non-Newtonian fluids. To realize this objective, non-Newtonian rheological simulants needed to be developed that were nonhazardous and similar in rheological nature to the actual Hanford waste material that will be processed in the WTP. Candidate materials were identified and recipes developed for non-hazardous rheological simulants. Both transparent and opaque simulants were developed for the testing. Results of this development and testing activity are reported in Poloski et al. (2004).

**Scaling Tests**. The technical basis for scale-up of the mixing induced by PJMs and steady jets (as induced by closed-loop recirculation) is a modification to turbulent jet theory to account for the non-Newtonian rheology and non-steady jets from the PJMs. Dimensional analysis (details in Appendix A) was used to identify the important dimensionless parameters and guide the experimental design. Mixing tests were conducted at three different physical scales to prove that testing at a reduced scale was adequate for assessing mixing performance. These included a large-scale (near full scale at the 336 Building), ~1/4 scale at the Applied Process Engineering Laboratory (APEL)], and small scale (~1/8) tests (at Savannah River Technology Center). Each of these vessels had a mixing system consisting of four PJMs, and they were geometrically similar. Theoretical analyses were used to develop scaling laws that related simulant properties and operating conditions in the different vessels. Mixing results were compared to demonstrate that testing at a reduced scale is a conservative way to predict full-scale mixing performance in WTP vessels. Results of that testing are reported separately.[a]

---

(a) WTP-RPT-113, "Technical Basis for Scaling of Pulsed Jet Mixer Performance with Non-Newtonian Slurries."

**Scaled Prototypic Testing**. The final component of the scaled test strategy was to test prototypic vessels at reduced scale. The seven vessels designed to contain and mix non-Newtonian simulants are adequately represented by a subset of three: the ultra-filtration process (UFP) vessel, the lag storage (LS) vessel, and the concentrate receipt vessel (CRV). Reduced-scale models (~1/4 scale) were fabricated maintaining the essential prototypic features (vessel geometry, number of PJMs, PJM geometry, operational parameters, and major vessel internals). These reduced-scale prototypic vessels allow for performance assessment of the baseline design, obtaining information on key operating parameters, and identifying PJM configurations with improved performance. The results of this component of the scaled test strategy are the subject of this report.

## 1.3 Scope of the Project

The scope of the work presented in this report involves testing PJMs in scaled UFP and LS vessels. The data presented in this report include 1) as-built descriptions of the test configurations, 2) simulant properties, 3) individual test operational parameters, and 4) results summarizing the test outcomes.

In the actual WTP, waste slurries with a sodium concentration of approximately 5 M are delivered to UFP-VSL-00002A/B for separation into solid (HLW) and liquid (LAW) fractions. The waste in the feed vessel is pumped through three bundles of cross-flow filters. The water and other soluble components of the waste permeate pass through the filter media and discharge into one of the permeate receipt vessels. The solids are recirculated into the feed vessels, where additional waste is received to replace the permeate and maintain a relatively constant volume [corresponding to a height to diameter ratio (H/D) of 1.4]. While the solids are being concentrated, the filters are back-pulsed periodically. Back-pulsing pushes permeate back through the filters into the concentrated slurry and dislodges solids that have built up on the filter surface, enhancing the overall permeate flux rate. The UFP vessels are equipped with PJMs, cooling jackets, high-pressure steam injectors, and chemical reagent feed lines. The cooling jackets control the slurry temperature while filtering and cool the waste after leaching. The filter pumps are relatively large and add a significant amount of heat energy to the waste. The high-pressure steam heats and holds the waste at an elevated temperature during the leach process. The chemical reagents are used for leaching and filter cleaning.

Solids treatment begins after the solids are concentrated to approximately 20 wt% (dry basis) for Envelopes A, B, and D and 15 wt% for Envelope C. First the solids are washed with process condensate using the same steps as solids filtering or concentration to remove soluble components. Process condensate is added to UFP-VSL-00002A/B to replace permeate that passes through the filters. After Envelope A, B, and D solids are washed, they are leached (except Envelope C solids are not leached) if warranted (corresponding to an H/D of 1.8 in the UFP vessels). The first step in leaching is to add 19 molar sodium hydroxide until a calculated value of 3-molar free hydroxide is reached for the batch. The solution is then heated with high-pressure steam to 176°–194°F and allowed to digest for eight hours. The slurry is then cooled and filtered until the solids concentration is back up to 20%. After the solids are reconcentrated, they are washed again with process condensate to remove residual sodium hydroxide and dissolved solids. Treated solids are discharged to LS (HLP-VSL-00027A/B) and chemical cleaning of the filters, if required, begins.

Normally LS vessels (HLP-VSL-00027A/B) receive treated solids from ultrafiltration, but treated solids can be sent directly to the blend vessel (HLP-VSL-00028) if necessary. Backup blend vessel HLP-VSL-00027B can receive the same waste transfers as HLP-VSL-00028. Treated HLW solids, concentrated Cs, and Sr/TRU solids (if available) are blended in HLP-VSL-00028, sampled, and routed to HLW vitrification.

## 1.4 Scaled Testing Description

For each tank a test system was prepared that included PJMs and important tank internals. Prototype tanks tested include the UFP vessel and a HLW LS vessel, the latter representing both LS and blend vessels. The scaled test tanks had diameters from 3 to 6 ft. Tank design details, internal components (number of pulse tubes, charge vessels, RFDs, etc.), system layout, utility requirements, simulants, along with the make-up instructions and number of tests) were used to design the initial test program.

Test Specification 24590-WTP-TSP-RT-03-008 Rev 0, detailing an initial test matrix, was supplied to PNWD. Additional specific testing requirements were provided during the tests based on results. PNWD assembled the system(s) and performed shakedown testing. Test Plan TP-RPP-WTP-296 was prepared by PNWD and approved by Bechtel National, Inc. (BNI).

Initial (physical) scaled testing confirmed in October 2003 that the baseline pulse jets in these vessels did not mix non-Newtonian slurries to the extent necessary to meet WTP design requirements. Phase I of the PJM program (the subject of this report) developed alternative “PJM-only” configurations that mixed the non-Newtonian slurries according to WTP design requirements toward the end of November 2003. The approach was to start with nominal PJM configurations from the current baseline plant design, perform scoping tests to identify whether those configurations were adequate, and begin geometric and operational parameter modifications based on observations from initial testing to find PJM-only mixing scenarios that delivered complete or nearly complete mixing/mobilization. An array of such tests, referred to as final PJM tests, were reviewed by the PJM steering committee to identify the configurations most likely to best serve the needs of the WTP (with proper weighting of WTP plant geometric and operational requirements and constraints). These final PJM configurations and operational parameters were tested in depth with the best available waste simulants. The final (referred to as “all-in”) tests resulted in the final recommended PJM configurations for the Phase 1 testing task.

The alternative PJM configurations were acceptable from a mixing/mobilization standpoint, but their implementation severely impacted WTP facility designs due to increased numbers of PJMs, additional piping, and the significantly increased air consumption required for operation. Other concerns relating to gas generation, retention, and release in the waste handling vessels were also heightened.

To minimize the impact to overall project cost and schedule, the PJM Task Team was directed to develop PJM hybrid mixing systems (which incorporate additional non-PJM mechanisms such as air sparging and closed-loop, pump-driven recirculation loops with steady jets to enhance performance). Phase II efforts were initiated to investigate in depth such alternative, PJM-based, hybrid mixing systems and to characterize not only mixing performance but also the effect of slurry rheology changes, reduced tank volume, PJM jet velocity and nozzle size, gas retention and release behavior, sparging, and recirculation pump operation. Phase II results are reported under separate cover.[a]

(a) WTP-RPT-128, "Performance Data for Hybrid Mixing Systems in Scaled Prototypic Ultrafiltration Feed Process (UFP) and HLW Lag Storage (LS) Vessels with Non-Newtonian Slurries."

# 2.0 Test Configurations

In this section, description of the initial and final LS and UFP test configurations are presented. The initial configurations were described in Test Specification 24590-WTP-TSP-RT-03-008 Rev 0 and represent the then current baseline designs of PJMs for the plant vessels. The final configurations, also called the “All-In” configurations, were described in a test exception (24590-WTP-TEF-RT-03-081). The final designs reference the performance observed during the course of geometrical and operating parameter variations to perform complete or at least acceptable mobilization/mixing of the target vessels. A first test exception (24590-WTP-TEF-RT-03-060) consisted of a modified test matrix building on knowledge gained from initial configuration tests. The complete text of the test exceptions is included as Appendix B to this report. Table 2.1 summarizes the geometrical and operational parameters for the scaled and full-scale tanks being investigated.

## 2.1 Initial Lag Storage Test Configuration

Initial testing hardware was provided by BNI and included the initial configuration of PJMs per the then-current (baseline) design for the LS vessel. The configuration was an approximately scaled configuration of the plant design LS PJM array.[a] The initial configuration is shown in Figure 2.1.

## 2.2 Final LS Test Configuration

Following initial testing with the initial, plant design PJM configuration and exercising a range of both PJM operating parameters and PJM geometrical arrays, a test exception was provided directing a final set of tests (referred to as the “All-In” test configurations) wherein decisions by the BNI-convened steering committee (consisting of BNI, PNWD, DOE, and expert consultants contracted by BNI) reviewed the entire set of prototype test results and observations and recommended a final best configuration for a final testing during the Phase 1 Prototype testing sequence. That final PJM configuration geometry recommended for the LS PJMs is shown below in Figures 2.2 (plan view) and 2.3 (elevation view). The design of the individual scaled LS PJMs as provided by BNI is shown in Figure 2.4. The full-scale PJM for use in the LS vessel is shown for comparison in Figure 2.5.

(a) Scaling was not exactly per the scale factor for the vessel due to limitations imposed by constructing PJM units from available standard pipe sizes and schedules.

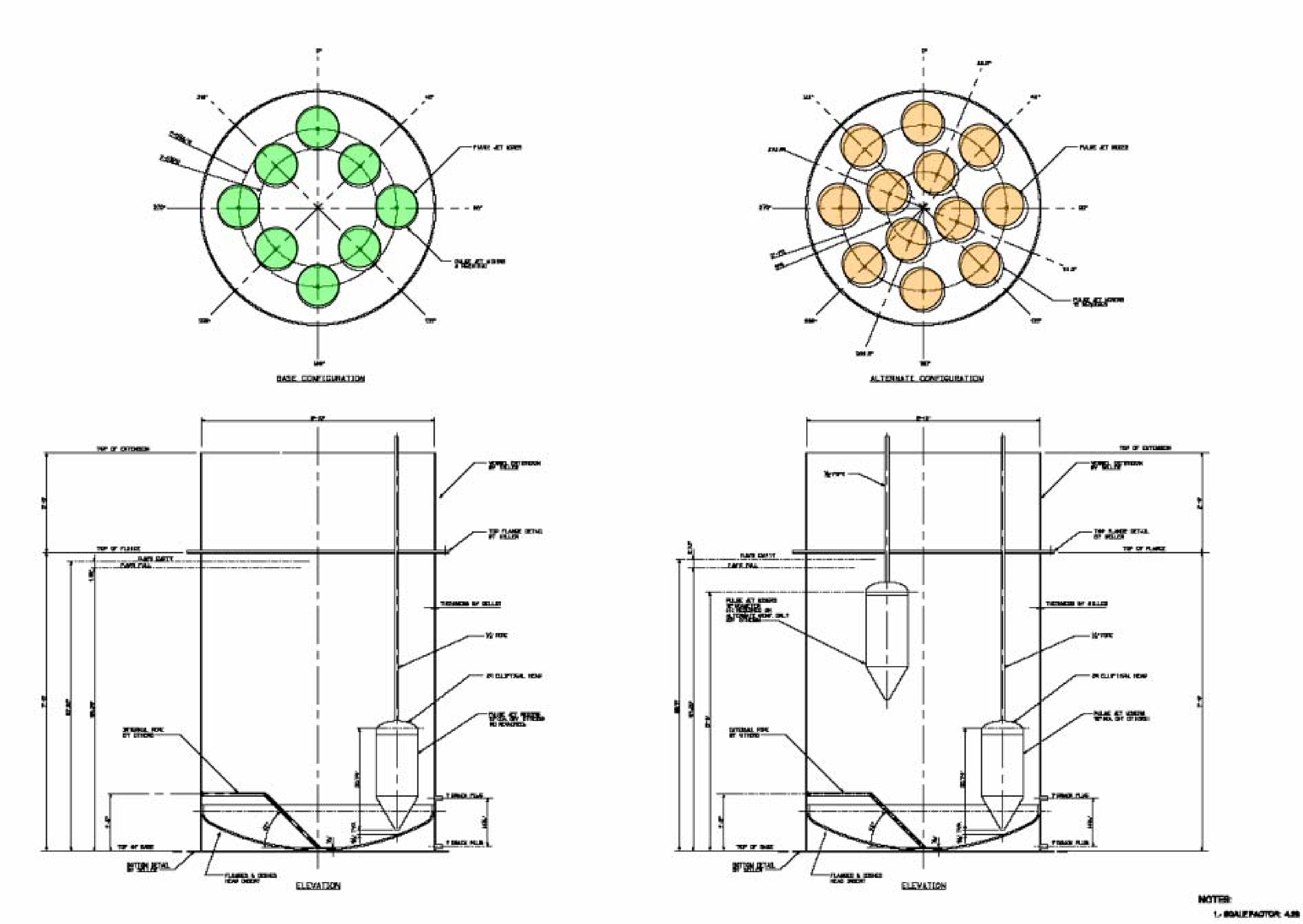


**Figure 2.1**. LS Vessel Showing Both Baseline (green) and Maximum Optional (orange) PJM Arrays

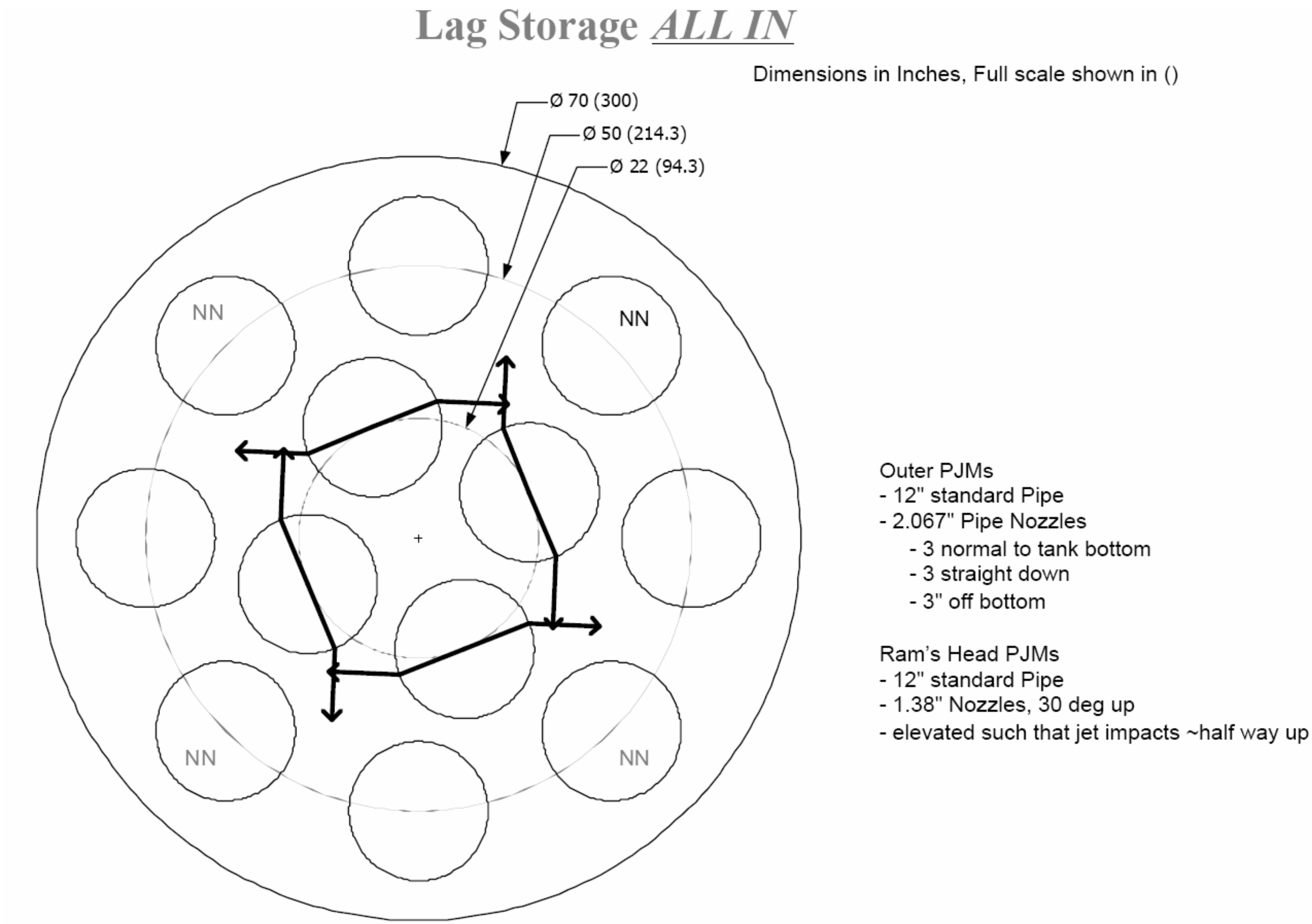


**Figure 2.2**. Lag Storage All-In Configuration

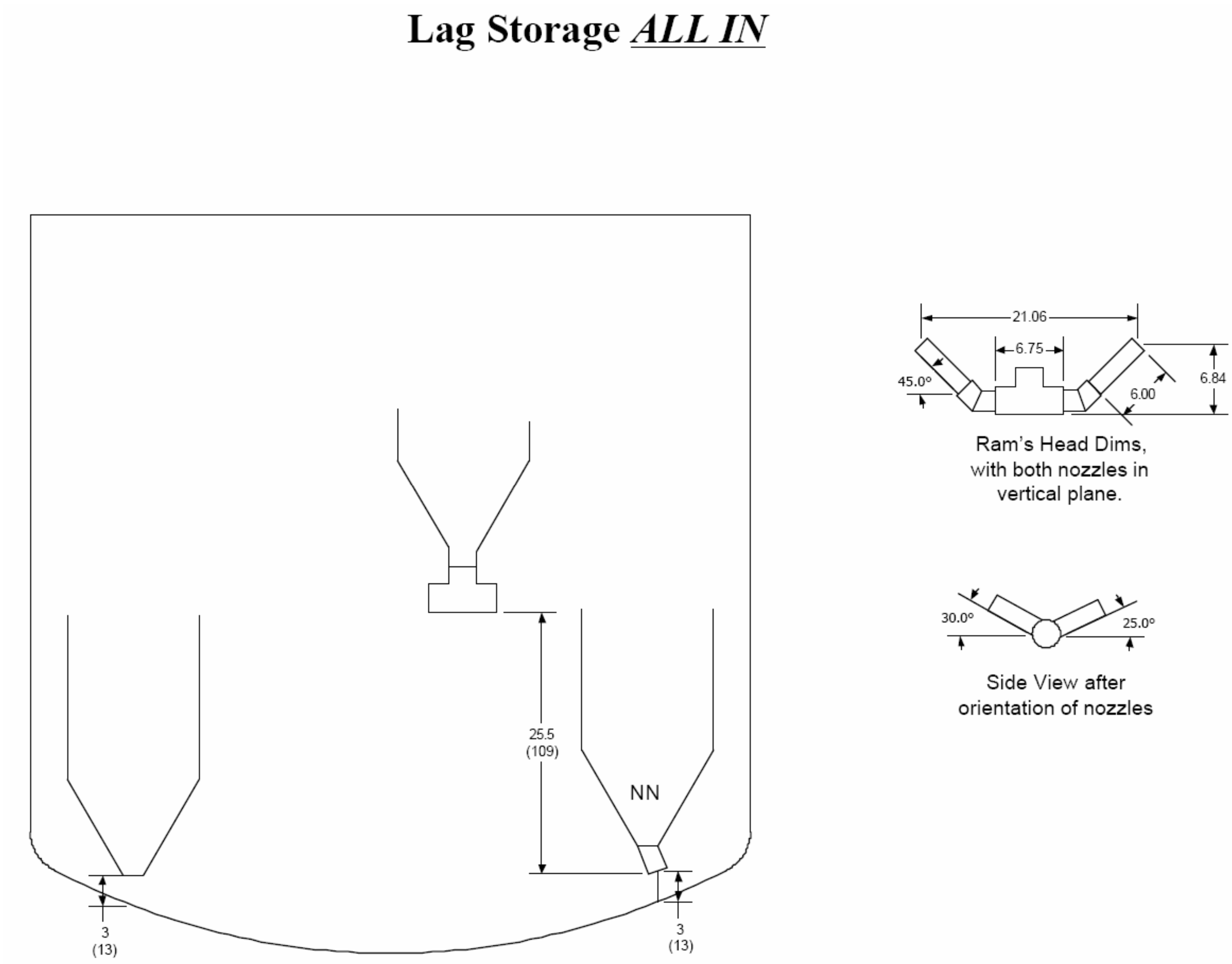


**Figure 2.3**. Elevation View - LS All-in Configuration

# Scaled HLP (LS)

**Title: Pulse Jet Mixer Sizing**

| Inputs | | |
|---|---|---|
| Inside Diameter= | 11.940 | in |
| Total Volume= | 18.430 | gal |
| NozzleDia= | 2.065 | in |

| | | |
|---|---|---|
| Head Volume= | 222.82 | $in^3$ |
| | 0.96 | gal |
| Head Height= | 2.99 | in |
| $h+h_b$= | 10.34 | in |
| h= | 8.55 | in |
| Volume of frustum= | 383.94 | $in^3$ |
| | 1.66 | gal |
| Cylindrical Volume= | 3,650.57 | $in^3$ |
| | 15.80 | gal |
| Cross. Area= | 111.97 | $in^2$ |
| Cylindrical Height= | 32.60 | in |
| Total Height = | 44.14 | in |

**Notes:**
Head is 2:1 SE
Angle of the cone is 60 deg

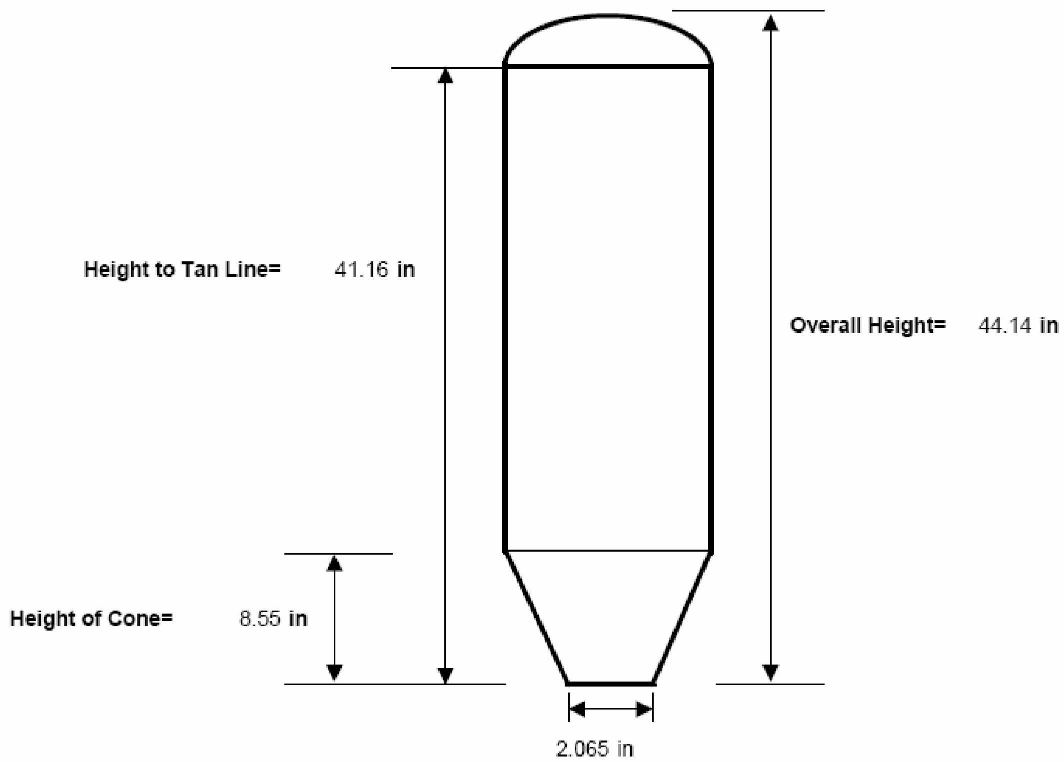


**Figure 2.4**. All-in LS Pulse Jets

# HLP (LS)

**Title: Pulse Jet Mixer Sizing**

| Inputs | | |
|---|---|---|
| Inside Diameter= | 52 | in |
| Total Volume= | 1451 | gal |
| NozzleDia= | 8.860 | in |

| | | |
|---|---|---|
| Head Volume= | 18,405.54 | $in^3$ |
| | 79.68 | gal |
| Head Height= | 13.00 | in |
| $h+h_b$= | 45.03 | in |
| h= | 37.36 | in |
| Volume of frustum= | 31,721.65 | $in^3$ |
| | 137.32 | gal |
| Cylindrical Volume= | 285,053.81 | $in^3$ |
| | 1,234.00 | gal |
| Cross. Area= | 2,123.72 | $in^2$ |
| Cylindrical Height= | 134.22 | in |
| Total Height = | 184.58 | in |

**Notes:**
Head is 2:1 SE
Angle of the cone is 60 deg

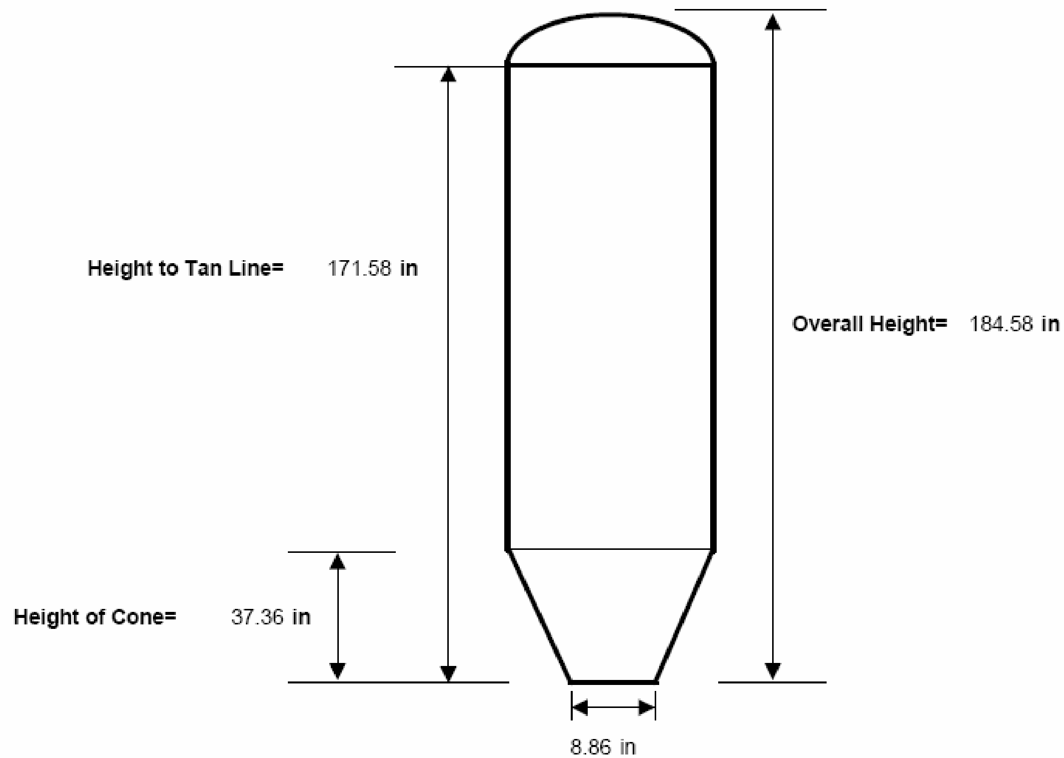


**Figure 2.5**. All-in LS Full-Scale Pulse Jets

**Table 2.1**. All-in Prototype Parameters (from Test Exception)

| Parameter | All In | | |
|---|---|---|---|
| | UFP | LS | CRV[(a)] |
| **Full-Scale** | | | |
| Vessel ID | 168 | 300 | 162 |
| PJM PCD (in.) | 113.6 | 214.3 | 72.0 |
| PJM ID (in.) | 32 | 52 | 32 |
| PJM OD (in.) | 32.75 | 52.75 | 32.75 |
| PJM Vol (gal) | 610 | 1451 | 448 |
| RH PJM PCD (in.) | 39.5 | 94.3 | 69.6 |
| RH PJM ID (in.) | 32 | 48 | 32 |
| RH PJM OD (in.) | 32.75 | 48.75 | 32.75 |
| RH PJM Vol (gal) | 610 | 1451 | 448 |
| Nozzle ID (in.) | 6.00 | 8.86 | 6.00 |
| RH Nozzle ID (in.) | 4.07 | 5.91 | 6.00 |
| Operating Level (in.) | 306 | 329 | 144 |
| H/D (operating) | 1.82 | 1.10 | 0.89 |
| **Small Scale** | | | |
| Vessel ID (in.) | 34 | 70 | 40.5 |
| Scale Factor | 4.94 | 4.29 | 4.00 |
| PJM PCD (in.) | 23 | 50 | 18 |
| PJM Pipe Size | 6 in. S40 | 12 in. S40 | 8 in. S5 |
| PJM ID (in.) | 6.065 | 11.94 | 8.407 |
| PJM OD (in.) | 6.625 | 12.75 | 8.625 |
| PJM Length (in.) | 43.39 | 43.6 | 39.3 |
| PJM Vol (gal) | 5.055 | 18.43 | 7 |
| RH PCD (in.) | 8 | 22 | 17.4 |
| Rh Pipe Size | 6 in. S40 | 12 in. S40 | 8 in. S10 |
| RH PJM ID (in.) | 6.065 | 11.94 | 8.329 |
| RH PJM OD (in.) | 6.625 | 12.75 | 6.625 |
| RH PJM Vol (gal) | 5.055 | 18.43 | 7 |
| Nozzle ID (in.) | 1.214 | 2.067 | 1.500 |
| RH Nozzle (in.) | 0.824 | 1.38 | 1.500 |
| Operating Level (in.) | 61.9 | 76.8 | 36.0 |
| H/D (operating) | 1.82 | 1.10 | 0.89 |

(a) CRV testing was done at SRTC and will be reported separately.
ID = inner diameter; PCD = Pitch circle diameter
OD = outer diameter; RH = ram's heads
H/D= height to diameter ratio.

## 2.3 Ram's Head Nozzle Arrangement for LS Final Configuration

Ram's head (RH) nozzle configurations were developed to allow split nozzle discharges from a single PJM. The dual or even triple nozzle discharges from the RH arrangements allowed alignment of nozzle flows in multiple directions as an enhancement to mobilization/mixing performance of the PJM discharge. The RH for the final LS configuration are made of standard PVC pipe components, as shown in Figure 2.6. A 2-in. tee is threaded onto the 2-in. male pipe on the end of the pulse tube conical end. At the branches of the tee the pipe size is bushed down to 1¼ inch and a 45-degree elbow cemented close to the

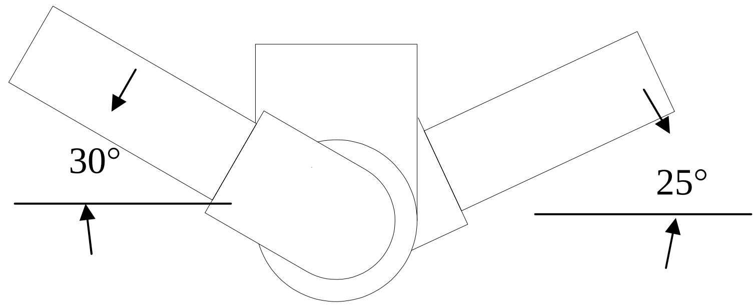


**Figure 2.6**. Actual Prototype Final LS PVC Nozzle Angles

bushing. A straight section of 1¼-in. schedule 40 PVC pipe is glued to the elbow and extends 6 in. past the elbow. When viewed along the horizontal axis of the tee, one nozzle is 30 degrees above horizontal and the other 25 degrees above horizontal.

The horizontal axis of the RH is tangent to the pitch circle of the upper pulse tubes (perpendicular to the radial direction). The nozzles from adjacent RH just miss touching by about ¼ in. at a distance of 3½ in. from the end of the nozzle. The following photos show the relative arrangement of the RH nozzles (Figure 2.7) and a view of the array from the bottom (Figure 2.8), also showing details of the RH configuration.

**Figure 2.7**. Final Prototype LS PVC Nozzle Relationship

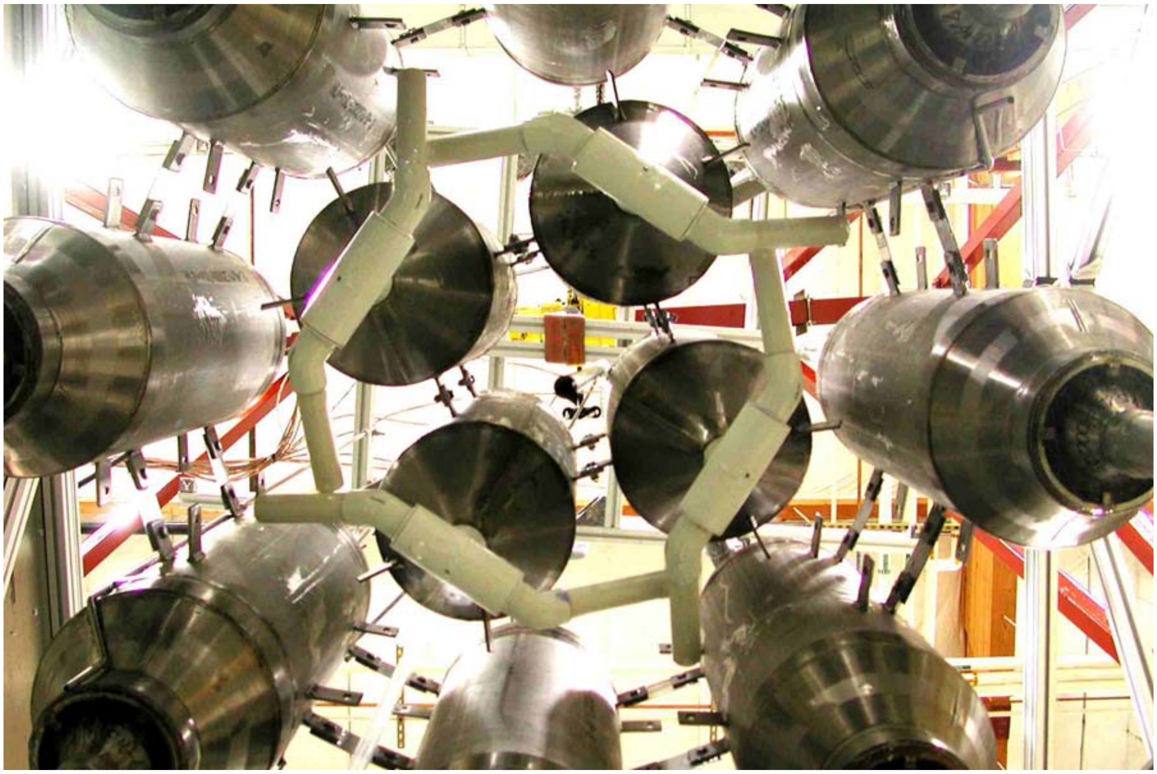

**Figure 2.8**. Final Prototype LS Nozzle Relationship; viewed looking up

## 2.4 Initial UFP Test Configuration

Initial testing hardware for the UFP scaled testing was also provided by BNI and included the initial configuration of PJMs as per the then current design for the UFP vessel. The configuration was an approximately scaled (scaling was again not exactly per the scale factor for the vessel due to limitations imposed by constructing PJM units from available standard pipe sizes and schedules) configuration of the then-current plant baseline design PJM array for the UFP vessel. That configuration is shown in Figure 2.9.

## 2.5 UFP Final Configuration

After testing with the initial PJM configuration, which included exercising a range of both PJM operating parameters and PJM geometrical arrays, a test exception was provided directing a final set of tests (referred to as the "All-In" test configurations). A BNI-convened Steering Committee, consisting of BNI, PNWD, DOE, and expert consultants (contracted by BNI) reviewed the entire set of prototype test results and observations and recommended a configuration to be used for final testing during the Phase 1 prototype testing sequence. The final PJM configuration recommended for the UFP PJMs is shown in Figures 2.10 (plan view) and 2.11 (elevation view).

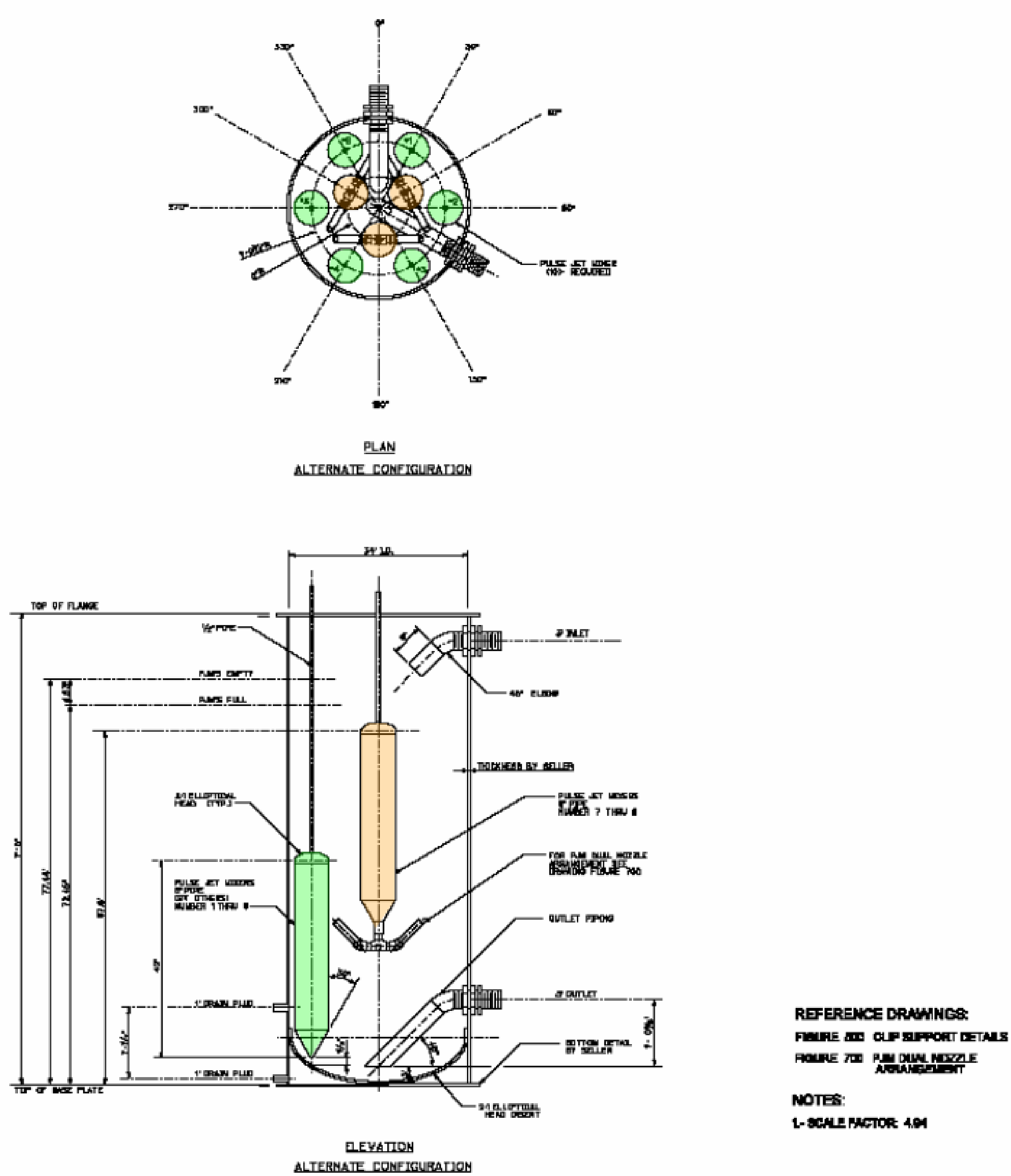


**Figure 2.9**. UFP Vessel Showing Both Baseline (green) and Maximum Optional (orange) PJM Arrays

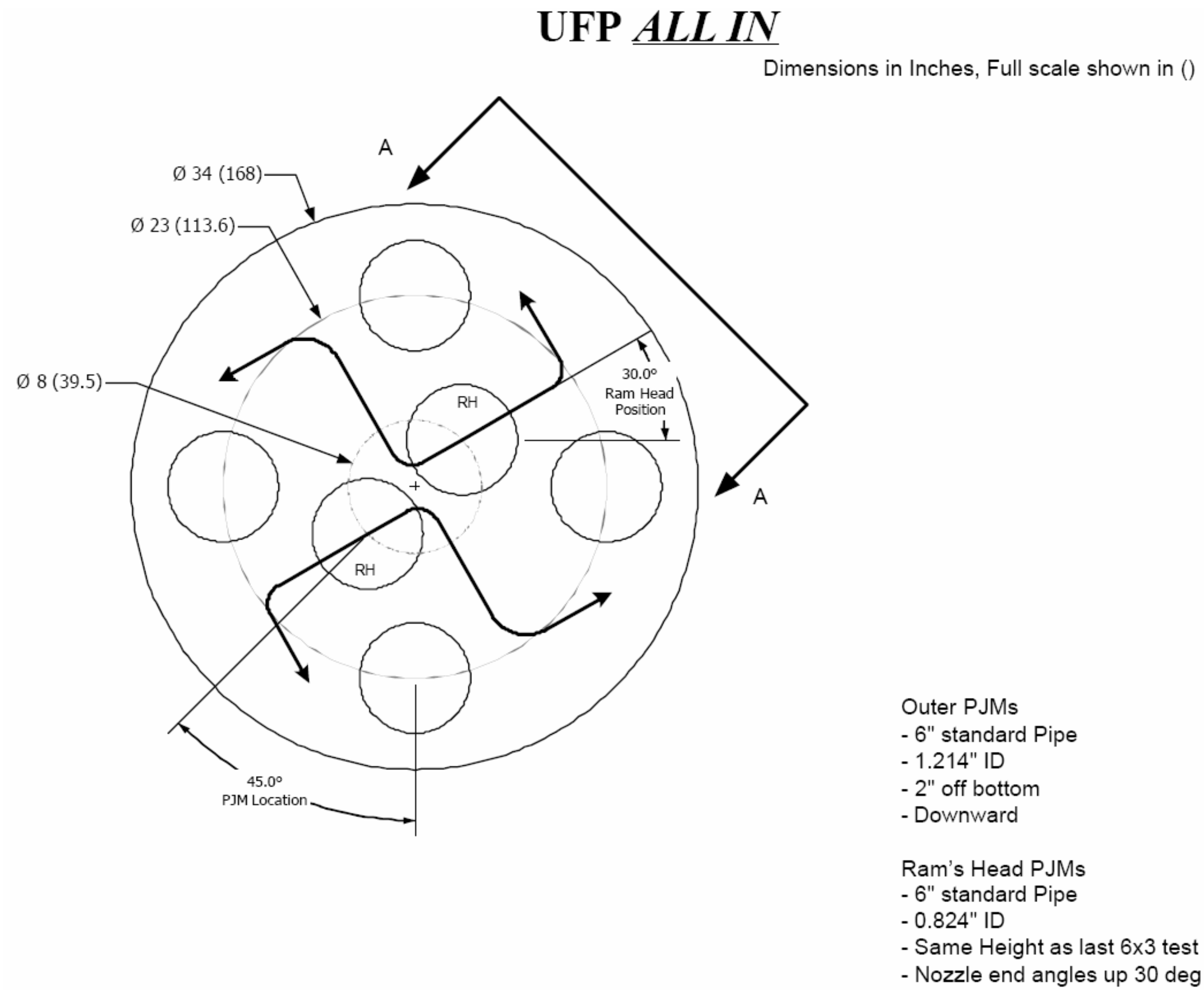


**Figure 2.10**. UFP All-in PJM Arrangement

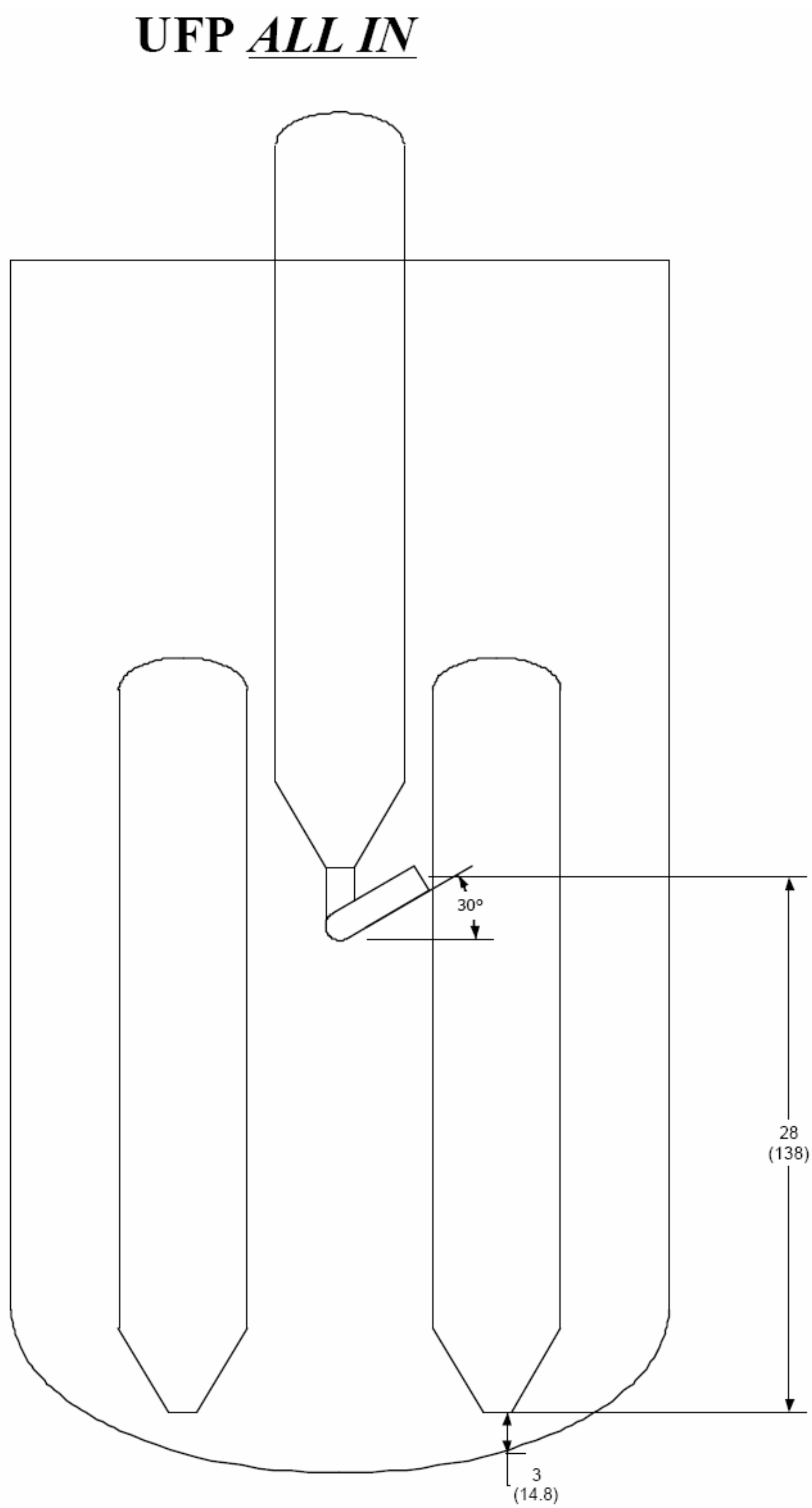


**Figure 2.11**. Prototype UFP All-In PJM Arrangement

## 2.6 Ram’s Head Nozzle Arrangement for UFP Final Configuration

The ram’s heads (RH) for the final UFP configuration are made of standard stainless steel pipe components. A 2-in. tee is threaded onto the 2-in. male pipe on the end of the pulse tube conical end. At the branches of the tee the pipe size is bushed down to 3/4 inch Schedule 40 pipe and 45-degree elbows fitted to appropriate length pipe nipples extending from the bushing and fittings added to arrive at the configuration shown in Figures 2.12 and 2.13. When viewed along the horizontal axis of the tee, each nozzle is 30 degrees above horizontal. The design of the individual scaled UFP PJMs as provided by BNI is shown in Figure 2.14, and the full-scale UFP PJM is shown in Figure 2.15 for comparison.

**Figure 2.12.** Actual Prototype Final UFP RH Discharge Nozzles

# UFP *ALL IN*

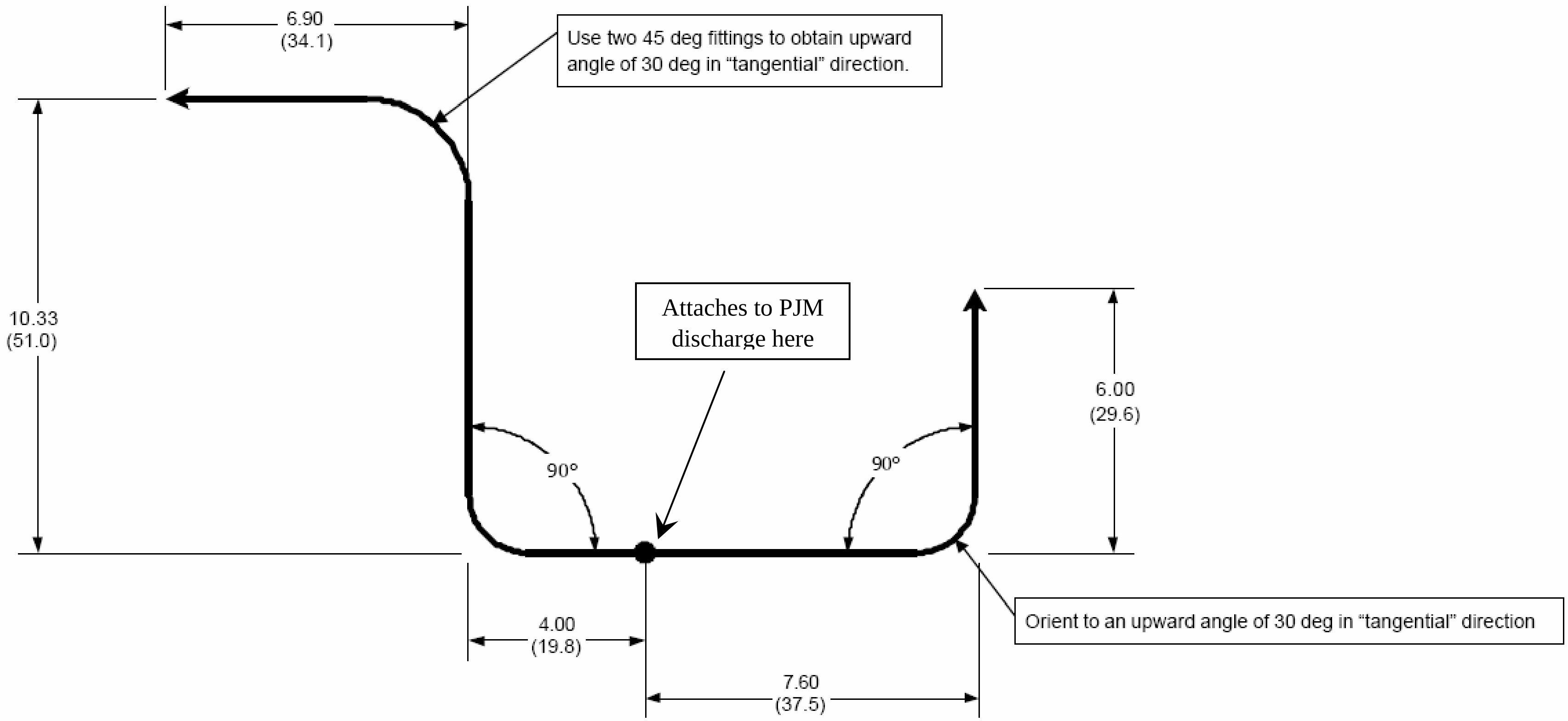


**Figure 2.13**. Prototype UFP RH Piping Detail (looking down; all pipe in same plane)

# Scaled UFP

Title: Pulse Jet Mixer Sizing

| Inputs | | |
|---|---|---|
| Inside Diameter= | 6.065 | in |
| Total Volume= | 5.055 | gal |
| NozzleDia= | 1.214 | in |

| | | |
|---|---|---|
| Head Volume= | 29.20 | $in^3$ |
| | 0.13 | gal |
| Head Height= | 1.52 | in |
| $h+h_b$= | 5.25 | in |
| h= | 4.20 | in |
| Volume of frustum= | 50.18 | $in^3$ |
| | 0.22 | gal |
| Cylindrical Volume= | 1,088.33 | $in^3$ |
| | 4.71 | gal |
| Cross. Area= | 28.89 | $in^2$ |
| Cylindrical Height= | 37.67 | in |
| Total Height = | 43.39 | in |

Notes:
Head is 2:1 SE
Angle of the cone is 60 deg

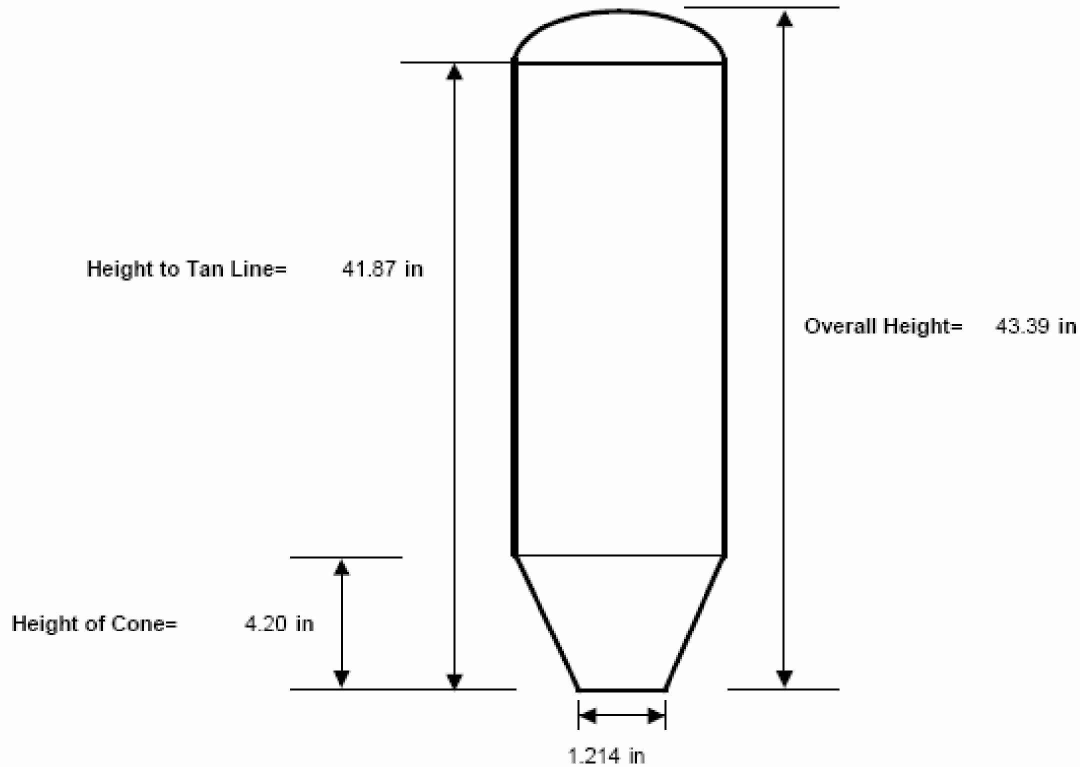


**Figure 2.14**. Final Prototype UFP Scaled Pulse Jets

## UFP

Title: Pulse Jet Mixer Sizing

| Inputs | | |
|---|---|---|
| Inside Diameter= | 32.000 | in |
| Total Volume= | 610 | gal |
| NozzleDia= | 6.000 | in |

| | | |
|---|---|---|
| Head Volume= | 4,289.32 | $in^3$ |
| | 18.57 | gal |
| Head Height= | 8.00 | in |
| $h+h_b$= | 27.71 | in |
| h= | 22.52 | in |
| Volume of frustum= | 7,380.35 | $in^3$ |
| | 31.95 | gal |
| Cylindrical Volume= | 129,240.33 | $in^3$ |
| | 559.48 | gal |
| Cross. Area= | 804.25 | $in^2$ |
| Cylindrical Height= | 160.70 | in |
| Total Height = | 191.21 | in |

Notes:
Head is 2:1 SE
Angle of the cone is 60 deg

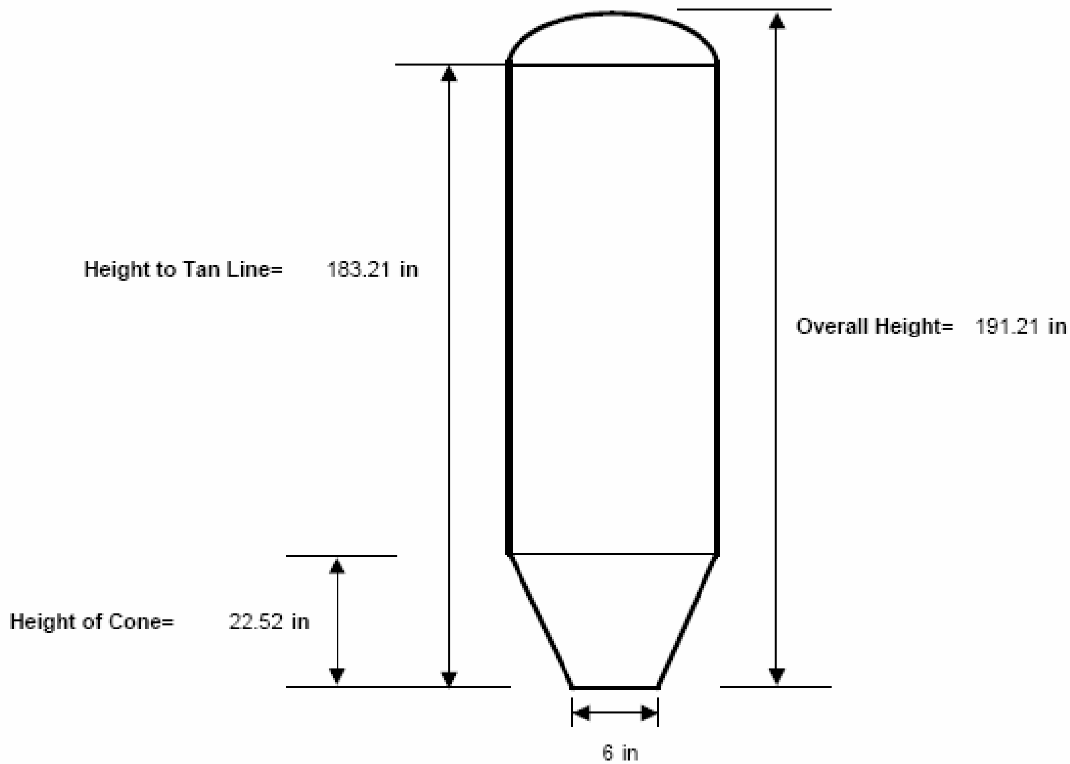


**Figure 2.15**. Final Full-Scale UFP PJMs

# 3.0 Experimental Approach

As discussed in Section 1, the primary data needed were 1) as-built descriptions of the test configurations, 2) rheological characterizations of the various simulants used in the scaled testing, 3) individual test operational parameters, and 4) results summarizing the test outcomes, i.e., observations and/or measurements defining the degree of mobilization achieved in the scaled test tanks. In this section, the experimental approaches used to measure the various items discussed above are presented.

## 3.1 Simulant

The simulant(s) were selected by the WTP PJM Steering Committee, which assumed that the WTP non-Newtonian waste stream is bounded by a Bingham plastic rheology. (For this test strategy, the critical rheological property is the shear strength, $\tau_{ss}$, as determined by a shear vane test. Because there are limited data on $\tau_{ss}$ recorded for actual waste, the approach used was to ensure that $\tau_{ss}$ meets or exceeds the bounding $\tau_{ys}$). Bounding values were $\tau_{ys}$ = 30 Pa and $\kappa$ = 30 cP.[a] This assumption provides a basis for the initial development and selection of a simulant to be used for this test effort.

Based on preliminary test results, the Bingham plastic rheological parameters, consistency index and yield stress, are considered less dominant in defining the cavern height due to the turbulent nature of pulse jet mixing (i.e., a high degree of turbulence is present).

Simulants identified for the non-Newtonian testing were evaluated for pH, shear strength, and rheological flow properties. These characteristics were determined in a laboratory environment, and then the requirements for simulant sampling and characterizations during the course of the scaled testing were determined. Rheological measurements were performed according to BNI Guidance 2450-WTP-GPG RTD-001 Rev. 0.[a]

Selected simulants had to be compatible with the facility use agreements (FUA) for the APEL. Disposal, storage, and handling requirements also must be identified and in place before simulants are received into the facility. Simulant selection took into consideration:

- the stability of the material over the duration of the test
- ease of preparation
- compatibility with instrumentation and experimental detection methods for measuring cavern size
- characterization of rheological properties
- physical representation of the WTP non-Newtonian waste stream
- procurement costs, availability, and disposal costs
- health and environmental risks and hazards associated with the material.

(a) See WTP-RPT-111, "Non-Newtonian Slurry Simulant Development and Selection for Pulse Jet Mixer Testing," for discussions of simulants and target properties.

The test strategy calls for the same simulant recipes for both scaled prototypic test platforms (UFP and LS). While simulant make-up activities strove to match rheological properties, minor variations between the platforms were not detrimental to the test objectives due to the ability to perform non-dimensional comparisons.

The two primary simulants were Laponite and a kaolin/bentonite clay mixture. Laponite is a thixotropic colloidal synthetic clay that forms a transparent gel when left unsheared. This simulant was used to assess the scale-up behavior of the PJMs and visualize flow behavior in the scaled prototypes. The kaolin/bentonite clay mixture exhibits a Bingham plastic rheology that closely represents the rheology of actual waste slurries. This simulant was used to investigate scale-up behavior as well as to assess the performance of the scaled prototype PJM-mixed vessels. (The simulant was also used in later gas retention and release testing that was beyond the scope of the current effort).

## 3.2 Test Setup

The 168-inch-diameter, full-scale UFP tank was represented by a 34-inch-ID acrylic vessel outfitted with a scaled array of PJMs and vessel internals. The 300-inch-diameter, full-scale LS tank was represented by a 70-inch-ID acrylic vessel outfitted with a scaled array of PJMs and vessel internals (Figure 3.1). The functionality of a PRESCON controller (the AEA-designed electronics package used for controlling full-scale PJM units in WTP) was mimicked by a Data Acquisition and Control System (DACS) array of solenoid valves controlling compressed air and vacuum supply sources. The control of solenoid valves exercised the PJMs in a time-scaled fashion (time scales as the inverse of the geometric scale factor); thus, for the prototypic UFP vessel, 168/34 = 4.94 and prototypic LS vessel, 300/70 = 4.29 scale factor relationships of these tests, all temporal events must occur in 1/4.94 and 1/4.29 time periods, respectively. The duration of large-scale events (45-second full-scale UFP PJM cycle time became 45/4.94 = 9.1 and LS cycles became 45/4.29 = 10.5-second small-scale cycle times).[a]

Asymmetries exist in the fabricated prototypic systems. These asymmetries along with the unknown asymmetries of the full-scale system prevent the creation of exact scaled replicas. Symmetry and geometric similarity were obtained to the degree achievable with practical, industrial fabrication tolerances.

The PJMs were fitted with capacitance-type level probes to monitor individual PJM liquid levels as a function of time. Additional instrumentation for the LS testing included camera wells at selected locations (specified in the test procedures) that allowed insertion of a miniature, traversable video camera for real-time visualization/detection of simulant mobilization ("cavern") elevations.

(a) WTP-RPT-128, Performance Data for Hybrid Mixing Systems in Scaled Prototypic Ultrafiltration Feed Process (UFP) and HLW Lag Storage (LS) Vessels with Non-Newtonian Slurries, Appendix A, "Technical Basis for Scaled Testing of WTP Mixing Vessels with Non-Newtonian Slurries."

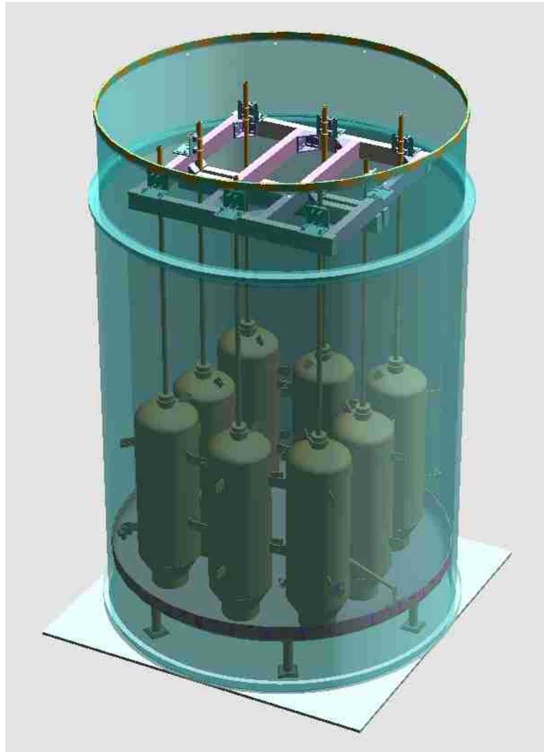

**Figure 3.1**. Lag Storage Vessel – Scaled Prototype Typical Assembly

## 3.3 Test Measurements

The primary measurement in the scaled prototypic test platforms is the size/extent of the mobilization cavern resulting from PJM operations. In the prototype transparent acrylic vessels, this was primarily accomplished by direct visual observations. Identification of the limits of the mobilized zone was enhanced by introduction of tracer dyes that better discriminated the bounds between mixed and unmixed zones of simulant. Movement of tank contents was documented on video when possible.

A secondary measurement technique was evaluated wherein electromagnetic and/or acoustic Doppler velocity sensors will be deployed on a local basis to detect local fluid velocity(s) indicative of the mobilization cavern. The velocity probes were evaluated in the APEL small-scale test tank with the same simulants as the prototype tanks in an attempt to capture the transient for the growth of the cavern. The results did not warrant deployment in the prototype tanks. Reportable measurements of distance were be made using standard commercially available equipment (e.g., tape measure, scale) accurate to within ±0.5 in. and requiring no formal calibration.

### 3.3.1 Mobilization Measurement

Visual observations using tape measures were highly effective in determining mobilized zones in the optically transparent Laponite simulants. Using both trapped air bubbles of sufficiently small size as to be fixed in place by the finite yield strengths of the simulant as well as various plastic, neutrally buoyant tracer particles in sparse populations made for effective visualization of simulant mobilization. Video tapes were used to capture tank mobilization behavior, although not all mobilization behavior was well captured; much of the observation of mobilization was made by a team of observers stationed around the test tanks during test operations, making periodic measurements and observations to test records of the observed degree/location of mobilization over the duration of the entire test. Additional observations were obtained of the tests in the scaled LS vessel by placing an optically transparent well in locations near tank center—where the optical path lengths made direct observation from the tank wall difficult even in the highly transparent Laponite-based simulants. By lowering a miniature video camera into the observation well, an observer could have a more direct view the degree of local simulant mobilization.

The kaolin/bentonite slurry simulants were totally opaque. Direct observations of simulant mobilization were possible only at the tank wall/simulant interface—and even here, very thin immobile layers could be misinterpreted as immobile bulk material. Alternative techniques were developed to allow determination of the degree of tank mobilization/mixing for testing with opaque simulants. These included quantitative dye injection/dilution determination via extracted sample analyses,[a] neutrally buoyant bead addition at the simulant surface and subsequent number counts from extracted core samples of the tank contents, and introduction and monitoring of radio frequency (RF) tagged particles and monitoring of number counts and frequencies at discreet locations around the periphery of the tank.

### 3.3.2 Pulse Tube Liquid Level Measurement

The change in liquid height in each pulse tube was measured using an ~4-ft.- (1.22-m-) long Teflon-coated capacitance liquid level sensors (fabricated by DrexelBrook Inc.) (see Appendix C). These sensors were statically calibrated in each test fluid used in completing the Phase 1 prototype testing efforts. Thus the calibration of the level probes was checked by users for indicated level output from 0 to 100% of span for water, Laponite, and kaolin/bentonite slurry simulants.

### 3.3.3 Nozzle Velocity Measurement

Nozzle velocities were not measured directly but calculated based on rate of change of fluid level in the PJM vessel and area ratios between the PJM vessel and nozzles. Average nozzle velocities were determined by the total volume divided by the total discharge time calculation.

### 3.3.4 Pressure Measurements

Pressure measurements were made with absolute pressure transducers (see Appendix C) installed in the PJM control manifold, with a separate transducer measuring pressure to each PJM supply line.

## 3.4 PJM Operation

PJM operations at full scale are controlled by an AEA-designed manifold using jet pump pairs for alternate pressurization, and vacuum refill operations are controlled with a PressCon® controller of AEA proprietary design. The functions of the PressCon controller that control discharge, refill, and inter-pulse

(a) WTP-RPT-121, 2004, *Chemical Tracer Techniques for Assessing Mixing Performance in Non-Newtonian Slurries for WTP Pulse Jet Mixer Systems*.

timing cycles were modeled using a control scheme developed with the commercial DACS software and hardware to control an array of solenoid operated valves connected to regulated pressure, vacuum, and vent sources.

## 3.5 Data Acquisition and Control System

The PJM Prototype Test Data Acquisition & Control System (DACS) software was a commercially available off-the-shelf product used without modification. General functionality using standard features of the commercial software was developed for BNI by PNWD. The following is a basic description of the PJM prototype test DACS to be used for LS and UFP scaled vessel testing conducted at PNWD.

The DACS software supported the PJM prototype tests performed in the APEL high-bay using the prototype-scale UFP and LS tanks and associated prototype PJMs. The software support included test logic, control, data acquisition, and data display, including data analysis, reporting, and archival storage. The PJM prototype test series employed PJMs in both a nominal design configuration and a series of optimization configurations. Test parameter studies included variations in:

- drive velocities (by variation of drive pressure)
- PJM nozzle diameters and geometries
- tank fill height (aspect ratio; H/D)
- simulant rheology using transparent Laponite and opaque kaolin-bentonite slurries.

The PJM prototype test DACS software requirements detailed here describe the operational requirements of the test equipment and the method of compliance with the applicable Waste Treatment Plant Support Project (WTPSP) Quality Assurance implementing procedures.

### 3.5.1 DACS Perspective

Figure 3.2 is a plan view of the PJM prototype test layout in the APEL facility. Figure 3.3 shows a schematic of the PJM prototype test DACS, showing the major components and interfaces.

#### 3.5.1.1 Analog Data Input Modules

Analog data input modules accommodate the following instrumentation signals from the PJMs and test equipment:

- One level probe and pressure transducer for each PJM, 0 to 20 mA output; for 12 PJMs, 24 inputs needed.
- Three Type K thermocouples, indicating tank fluid temperatures and ambient air temperature.
- Spare signals for additional transducers added during the course of testing, 0-20 mA and ±5 V.

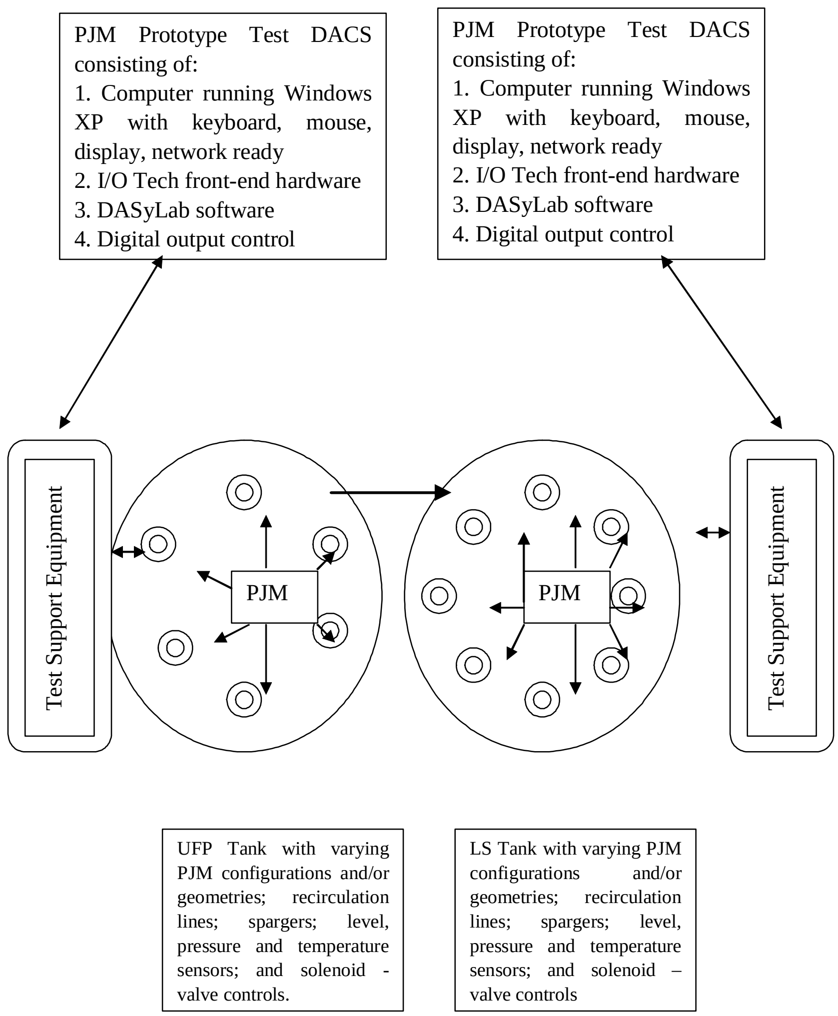


**Figure 3.2**. PJM Prototype Test DACS Overview

#### 3.5.1.2 DACS Desktop PC

The central control console with monitors, keyboard, and mouse provides the operator-DACS interface for the PJM system and data collection, and include the following minimum equipment:

- Multiple power supplies to supply 5 V DC power to the input and output modules as needed.
- A PC interface controller card that receives data from the input modules via the primary elements, transmits digital output signals to the output modules/solid-state relays (SSR), and provides data processing and display functions.

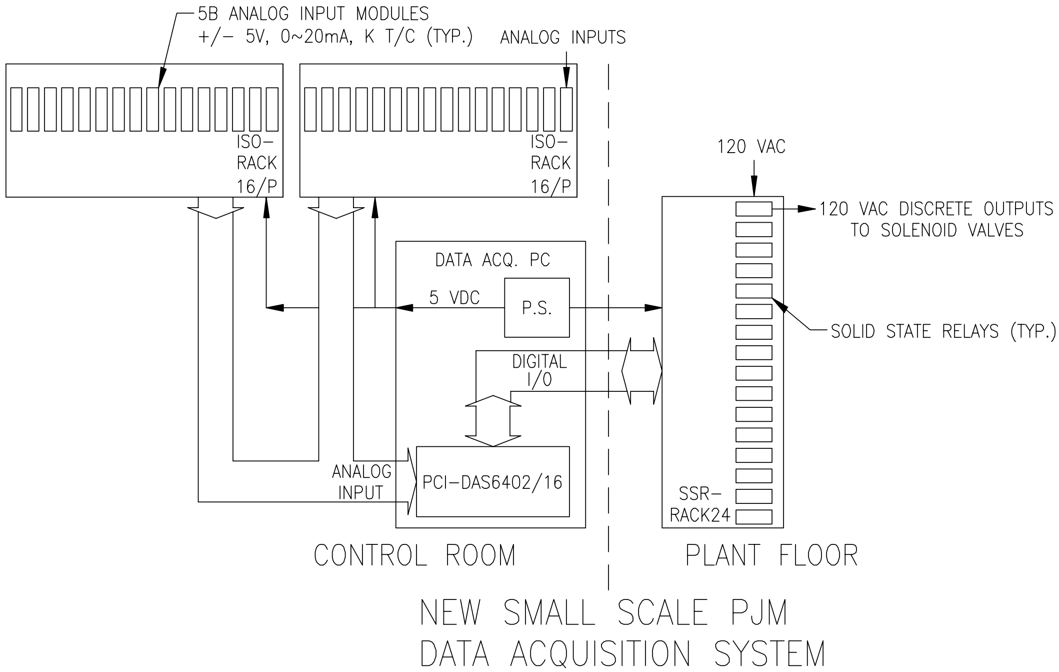


**Figure 3.3**. Schematic of PJM Prototype Test DACS

#### 3.5.1.3 Digital Output Modules

These modules control the solenoid valves that apply pressure and vacuum to the PJMs. Each PJM air supply line must be equipped with three solenoid valves to control pressure, vent, and vacuum; for the maximum 12-PJM configuration, 36 relays were required, plus spares.

#### 3.5.1.4 Product Functions

Each tank was filled with a non-Newtonian fluid for characterizing the mixing capabilities of various PJM configurations and drive parameters. The variables to be set and controlled by the DACS include timing of pressure, vacuum, and vent (controlling drive velocity and length of stroke).

The nozzle velocity of the PJM is calculated by the DACS using PJM pulse-tube level measurements and the cross-sectional area ratio of the pulse tubes and nozzles. The DACS is capable of independently controlling the drive/refill cycle of multiple arrays of PJMs. Data recorded by the DACS included pressure (±) in each PJM head space, continuous liquid level in each PJM, recirculation line flow rate and pressure, and liquid/ambient air temperatures.. The DACS data are

- recorded to a hard drive of sufficient size to hold continuous data for each test series
- downloadable onto electronic media in ASCI, tab delimited format for each test run
- displayed with all required parameters in support of operations and data collection
- received from the PJM test stand and collected, reduced to engineering units, analyzed, and results presented.

Five-volt DC power is supplied to the input and output modules.

### 3.5.2 Overview of Data Flow

Figure 3.4 shows an overview of the data flow, including the test control functions, DACS data analysis, manual data analysis, and data from sample analysis functions. Figure 3.5 shows the data flow between the DACS, test tanks, and the test engineer and includes manually recorded data as well as DACS data.

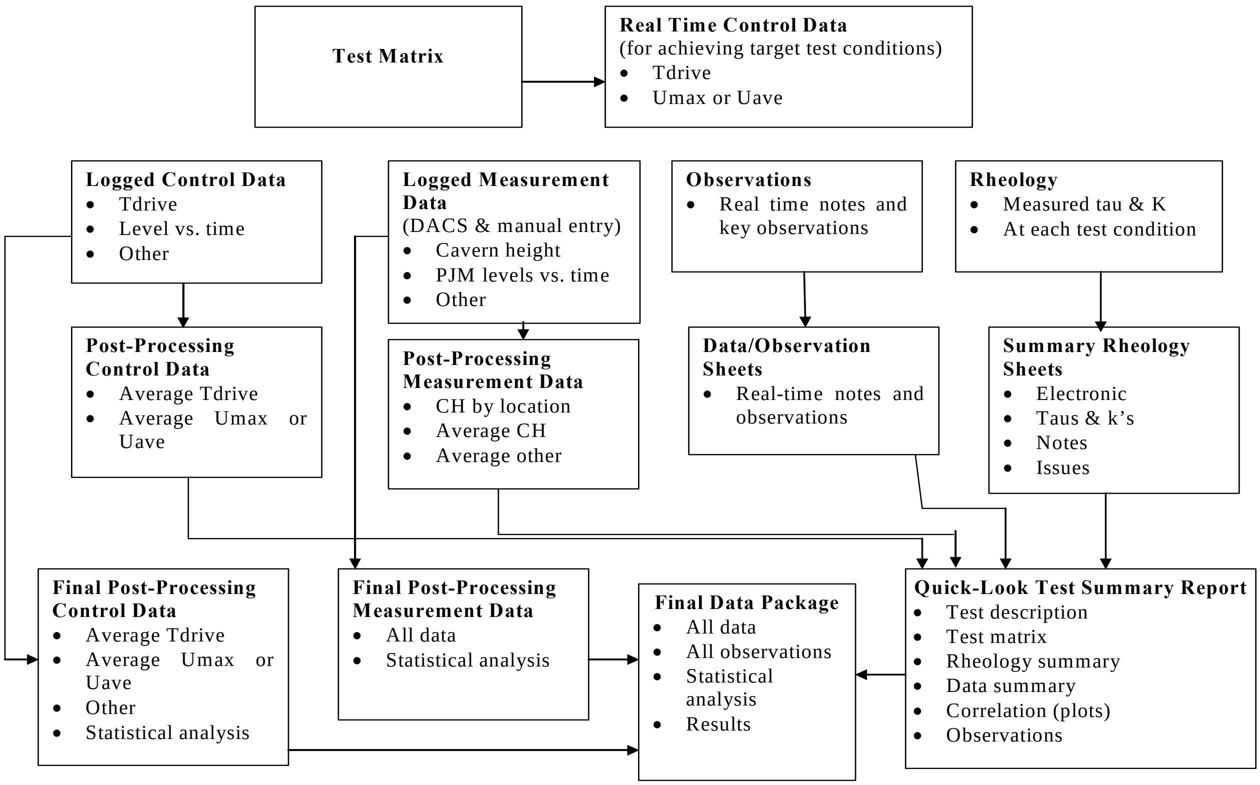


**Figure 3.4.** Overview of the Data Flow

### 3.5.3 Test Control

The DACS stored the test parameter inputs, used these parameters to control the PJM cycle, initiated the PJM operations from a "start" input from the test operator, repeated the PJM cycle for as long as required, and stopped the PJM cycle when a "stop" input is received from the test operator.

### 3.5.4 Calibration Requirements

The transducers that provide input signals to the DACS are under calibration control per the appropriate project Quality Assurance implementing procedures and are not considered part of the requirements for the DACS.

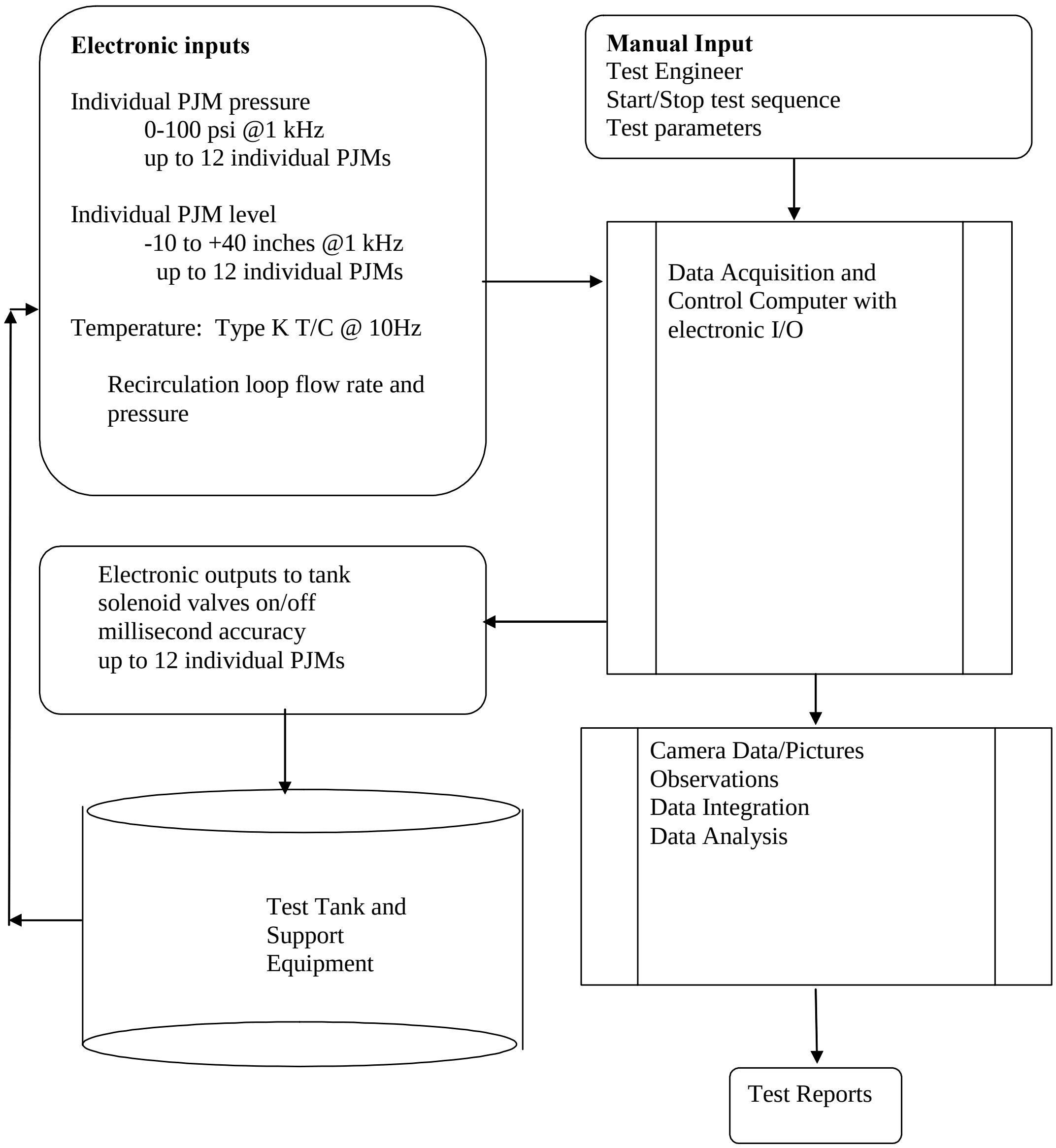


**Figure 3.5**. Data Flow Between the DACS, Test Tanks, and Test Engineer

Processing the input data signals by the DACS and any data signals generated by the DACS satisfies the WTP Quality Assurance requirements for software control for procured systems. The DACS system includes documentation necessary to demonstrate compliance with QA procedures (QA-ORP-WTP 1201, Calibration Control System, and QA-ORP-WTP 1601, Software Control).

### 3.5.5 Manually Recorded Data

Some data are recorded by visual observation on data sheets and are input to another computer system for analysis. These data and the analytical systems are not considered to be part of the Prototype DACS and thus their requirements are not included in this discussion. They are included in Figure 3.5 to show their relationship to the DACS data, which consist of measurements defining the cavern size and shape, recorded from manual observations, and the data defining the corresponding operation of the PJMs, recorded by the DACS.(a)

### 3.5.6 Test Parameters for Each PJM

- Open and close times for the pressure solenoid valve, total drive time, $t_{drive}$, relative to the open pressure solenoid valve time.
- Open and close times for the vent solenoid valve, total vent time, $t_{vent}$.
- Open and close times for the vacuum solenoid valve, total refill time, $t_{refill}$, relative to the open pressure solenoid valve time.
- Total cycle time, $t_{cycle} = t_{drive} + t_{vent} + t_{fill}$ + any wait time (wait time is typically zero).
- Maximum velocity, $U_{max}$ (calculated from change in level, and elapsed time).
- Maximum PJM fluid level, $L_{max}$
- Minimum PJM fluid level, $L_{min}$. Figure 3.6 is a visual representation of these parameters.

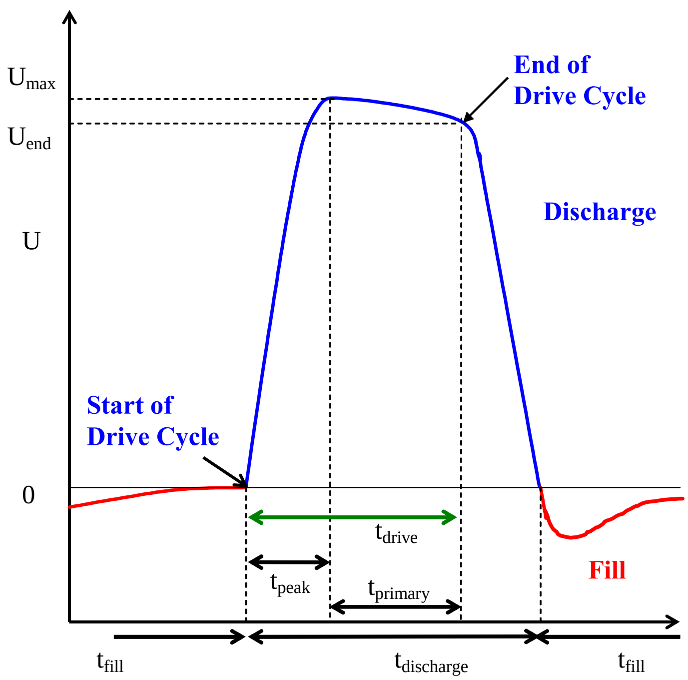


**Figure 3.6**. Velocity Profile

(a) Enderlin CW and JM Bates. 2003. "Test Plan for Determining Scalability of PJM Performance in Non-Newtonian Fluids." TP-RPP-WTP-290, Rev. 0, PNWD, Richland, WA.

# 4.0 Results

The primary focus of the mobilization tests was to determine the relative amount of mobilization with different hardware configurations and PJM operating parameters. In this section, a brief discussion of the results in terms of the flow field symmetry is presented.

All of the individual tests conducted in the course of the Phase 1 LS and UFP vessel testing are summarized in Tables 4.1 and 4.2 for LS and 4.3 and 4.4 for the UFP vessel. Summary final observations for the testing performed on the LS vessel are presented in Table 4.1 and comprehensive test descriptions in Table 4.2. Testing performed on the UFP vessel is likewise presented in Tables 4.3 and 4.4. Explanations for the column headings in Tables 4.2 and 4.4 are listed in Appendix D.

**Table 4.1.** LS Prototype Tests with Favorable Mobilization/Mixing Observations—Summary of Results[a,b]

| Test Date | PJM Configuration | Nozzle Diameter (in.) | Target Nozzle Vel. (m/s) | Actual Nozzle Vel. Peak Average (m/s) | Actual Nozzle Vel. Pulse Average (m/s)[c] | PJM ΔH (cm) | Actual Drive Time (s) | Cycle Time (s) | Mixing Pattern Observed[d] | Yield, Actual (Pa) | Actual H/D |
|---|---|---|---|---|---|---|---|---|---|---|---|
| 10/7/2003 | Baseline 8 | 0.93 | 8 | na | na | 90 | 18 | 79.2 | Type 3 | 80 | 1.06 |
| 10/24/2003 | Baseline 8 | 2.065 | 8 | 8.1 | 7.1 | 80 | 3.2 | 79.2 | Type 3 | 67 | 1.06 |
| 10/24/2003 | Baseline 8 | 2.065 | 12 | 10.8 | 9.0 | 80 | 3 | 79.2 | Type 3+++ | 67 | 1.06 |
| 10/24/2003 | Baseline 8+4 with RH | 2.065 | 8 | 7.1 | 6.3 | 80 | 3.2 | 79.2 | Type 3- | 67 | 1.06 |
| 10/25/2003 | Baseline 8 | 2.065 | 8 | 7.3 | 6.6 | 80 | 3.8 | 21 | Type 3++ | 77 | 1.05 |
| 10/25/2003 | Baseline 8 | 2.065 | 12 | 10.4 | 9.0 | 80 | 2.8 | 18.7 | Type 3+ | 77 | 1.05 |
| 10/25/2003 | Baseline 8+4 with RH | 2.065 | 8 | 7.3 | 6.2 | 80 | 4 | 35 | Type 4- | 77 | 1.05 |
| 10/25/2003 | Baseline 8+4 with RH | 2.065 | 10.5 | 9.3 | 7.5 | 80 | 3.3 | 35 | Type 4- | 77 | 1.05 |
| 11/3/2003 | Baseline 8 4/4 asynchronous | 2.065 | 8 | 8.7 | 6.6 | 80 | 3.2 | 35 | Type 3 - | 102 | 1.06 |
| 11/3/2003 | Baseline 8 4/4 asynchronous | 2.065 | 12 | 12.5 | 9.2 | 80 | 2.1 | 25 | Type 3+++ | 102 | 1.05 |
| 11/3/2003 | Baseline 8+4 with RH asynchronous | 2.065 | 8 | 8.9 | 6.8 | 80 | 3.2 | 35 | Type 3++ | 102 | 1.05 |
| 11/3/2003 | Baseline 8+4 with RH asynchronous | 2.065 | 12 | 11.5 | 8.4 | 80 | 2.1 | 35 | Type 4- | 102 | 1.05 |
| 11/4/2003 | Baseline 8 4/4 asynchronous odd no. w/ext | 2.065 | 8 | 8.7 | 6.6 | 80 | 3.2 | 25 | Type 3 -- | 88 | 1.05 |
| 11/4/2003 | Baseline 8 4/4 synchronous odd no. w/ext | 2.065 | 8 | 7.9 | 6.3 | 80 | 3.2 | 25 | Type 3 - | 88 | 1.05 |
| 11/5/2003 | Baseline 8 4/4 synchronous odd numbers w/normal nozzles + RH | 2.065 | 8 | 7.9 | 6.0 | 80 | 3.2 | 25 | Type 4 | 86 | 1.04 |
| 11/5/2003 | Baseline 8 4/4 synchronous odd no. w/normal nozzles + RH | 2.065 | 12 | | Not initiated due to Type 4 w/8 m/s | | | | | | |
| 11/10/2003 | Baseline 8 odd no. w/normal nozzles asynchronous w/RH first | 2.065 | 8 | 8.4 | 7.0 | 80 | 3.2 | 25 | Type 3 - | 73 | 1.04 |
| 11/10/2003 | Baseline 8 odd no. w/normal nozzles asynchronous w/RH first | 2.065 | 12 | 10.5 | 8.5 | 80 | 2.3 | 25 | Type 3 | 73 | 1.04 |
| 11/10/2003 | Baseline 8 odd no. w/normal nozzles asynchronous 4/4 w/RH first | 2.065 | 12 | 11.7 | 9.1 | 80 | 2.3 | 25 | Type 3 | 73 | 1.04 |
| 11/11/2003 | Baseline 8 odd no. w/normal nozzles asynchronous 4/4 w/RH first | 2.065 | 12 | 11.3 | 8.8 | 80 | 2.3 | 25 | Type 3 | 85 | 1.02 |
| 11/13/2003 | Baseline 8 | 0.93 | 12 | 14.8 | | 80 | 8 | 45 | Type 3 -- | 75 | 1.03 |
| 11/13/2003 | Baseline 8 4/4 asynchronous | 0.93 | 12 | 13.9 | | 80 | 8 | 45 | Type 3 -- | 75 | 1.03 |
| 11/13/2003 | Baseline 8 | 0.93 | 12 | 14.6 | | 80 | | 45 | Type 3+++ | 29-40 | 1.07 |
| 11/14/2003 | Baseline 8 | 0.93 | 12 | 13.5 | | 80 | 8 | 45 | Type 3++ | 32 | 1.02 |
| 11/22/2004 | 8 PJM Chandelier | 2.065 | 8 | 8.1 | | 80 | 3 | 30 | Type 1 | 65 | 1.07 |
| 11/22/2004 | 8 PJM Chandelier | 2.065 | 11 | 10.6 | | 80 | 2.1 | 30 | Type 1 | 65 | 1.07 |
| 12/13/2004 | All-in test–baseline 8 w/normal nozzles | 2.065 | 8 | 8.7 | | 80 | 3.2 | 25 | see dye results | 26/28 | 1.07 |

(a) Laponite was the simulant in all the tests except 12/13/2004, when kaolin-bentonite was used.

(b) Cavern height was 'breakthrough,' meaning mobilization was observed at the free surface of the simulant, in all tests except 10/7/2003 (na) and chandelier tests, where cavern heights were ~42 and ~ 48 inches, respectively.

(c) Peak average is average velocity over time period $t_{primary}$ as shown in Figure 3.6. See Appendix A for more thorough descriptions.

(d) + and - suffix to mixing observation is intended as relative indication of degree of recirculation observed in Type 2 and 3 mixing patterns. A type 4- designation indicates there were appreciable unmobilized areas in the test vessel.

**Table 4.2**. Summary Results: LS Tests (shaded rows depict “final” tests exhibiting Type 3 or better mobilization states)

| Test date | Test type | PJM config | Nozzle dia (in.) | Nozzle velocity (m/s) | PJM ΔH (cm) | Nom. drive time (sec) | Actual drive time (sec) | Cycle time (sec) | DACS files | Mixing pattern observed | Cavern height if appropriate (in.) | Simulant | Yield, nominal (Pa) | Yield, actual (Pa) | Target h/d fill | Actual h/d | Recirc. y/n | Ops notes | Scoping (S) or final (F) |
|---|---|---|---|---|---|---|---|---|---|---|---|---|---|---|---|---|---|---|---|
| 10/6/2003 | LS | Baseline 8 | 0.93 | 8 | 90 | 19.8 | 18 | 59.4 | LS031006R1a.ASC<br>LS031006R1b.ASC<br>LS031006R1c.ASC | Type 1 * | Breakthrough only after camera insertion for cavern observation | Laponite | 70 | 74 | 1.067 | 1.07 | N | | S |
| 10/6/2003 | LS | Baseline 8 | 0.93 | 12 | 90 | 13.2 | 13.2 | 75 | p031006R2a.ASC<br>p031006R2b.ASC<br>p031006R2c.ASC | Type 2 | Breakthrough possibly due to camera well insertion disturbance | Laponite | 70 | 78 | 1.067 | 1.07 | N | | S |
| 10/8/2003 | LS | Baseline 8 | 0.93 | 8 | 80 | 19.8 | 16 | 79.2 | LS031008R1a.ASC<br>LS031008R1b.ASC<br>LS031008R1c.ASC | Type 2 ++ | 59 +1 | Laponite | 70 | 80 | 1.067 | 1.06 | N | | S |
| 10/18/2003 | LS | Baseline 8+4 w/RH | 0.93 | 8 | 80 | 19.8 | 16 | 69.2 | LS031018R1a.ASC<br>LS031018R1b.ASC<br>LS031018R1c.ASC | Type 2 ++ | Breakthrough | Laponite | 70 | 92 | 1.067 | 1.03 | N | | S |
| 10/18/2003 | LS | Baseline 8+4 w/RH | 0.93 | 12 | 80 | 13.2 | 9 | 62.2 | LS031018R2a.ASC<br>LS031018R2b.ASC<br>LS031018R2c.ASC | Type 2 ++++ | Breakthrough | Laponite | 70 | 92 | 1.067 | 1.03 | N | | S |
| 10/20/2003 | LS | Baseline 8+4 w/RH | 0.93 | 12 | 40 | 13.2/2 | 4 | 26.5 | LS031020R1a.ASC<br>LS031020R1b.ASC<br>LS031020R1c.ASC | Unmixed annular areas near bottom | Breakthrough | Laponite | 70 | 90 | 1.067 | 1.03 | N | | S |
| 10/24/2003 | LS | Baseline 8 | 2.065 | 4 | 80 | 8.0 | 6.4 | 79.2 | LS031024R1a.ASC<br>LS031024R1b.ASC<br>LS031024R1c.ASC | Type 1 | 43.75 | Laponite | 70 | 67 | 1.067 | 1.06 | N | | S |
| 10/29/2003 | LS | Baseline 8+4 w/RH | 2.065 | 12 | 80 | 2.7 | 2.3 | 35 | LS031029R1a.ASC<br>LS031029R1b.ASC<br>LS031029R1c.ASC | Trial scoping test only | Breakthrough | Laponite | 70 | 81 | 1.067 | 1.06 | N | | S |
| 10/30/2003 | LS | Baseline 8+4 w/RH | 2.065 | 12 | 80 | 2.7 | 2.3 | 35 | LS031030R1a.ASC<br>LS031030R1b.ASC<br>LS031030R1c.ASC | Trial scoping test only | | | | | | | | | S |
| 11/4/2003 | LS | Baseline 8 4/4 synchronous odd no. w/ext | 2.065 | 12 | 80 | 2.7 | 2.1 | 25 | LS031104R3a.ASC<br>LS031104R3b.ASC<br>LS031104R3c.ASC | Incomplete test due to overblow | Breakthrough | Laponite | 70 | 88 | 1.067 | 1.05 | N | | S |
| 11/4/2003 | LS | Baseline 8 4/4 asynchronous odd no. w/ext | 2.065 | 12 m/s | 80 | 2.7 | | | | Not initiated due to overblow | | | | | | | | | S |
| 11/5/2003 | LS | Baseline 8 4/4 asynchronous odd no. w/normal nozzles | 2.065 | 8 m/s | 80 | 4.0 | 3.2 | 25 | LS031105R1a.ASC<br>LS031105R1b.ASC<br>LS031105R1c.ASC | Type 1+ | 68-71 in. cavern height | Laponite | 70 | 86 | 1.067 | 1.04 | N | asynchronous ops | S |
| 11/5/2003 | LS | Baseline 8 4/4 asynchronous odd no. w/normal nozzles | 2.065 | 12 m/s | 80 | 2.7 | 2.1 | 25 | LS031105R2a.ASC<br>LS031105R2b.ASC<br>LS031105R2c.ASC | Type 2 + | Breakthrough | Laponite | 70 | 86 | 1.067 | 1.04 | N | asynchronous ops | S |
| 11/5/2003 | LS | Baseline 8 4/4 synchronous odd no. w/normal nozzles | 2.065 | 8 m/s | 80 | 4.0 | 3.2 | 25 | LS031105R3a.ASC<br>LS031105R3b.ASC<br>LS031105R3c.ASC | Type 2 + | Breakthrough | Laponite | 70 | 86 | 1.067 | 1.04 | N | | S |
| 11/5/2003 | LS | Baseline 8 4/4 synchronous odd no. w/ normal nozzles | 2.065 | 12 m/s | 80 | 2.7 | 2.1 | 25 | LS031105R4a.ASC<br>LS031105R4b.ASC<br>LS031105R4c.ASC | Type 2 + | Breakthrough | Laponite | 70 | 86 | 1.067 | 1.04 | N | | S |
| 11/5/2003 | LS | Baseline 8 4/4 synchronous odd no. w/normal nozzles/RH | 2.065 | 12 m/s | | | | | | Not initiated due to type 4 w/ 8 m/s | | | | | | | | | S |

**Table 4.2**. Summary Results: LS Tests (shaded rows depict “final” tests exhibiting Type 3 or better mobilization states)

| Test date | Test type | PJM config | Nozzle dia (in.) | Nozzle velocity (m/s) | PJM ΔH (cm) | Nom. drive time (sec) | Actual drive time (sec) | Cycle time (sec) | DACS files | Mixing pattern observed | Cavern height if appropriate (in.) | Simulant | Yield, nominal (Pa) | Yield, actual (Pa) | Target h/d fill | Actual h/d | Recirc. y/n | Ops notes | Scoping (S) or final (F) |
|---|---|---|---|---|---|---|---|---|---|---|---|---|---|---|---|---|---|---|---|
| 11/13/2003 | LS | Baseline 8 | 0.93 | 8 m/s | 80 | 19.8 | 16 | 60 | LS031113R1a.ASC<br>LS031113R1b.ASC<br>LS031113R1c.ASC | Type 1 | 35 inch cavern height | Laponite | 70 | 62 | 1.067 | 1.03 | N | synchronous ops | S |
| 11/14/2003 | LS | Baseline 8 | 0.93 | 8 m/s | 80 | 19.8 | 16 | 60 | LS031114R1a.ASC<br>LS031114R1b.ASC<br>LS031114R1c.ASC | Type 1 | 44 inch cavern height | Laponite | 30 | 32 | 1.067 | 1.02 | N | synchronous ops | S |
| 11/19/2003 | LS | Baseline 6+2 w/3 leg RH | 2.065 | 8 m/s | 80 | 4.0 | 3 | 30 | LS031119R1a.ASC<br>LS031119R1b.ASC<br>LS031119R1c.ASC | Type 1 | 48 in. cavern height | Laponite | 70 | 71 | 1.067 | 1.08 | N | synchronous ops | S |
| 11/19/2003 | LS | Baseline 6+2 w/3 leg RH asynchronous | 2.065 | 8 m/s | 80 | 4.0 | 3 | 30 | LS031119R2a.ASC<br>LS031119R2b.ASC<br>LS031119R2c.ASC | Type 1 | 48 in. cavern height | Laponite | 70 | 71 | 1.067 | 1.08 | N | asynchronous ops | S |
| 11/19/2003 | LS | Baseline 6+2 w/3 leg RH synchronous | 2.065 | 12 m/s | 80 | 2.7 | 1.5 | 30 | LS031119R3a.ASC<br>LS031119R3b.ASC<br>LS031119R3c.ASC | Type 1 | 54 in. cavern height | Laponite | 70 | 71 | 1.067 | 1.08 | N | synchronous ops | S |
| 12/4/2003 | LS | Baseline 8 4/4 synchronous odd no. w/normal nozzles/RH | 2.065 | 8 m/s | 80 | 4.0 | 3.2 | 25 | LS031204R2a.ASC<br>LS031204R2b.ASC<br>LS031204R2c.ASC | Determine by RF tags/beads | Breakthrough | Kaolin-Bentonite slurry | 30/30 yld/ consist | 26/27 yld/ consist | 1.067 | 1.07 | N | synchronous ops | S |
| 12/18/2003 | LS | All-In Test - baseline 8 w/normal nozzles | 2.065 | 8 m/s | 80 | 4.0 | 3.2 | 25 | LS031218R1a.ASC<br>LS031218R1b.ASC<br>LS031218R1c.ASC | Tour demo only | | Kaolin-Bentonite slurry | 30/30 yld/ consist | | 1.067 | 1.07 | N | synchronous ops | S |
| 10/7/2003 | LS | Baseline 8 | 0.93 | 8 m/s | 90 | 19.8 | 18 | 79.2 | LS031007R1a.ASC<br>LS031007R1b.ASC<br>LS031007R1c.ASC | Type 3 | NA | Laponite | 70 | 80 | 1.067 | 1.06 | N | | F |
| 10/8/2003 | LS | Baseline 8 | 0.93 | 12 m/s | 80 | 13.2 | 9 | 77.8 | LS031008R2a.ASC<br>LS031008R2b.ASC<br>LS031008R2c.ASC | Type 3 | Breakthrough | Laponite | 70 | 80 | 1.067 | 1.05 | N | | F |
| 10/24/2003 | LS | Baseline 8 | 2.065 | 8 m/s | 80 | 4.0 | 3.2 | 79.2 | LS031024R2a.ASC<br>LS031024R2b.ASC<br>LS031024R2c.ASC | Type 3 | Breakthrough | Laponite | 70 | 67 | 1.067 | 1.06 | N | | F |
| 10/24/2003 | LS | Baseline 8 | 2.065 | 12 m/s | 80 | 2.7 | 3 | 79.2 | LS031024R3a.ASC<br>LS031024R3b.ASC<br>LS031024R3c.ASC | Type 3+++ | Breakthrough | Laponite | 70 | 67 | 1.067 | 1.06 | N | | F |
| 10/24/2003 | LS | Baseline 8+4 w/RH | 2.065 | 8 m/s | 80 | 4.0 | 3.2 | 79.2 | LS031024R4a.ASC<br>LS031024R4b.ASC<br>LS031024R4c.ASC | Type 3- | Breakthrough | Laponite | 70 | 67 | 1.067 | 1.06 | N | | F |
| 10/25/2003 | LS | Baseline 8 | 2.065 | 8 m/s | 80 | 4.0 | 3.8 | 21 | LS031025R1a.ASC<br>LS031025R1b.ASC<br>LS031025R1c.ASC | Type 3++ | Breakthrough | Laponite | 70 | 77 | 1.067 | 1.05 | N | | F |
| 10/25/2003 | LS | Baseline 8 | 2.065 | 12 m/s | 80 | 2.7 | 2.8 | 18.7 | LS031025R2a.ASC<br>LS031025R2b.ASC<br>LS031025R2c.ASC | Type 3+ | Breakthrough | Laponite | 70 | 77 | 1.067 | 1.05 | N | | F |
| 10/25/2003 | LS | Baseline 8+4 w/RH | 2.065 | 8 m/s | 80 | 4.0 | 4 | 35 | LS031025R3a.ASC<br>LS031025R3b.ASC<br>LS031025R3c.ASC | Type 4- | Breakthrough | Laponite | 70 | 77 | 1.067 | 1.05 | N | | F |
| 10/25/2003 | LS | Baseline 8+4 w/RH | 2.065 | 10.5 | 80 | 2.6 | 3.3 | 35 | LS031025R4a.ASC<br>LS031025R4b.ASC<br>LS031025R4c.ASC | Type 4- | Breakthrough | Laponite | 70 | 77 | 1.067 | 1.05 | N | | F |
| 11/3/2003 | LS | Baseline 8 4/4 asynchronous | 2.065 | 8 m/s | 80 | 4.0 | 3.2 | 35 | LS031103R1a.ASC<br>LS031103R1b.ASC | Type 3 - | Breakthrough | Laponite | 70 | 102 | 1.067 | 1.06 | N | asynchronous ops | F |

**Table 4.2**. Summary Results: LS Tests (shaded rows depict "final" tests exhibiting Type 3 or better mobilization states)

| Test date | Test type | PJM config | Nozzle dia (in.) | Nozzle velocity (m/s) | PJM $\Delta H$ (cm) | Nom. drive time (sec) | Actual drive time (sec) | Cycle time (sec) | DACS files | Mixing pattern observed | Cavern height if appropriate (in.) | Simulant | Yield, nominal (Pa) | Yield, actual (Pa) | Target h/d fill | Actual h/d | Recirc. y/n | Ops notes | Scoping (S) or final (F) |
|---|---|---|---|---|---|---|---|---|---|---|---|---|---|---|---|---|---|---|---|
| | | | | | | | | | LS031103R1c.ASC | | | | | | | | | | |
| 11/3/2003 | LS | Baseline 8 4/4 asynchronous | 2.065 | 12 m/s | 80 | 2.7 | 2.1 | 25 | LS031103R2a.ASC LS031103R2b.ASC LS031103R2c.ASC | Type 3+++ | Breakthrough | Laponite | 70 | 102 | 1.067 | 1.05 | N | asynchronous ops | F |
| 11/3/2003 | LS | Baseline 8+4 w/RH asynchronous | 2.065 | 8 m/s | 80 | 4.0 | 3.2 | 35 | LS031103R3a.ASC LS031103R3b.ASC LS031103R3c.ASC | Type 3++ | Breakthrough | Laponite | 70 | 102 | 1.067 | 1.05 | N | asynchronous ops | F |
| 11/3/2003 | LS | Baseline 8+4 w/RH asynchronous | 2.065 | 12 m/s | 80 | 2.7 | 2.1 | 35 | LS031103R4a.ASC LS031103R4b.ASC LS031103R4c.ASC | Type 4- | Breakthrough | Laponite | 70 | 102 | 1.067 | 1.05 | N | asynchronous ops | F |
| 11/4/2003 | LS | Baseline 8 4/4 asynchronous odd no. w/ext | 2.065 | 8 m/s | 80 | 4.0 | 3.2 | 25 | LS031104R1a.ASC LS031104R1b.ASC LS031104R1c.ASC | Type 3 -- | Breakthrough | Laponite | 70 | 88 | 1.067 | 1.05 | N | asynchronous ops | F |
| 11/4/2003 | LS | Baseline 8 4/4 synchronous odd no. w/ext | 2.065 | 8 m/s | 80 | 4.0 | 3.2 | 25 | LS031104R2a.ASC LS031104R2b.ASC LS031104R2c.ASC | Type 3 - | Breakthrough | Laponite | 70 | 88 | 1.067 | 1.05 | N | | F |
| 11/5/2003 | LS | Baseline 8 4/4 synchronous odd no. w/normal nozzles/RH | 2.065 | 8 m/s | 80 | 4.0 | 3.2 | 25 | LS031105R5a.ASC LS031105R5b.ASC LS031105R5c.ASC | Type 4 | Breakthrough | Laponite | 70 | 86 | 1.067 | 1.04 | N | | F |
| 11/10/2003 | LS | Baseline 8 odd no. w/normal nozzles asynchronous w/RH first | 2.065 | 8 m/s | 80 | 4.0 | 3.2 | 25 | LS031110R1a.ASC LS031110R1b.ASC LS031110R1c.ASC | Type 3 - | Breakthrough | Laponite | 70 | 73 | 1.067 | 1.04 | N | asynchronous ops | F |
| 11/10/2003 | LS | Baseline 8 odd no. w/normal nozzles asynchronous w/RH first | 2.065 | 12 m/s | 80 | 2.7 | 2.3 | 25 | LS031110R2a.ASC LS031110R2b.ASC LS031110R2c.ASC | Type 3 | Breakthrough | Laponite | 70 | 73 | 1.067 | 1.04 | N | asynchronous ops | F |
| 11/10/2003 | LS | Baseline 8 odd no. w/normal nozzles asynchronous 4/4 w/RH first | 2.065 | 12 m/s | 80 | 2.7 | 2.3 | 25 | LS031110R3a.ASC LS031110R3b.ASC LS031110R3c.ASC | Type 3 | Breakthrough | Laponite | 70 | 73 | 1.067 | 1.04 | N | asynchronous ops | F |
| 11/11/2003 | LS | Baseline 8 odd no. w/normal nozzles asynchronous 4/4 w/RH first | 2.065 | 12 m/s | 80 | 2.7 | 2.3 | 25 | LS031111R1a.ASC LS031111R1b.ASC LS031111R1c.ASC | Type 3 | Breakthrough | Laponite | 70 | 85 | 1.067 | 1.02 | N | asynchronous ops | F |
| 11/13/2003 | LS | Baseline 8 | 0.93 | 12 m/s | 80 | 13.2 | 8 | 45 | LS031113R2a.ASC LS031113R2b.ASC LS031113R2c.ASC | Type 3 -- | Breakthrough | Laponite | 70 | 75 | 1.067 | 1.03 | N | synchronous ops | F |
| 11/13/2003 | LS | Baseline 8 4/4 asynchronous | 0.93 | 12 m/s | 80 | 13.2 | 8 | 45 | LS031113R3a.ASC LS031113R3b.ASC LS031113R3c.ASC | Type 3 -- | Breakthrough | Laponite | 70 | 75 | 1.067 | 1.03 | N | asynchronous ops | F |
| 11/13/2003 | LS | Baseline 8 | 0.93 | 12 m/s | 80 | 13.2 | | 45 | LS031113R4a.ASC LS031113R4b.ASC LS031113R4c.ASC | Type 3+++ | Breakthrough | Laponite | 30 | 29-40 | 1.067 | 1.07 | N | synchronous ops | F |
| 11/14/2003 | LS | Baseline 8 | 0.93 | 12 m/s | 80 | 13.2 | 8 | 45 | LS031114R2a.ASC LS031114R2b.ASC LS031114R2c.ASC | Type 3++ | Breakthrough | Laponite | 30 | 32 | 1.067 | 1.02 | N | synchronous ops | F |
| 11/22/2003 | LS | 8 PJM Chandelier | 2.065 | 8 m/s | 80 | | 3 | 30 | LS031122R1a.ASC LS031122R1b.ASC | Type 1 | ~42 high turb | Laponite | 70 | 65 | 1.067 | 1.07 | N | synchronous ops | F |

**Table 4.2**. Summary Results: LS Tests (shaded rows depict "final" tests exhibiting Type 3 or better mobilization states)

| Test date | Test type | PJM config | Nozzle dia (in.) | Nozzle velocity (m/s) | PJM ΔH (cm) | Nom. drive time (sec) | Actual drive time (sec) | Cycle time (sec) | DACS files | Mixing pattern observed | Cavern height if appropriate (in.) | Simulant | Yield, nominal (Pa) | Yield, actual (Pa) | Target h/d fill | Actual h/d | Recirc. y/n | Ops notes | Scoping (S) or final (F) |
|---|---|---|---|---|---|---|---|---|---|---|---|---|---|---|---|---|---|---|---|
| | | | | | | | | | LS031122R1c.ASC | | | | | | | | | | |
| 11/22/2003 | LS | 8 PJM Chandelier | 2.065 | 11 m/s | 80 | | 2.1 | 30 | LS031122R2a.ASC LS031122R2b.ASC LS031122R2c.ASC | Type 1 | ~48 high turb | Laponite | 70 | 65 | 1.067 | 1.07 | N | synchronous ops | F |
| 11/30/2003 | LS | Baseline 8 4/4 synchronous odd no. w/normal nozzles/RH | 2.065 | 8 m/s | 80 | 4.0 | 3.2 | 25 | LS031130R1a.ASC LS031130R1b.ASC LS031130R1c.ASC | Type 4- | Breakthrough | Laponite | 70 | 76 | 1.067 | 1.07 | N | synchronous ops | F |
| 12/4/2003 | LS | Baseline 8 4/4 synchronous odd no. w/normal nozzles/RH | 2.065 | 8 m/s | 80 | 4.0 | 3.2 | 25 | LS031204R1a.ASC LS031204R1b.ASC LS031204R1c.ASC | TBD by dye - results ~96% mixed | Breakthrough | Kaolin-Bentonite slurry | 30/30 yld/ consist | 26/27 yld/ consist | 1.067 | 1.07 | N | synchronous ops | F |
| 12/10/2003 | LS | Baseline 8 4/4 synchronous odd no. w/normal nozzles/RH | 2.065 | 6m/s | 80 | 5.4 | 4.8 | 25 | LS031210R1a.ASC LS031210R1b.ASC LS031210R1c.ASC | Type 3 | | Kaolin-Bentonite slurry | 30/30 yld consist | | 1.067 | 1.07 | N | synchronous ops | F |
| 12/10/2003 | LS | Baseline 8 4/4 synchronous odd no. w/normal nozzles/RH | 2.065 | 8 m/s | 80 | 4.0 | 3.5 | 25 | LS031210R2a.ASC LS031210R2b.ASC LS031210R2c.ASC | Type 3 | | Kaolin-Bentonite slurry | 30/30 yld/ consist | | 1.067 | 1.06 | N | synchronous ops | F |
| 12/10/2003 | LS | Baseline 8 4/4 synchronous odd no. w/normal nozzles/RH | 2.065 | 12 m/s | 80 | 1.9 | 2.1 | 25 | LS031210R3a.ASC LS031210R3b.ASC LS031210R3c.ASC | Type 3 | | Kaolin-Bentonite slurry | 30/30 yld/ consist | | 1.067 | 1.06 | N | synchronous ops | F |
| 12/13/2003 | LS | All-In Test - baseline 8 w/normal nozzles | 2.065 | 8 m/s | 80 | 4.0 | 3.2 | 25 | LS031213R1a.ASC LS031213R1b.ASC LS031213R1c.ASC | Determine by dye tracer | | Kaolin-Bentonite slurry | 30/30 yld/ consist | 26/28 yld/ consist | 1.067 | 1.07 | N | synchronous ops | F |

**Table 4.3**. UFP Prototype Tests with Favorable Mobilization/Mixing Observations—Summary of Results[(a)]

| Test date | PJM config | Nozzle diameter (in.) | Target avg. nozzle vel. (m/s) | Actual nozzle vel. peak avg (m/s)[(b)] | Actual avg vel. (m/s) | PJM $\Delta$H (cm) | Actual drive time (s) | Cycle time (s) | Mixing pattern observed[(c)] | Cavern height | Actual yield (Pa) | Actual H/D | Recirc Y/N | Recirc flow (gpm) or synchr/asychr. |
|---|---|---|---|---|---|---|---|---|---|---|---|---|---|---|
| 10/1/2003 | Baseline 6+recirc | 0.81 | 12 | 11 | 8.0 | 90 | 4.2 | 27.7 | Type 4 | NA | 84 | 1.86 | Y | 90, 2 ea. 45° nozzles |
| 10/3/2003 | Baseline 6+recirc | 0.81 | 12 | 10.4 | 8.3 | 90 | 4.2 | 27.7 | Type 4 | NA | 48 | 1.86 | Y | |
| 10/3/2003 | Baseline 6+recirc | 0.81 | 12 | na | na | 90 | 4.2 | 27.7 | Type 4 | NA | 33 | 1.86 | Y | |
| 10/10/2003 | Baseline 6+3 w/RH | 0.81 | 12 | 13 | 9.1 | 80 | 3 | 27.7 | Type 4 | Breakthrough | 36 @ start<br>40 @ finish | 1.82 | N | |
| 10/11/2003 | Baseline 6+3 w/RH | 0.81 | 12 | 13.5 | 8.9 | 80 | 3 | 27.7 | Type 4 | Breakthrough | 72-75 | 1.86 | N | |
| 11/10/2003 | Baseline 6+3 w/5" ext RH-asynchronous | 0.81 | 12 | 12.1 | 9.1 | 80 | 3.5 | 30 | Type 4- | Breakthrough | 70 | 1.77 | N | asynchronous ops |
| 11/10/2003 | Baseline 3 on/3 off + 3 enh. w/5" ext. RH asynchronous | 0.81 | 12 | 12 | 8.6 | 80 | 3.5 | 30 | Type 4 | Breakthrough | 70 | 1.77 | N | asynchronous ops |
| 11/17/2003 | Baseline 4+2 w/RH synchronous | 1.21 | 8 | 7.7 | 5.6 | 80 | 2.5 | 20 | Type 4- | Breakthrough | 81 | 1.82 | N | synchronous ops |
| 11/17/2003 | Baseline 4+2 w/RH asynchronous | 1.21 | 8 | 7.8 | 5.8 | 80 | 2.5 | 20 | Type 3 - | Breakthrough | 81 | 1.82 | N | asynchronous ops |
| 11/17/2003 | Baseline 4+2 w/RH asynchronous | 1.21 | 12 | 12.4 | 7.5 | 80 | 1 | 20 | Type 4- | Breakthrough | 81 | 1.82 | N | asynchronous ops |
| 11/17/2003 | Baseline 4+2 w/RH synchronous | 1.21 | 12 | 12.8 | 7.7 | 80 | 1 | 20 | Type 4- | Breakthrough | 81 | 1.82 | N | synchronous ops |
| 11/18/2003 | Baseline 4+2 w/RH synchronous | 1.21 | 12 | 12.6 | 7.5 | 80 | 1 | 20 | Type 4- | Breakthrough | 61 | 1.87 | N | synchronous ops |
| 11/20/2003 | Baseline 4 (8")+2 (6") w/RH synchronous | 1.21 | 8 | 8.3 | 6.7 | 80 | 3.2/2.5 | 20 | 3+ | Breakthrough | 65 | 1.85 | N | synchronous ops |
| 11/20/2003 | Baseline 4 (8")+2 (6") w/RH asynchronous | 1.21 | 8 | 8.2 | 6.5 | 80 | 3.2/2.5 | 20 | 3- | Breakthrough | 65 | 1.85 | N | asynchronous ops |
| 11/20/2003 | Baseline 4 (8")+2 (6") w/RH synchronous | 1.21 | 10 | 9.9 | 7.5 | 80 | 2.5/1.6 | 20 | 4- | Breakthrough | 65 | 1.85 | N | synchronous ops |
| 11/20/2003 | Baseline 4 (8")+2 (6") w/RH synchronous | 1.21 | 12 | 12.3 | 8.4 | 80 | 2.0/1.1 | 20 | 4- | Breakthrough | 65 | 1.85 | N | synchronous ops |
| 11/29/2003 | All-In Test - Baseline 4 (6")+2 (6") w/RH synchronous | 1.21 | 8 | 10.4 | 6.6 | 80 | 2.2 | 30 | see dye test results | Breakthrough | 30/30 | 24/27 | N | synchronous ops |
| 11/29/2003 | All-In Test - baseline 4 (6")+2 (6") w/RH synchronous | 1.21 | 10 | 11.6 | 7.3 | 80 | 1.2 | 20 | see dye test results | Breakthrough | 30/30 | 24/27 | N | synchronous ops |

(a) Laponite was the simulant used in all tests except those on 11/29/2003, when kaolin-bentonite was used.
(b) Peak average is average velocity over time period $t_{primary}$ as shown in Figure 3.6. See Appendix A for more thorough descriptions.
(c) + and - suffix to mixing observation is intended as relative indication of degree of recirculation observed in Type 2 and 3 mixing patterns. A type 4- designation indicates there were appreciable unmobilized areas in the test vessel.

**Table 4.4**. Summary Results: UFP Tests (shaded rows indicate ‘final’ tests exhibiting Type 3 or better mobilization states)

| Test date | Test type | PJM config | Nozzle dia. (in.) | Nozzle vel. (m/s) | PJM $\Delta H$ (cm) | Nom. drive time (sec) | Actual drive time (sec) | Cycle time (sec) | DACS files | Mixing pattern observed | Cavern height if appropriate (in.) | Simulant | Yield, nom | Yield, actual | Target H/D fill | Actual H/D | Recirc Y/N | Recirc flow (gpm) | Scoping (S) or final (F) |
|---|---|---|---|---|---|---|---|---|---|---|---|---|---|---|---|---|---|---|---|
| 9/19/2003 | UFP | Baseline 6 | 0.81 | 8 | 85 | 7.4 | 6.9 | 29.7 | p030919R1a.ASC p030919R1a2.ASC | Type 1 | 38 ±2 inches | Laponite | 100 | | 1.845 | | N | | S |
| 9/22/2003 | UFP | Baseline 6 | 0.81 | 8 | 85 | 7.4 | 6.9 | 29.7 | p030922R1a.ASC p030922R1b.ASC | Type 1 | 37 ±2 inches | Laponite | 100 | 115 | 1.845 | 1.87 | N | | S |
| 9/22/2003 | UFP | Baseline 6 | 0.81 | 12 | 85 | 4.9 | | 29.7 | p030922R2a.ASC p030922R2b.ASC | Type 1 | 46 ±2 inches | Laponite | 100 | | 1.845 | | N | | S |
| 9/22/2003 | UFP | Baseline 6 | 0.81 | ~17 | 85 | 3.0 | | | p030922R3a.ASC p030922R3b.ASC | Type 1 | 48 ±2 inches | Laponite | 100 | | 1.845 | 1.86 | N | | S |
| 9/23/2003 | UFP | Baseline 6 + recirc | 0.81 | 8 | 85 | 7.4 | 6.3 | 29.7 | p030923R1a.ASC p030923R1b.ASC | Type 2 | NA | Laponite | 100 | 119 | 1.845 | 1.85 | Y | 90, 2 ea. 30 deg. noz | S |
| 9/23/2003 | UFP | Baseline 6 + recirc | 0.81 | 17 | 85 | 3.0 | | 29.7 | p030923R2a.ASC p030923R2b.ASC | Type 2 | NA | Laponite | 100 | | | | | | S |
| 9/25/2003 | UFP | Baseline 6 | 0.81 | 8 | 90 | 7.4 | 6.9 | 29.7 | p030925R1a.ASC p030925R1b.ASC | Incomplete test due to overblow | NA | Laponite | 100 | | 1.845 | 1.88 | Y | 50, top bucket | S |
| 9/27/2003 | UFP | Baseline 6 | 0.81 | 8 | 90 | 7.4 | 6.9 | 29.7 | p030927R1a.ASC p030927R1b.ASC | Type 1 | 38 ±2 inches | Laponite | 70 | 89 | 1.845 | 1.85 | N | | S |
| 9/27/2003 | UFP | Baseline 6 | 0.81 | 12 | 90 | 4.9 | 4.2 | 29.7 | p030927R2a.ASC p030927R2b.ASC | Type 2 | Breakthrough | Laponite | 70 | 89 | 1.845 | 1.85 | N | | S |
| 9/30/2003 | UFP | Baseline 6 | 0.81 | 12 | 90 | 4.9 | 4.2 | 29.7 | p030930R1a.ASC p030930R1b.ASC | Type 2 | Breakthrough | Laponite | 70 | 76 | 1.845 | 1.84 | N | | S |
| 9/30/2003 | UFP | Baseline 6 + recirc | 0.81 | 12 | 90 | 4.9 | 4.2 | 29.7 | p030930R2a.ASC p030930R2b.ASC | Type 2 | Breakthrough | Laponite | 70 | 77 | 1.845 | 1.84 | Y | 1 hand held, 60-70 | S |
| 9/30/2003 | UFP | Baseline 6 + recirc | 0.81 | 12 | 90 | 4.9 | 4.2 | 29.7 | p030930R6a.ASC p030930R6b.ASC | Type 2 | Breakthrough | Laponite | 70 | 77 | 1.845 | 1.84 | Y | | S |
| 9/30/2003 | UFP | Baseline-2 on, 4 off +recirc | 0.81 | 12 | 90 | 4.9 | 4.2 | 29.7 | p030930R4a.ASC p030930R4b.ASC | Type 2 | Breakthrough | Laponite | 70 | 77 | 1.845 | 1.84 | Y | | S |
| 9/30/2003 | UFP | Baseline-3 on, 3 off + recirc | 0.81 | 12 | 90 | 4.9 | 4.2 | 29.7 | p030930R3a.ASC p030930R3b.ASC | Type 2 | Breakthrough | Laponite | 70 | 77 | 1.845 | 1.84 | Y | | S |
| 9/30/2003 | UFP | Baseline-3 on, 3 off + recirc | 0.81 | 17 | 90 | 4.9 | 4.2 | 29.7 | p030930R5a.ASC p030930R5b.ASC | Type 2 | Breakthrough | Laponite | 70 | 77 | 1.845 | 1.84 | Y | | S |
| 10/2/2003 | UFP | Baseline 6 + recirc | 0.81 | 12 | 90 | 4.9 | 4.2 | 27.7 | p031002R1a.ASC p031002R1b.ASC | Type 2 ++ | NA | Laponite | 70 | 87 | 1.845 | 1.83 | Y | | S |
| 10/2/2003 | UFP | Baseline-2 on, 4 off +recirc | 0.81 | 12 | 90 | 4.9 | 4.2 | 27.7 | p031002R2a.ASC p031002R2b.ASC | Type 2 ++ | NA | Laponite | 70 | 87 | 1.845 | 1.83 | Y | | S |
| 10/3/2003 | UFP | Baseline 6 | 0.81 | 8 | 90 | 7.4 | 6.9 | 29.7 | p031003R1a.ASC p031003R1b.ASC | Type 2 | Breakthrough | Laponite | 30 | 48 | 1.845 | 1.86 | N | | S |
| 10/3/2003 | UFP | Baseline 6 | 0.81 | 12 | 90 | 4.9 | 4.2 | 27.7 | p031003R2a.ASC p031003R2b.ASC | Type 2 | Breakthrough | Laponite | 30 | 48 | 1.845 | 1.86 | N | | S |

**Table 4.4**. Summary Results: UFP Tests (shaded rows indicate ‘final’ tests exhibiting Type 3 or better mobilization states)

| Test date | Test type | PJM config | Nozzle dia. (in.) | Nozzle vel. (m/s) | PJM ΔH (cm) | Nom. drive time (sec) | Actual drive time (sec) | Cycle time (sec) | DACS files | Mixing pattern observed | Cavern height if appropriate (in.) | Simulant | Yield, nom | Yield, actual | Target H/D fill | Actual H/D | Recirc Y/N | Recirc flow (gpm) | Scoping (S) or final (F) |
|---|---|---|---|---|---|---|---|---|---|---|---|---|---|---|---|---|---|---|---|
| 10/3/2003 | UFP | Baseline 6 | 0.81 | 8 | 90 | 7.4 | 6.9 | 29.7 | p031003R4a.ASC p031003R4b.ASC | Type 1 | 58 ±2 | Laponite | 30 | 26 | 1.845 | 1.86 | Y | 90, top bucket | S |
| 10/3/2003 | UFP | Baseline 6 | 0.81 | 12 | 90 | 4.9 | 4.2 | 29.7 | p031003R5a.ASC p031003R5b.ASC | Type 2 | Breakthrough | Laponite | 30 | 27 | 1.845 | 1.86 | Y | 90, top bucket | S |
| 10/7/2003 | UFP | Baseline 6 | 0.81 | 8 | 65 | 7.4 | 4.2 | 29.7 | p031007R1a.ASC p031007R1b.ASC | Type 2 ?? | | Laponite | 30 | 55 | 1.3 | 1.33 | Y | 90, top bucket | S |
| 10/10/2003 | UFP | Baseline 6 + 3 w/ RH | 0.81 | 8 | 80 | 7.4 | 5.0 RH, 5.2 Baselines | 29.7 | p031010R1a.ASC p031010R1b.ASC p031010R1c.ASC | Type 2 ++ | Breakthrough | Laponite | 30 | 34 | 1.845 | 1.82 | N | | S |
| 10/11/2003 | UFP | Baseline 6 + 3 w/ RH | 0.81 | 8 | 80 | 7.4 | 5.0 RH, 6.0 baselines | 29.7 | p031011R1a.ASC p031011R1b.ASC p031011R1c.ASC | Type 2 +++ | Breakthrough | Laponite | 70 | 75 | 1.845 | 1.86 | N | | S |
| 10/18/2003 | UFP | Baseline 6 + 3 w/ extend. RH | 0.81 | 8 | 80 | 7.4 | 4.5-5.0 RH, 6.0 baselines | 29.7 | p031018R1a.ASC p031018R1b.ASC p031018R1c.ASC | Type 1 | 60 ±2 | Laponite | 70 | 83 | 1.845 | 1.83 | Y | 90, top bucket | S |
| 10/18/2003 | UFP | Baseline 6 + 3 w/ extend. RH | 0.81 | 12 | 80 | 4.9 | 3 | 27.7 | p031018R2a.ASC p031018R2b.ASC p031018R2c.ASC | Type 1 ++ | Minimal breakthrough | Laponite | 70 | 83 | 1.845 | 1.83 | N | | S |
| 10/20/2003 | UFP | Baseline 6 + 3 w/ extend. RH | 0.81 | 12 | 80 | 4.9 | 2.5 RH, 3.0 baselines | 27.7 | p031020R1a.ASC p031020R1b.ASC p031020R1c.ASC | Type 1 ++ | 58 ± 2 with minimal breakthrough | Laponite | 70 | 101.5 | 1.845 | 1.79 | N | | S |
| 10/29/2003 | UFP | Baseline 6 + 3 w/ extend. RH | 0.93 | | | | | | p031029R1a.ASC p031029R1b.ASC p031029R1c.ASC | Scoping test only?? | | | | | | | | | S |
| 11/10/2003 | UFP | Baseline 6 + 3 w/ 5" extend. RH | 0.81 | 8 | 80 | 7.4 | 4.5 | 30 | p031110R1a.ASC p031110R1b.ASC p031110R1c.ASC | Type 2 + | | Laponite | 70 | 70 | 1.845 | 1.77 | N | | S |
| 11/15/2003 | UFP | Baseline 4 + 2 w/ RH | 1.21 | 3.9** DACS calc error | 80 | 5.9 | 5 | 30 | p031115R1a.ASC p031115R1b.ASC p031115R1c.ASC | Type 1 | No breakthrough | Laponite | 70 | 70 | 1.845 | 1.86 | N | synch ops | S |
| 11/15/2003 | UFP | Baseline 4 + 2 w/ RH | 1.21 | 5.4** DACS calc error | 80 | | | | p031115R2a.ASC p031115R2b.ASC p031115R2c.ASC | Overblow - test terminated | | Laponite | 70 | 70 | 1.845 | 1.86 | N | synch ops | S |
| 11/25/2003 | UFP | Baseline 4(6") + 2 (6") w/ RH synchronous | 1.21 | 8 | 80 | 2.5 | 2.2 | 20 | p031125R1a.ASC p031125R1b.ASC p031125R1c.ASC | Type 4- | Breakthrough | Laponite | 70 | 61.9 | 1.845 | 1.81 | N | synch ops | S |
| 12/1/2003 | UFP | Baseline 4(6") + 2 (6") w/ RH synchronous | 1.21 | 12 | 80 | 1.9 | 1.2 | 20 | | | Breakthrough | Kaolin-Bentonite slurry | 30/30 yld/consist | | 1.845 | | N | synch ops | S |
| 12/2/2003 | UFP | Baseline 4(6") + 2 (6") w/ RH synchronous | 1.21 | 12 | 80 | 1.9 | 1.2 | 20 | p031202R1a.ASC p031202R1b.ASC p031202R1c.ASC | | | Kaolin-Bentonite slurry | 30/30 yld/consist | | 1.845 | | N | synch ops | S |
| 12/3/2003 | UFP | Baseline 4(6") + 2 (6") w/ RH synchronous | 1.21 | 12 | 80 | 1.9 | 1.2 | 20 | p031203R1a.ASC p031203R1b.ASC p031203R1c.ASC | | | Kaolin-Bentonite slurry | 30/30 yld/consist | | 1.845 | | N | synch ops | S |
| 10/1/2003 | UFP | Baseline 6 + recirc | 0.81 | 12 | 90 | 4.9 | 4.2 | 27.7 | p031001R1a.ASC p031001R1b.ASC | Type 4 | NA | Laponite | 70 | 84 | 1.845 | 1.86 | Y | | F |
| 10/3/2003 | UFP | Baseline 6 + recirc | 0.81 | 12 | 90 | 4.9 | 4.2 | 27.7 | p031003R3a.ASC p031003R3b.ASC | Type 4 | NA | Laponite | 30 | 48 | 1.845 | 1.86 | Y | | F |

**Table 4.4**. Summary Results: UFP Tests (shaded rows indicate 'final' tests exhibiting Type 3 or better mobilization states)

| Test date | Test type | PJM config | Nozzle dia. (in.) | Nozzle vel. (m/s) | PJM ΔH (cm) | Nom. drive time (sec) | Actual drive time (sec) | Cycle time (sec) | DACS files | Mixing pattern observed | Cavern height if appropriate (in.) | Simulant | Yield, nom | Yield, actual | Target H/D fill | Actual H/D | Recirc Y/N | Recirc flow (gpm) | Scoping (S) or final (F) |
|---|---|---|---|---|---|---|---|---|---|---|---|---|---|---|---|---|---|---|---|
| 10/3/2003 | UFP | Baseline 6 + recirc | 0.81 | 12 | 90 | 4.9 | 4.2 | 27.7 | p031003R6a.ASC p031003R6b.ASC | Type 4 | NA | Laponite | 30 | 33 | 1.845 | 1.86 | Y | | F |
| 10/10/2003 | UFP | Baseline 6 + 3 w/RH | 0.81 | 12 | 80 | 4.9 | 3 | 27.7 | p031010R2a.ASC p031010R2b.ASC p031010R2c.ASC | Type 4 | Breakthrough | Laponite | 30 | 36 @ start 40 @ finish | 1.845 | 1.82 | N | | F |
| 10/11/2003 | UFP | Baseline 6 + 3 w/RH | 0.81 | 12 | 80 | 4.9 | 3 | 27.7 | p031011R2a.ASC p031011R2b.ASC p031011R2c.ASC | Type 4 | Breakthrough | Laponite | 70 | 72-75 | 1.845 | 1.86 | N | | F |
| 11/10/2003 | UFP | Baseline 6 + 3 w/ 5" ext. RH asynchronous | 0.81 | 12 | 80 | 4.9 | 3.5 | 30 | p031110R2a.ASC p031110R2b.ASC p031110R2c.ASC | Type 4- | Breakthrough | Laponite | 70 | 70 | 1.845 | 1.77 | N | | F |
| 11/10/2003 | UFP | Baseline 3 on/3 off + 3 enhanced w/ 5" ext. RH asynchronous | 0.81 | 12 | 80 | 4.9 | 3.5 | 30 | p031110R3a.ASC p031110R3b.ASC p031110R3c.ASC | Type 4 | Breakthrough | Laponite | 70 | 70 | 1.845 | 1.77 | N | | F |
| 11/17/2003 | UFP | Baseline 4 + 2 w/RH synchronous | 1.21 | 8 | 80 | 3.3 | 2.5 | 20 | p031117R1a.ASC p031117R1b.ASC p031117R1c.ASC | Type 4- | Breakthrough | Laponite | 70 | 81 | 1.845 | 1.82 | N | synch ops | F |
| 11/17/2003 | UFP | Baseline 4 + 2 w/RH asynchronous | 1.21 | 8 | 80 | 3.3 | 2.5 | 20 | p031117R2a.ASC p031117R2b.ASC p031117R2c.ASC | Type 3 - | Breakthrough | Laponite | 70 | 81 | 1.845 | 1.82 | N | | F |
| 11/17/2003 | UFP | Baseline 4 + 2 w/RH asynchronous | 1.21 | 12 | 80 | 2.5 | 1 | 20 | p031117R3a.ASC p031117R3b.ASC p031117R3c.ASC | Type 4- | Breakthrough | Laponite | 70 | 81 | 1.845 | 1.82 | N | | F |
| 11/17/2003 | UFP | Baseline 4 + 2 w/RH synchronous | 1.21 | 12 | 80 | 2.5 | 1 | 20 | p031117R4a.ASC p031117R4b.ASC p031117R4c.ASC | Type 4- | Breakthrough | Laponite | 70 | 81 | 1.845 | 1.82 | N | synch ops | F |
| 11/18/2003 | UFP | Baseline 4 + 2 w/RH synchronous | 1.21 | 12 | 80 | 2.5 | 1 | 20 | p031118R1a.ASC p031118R1b.ASC p031118R1c.ASC | Type 4- | Breakthrough | Laponite | 70 | 61 | 1.845 | 1.87 | N | synch ops | F |
| 11/20/2003 | UFP | Baseline 4 (8") + 2 (6") w/RH synchronous | 1.21 | 8 | 80 | 6.2/3.3 | 3.2/2.5 | 20 | p031120R1a.ASC p031120R1b.ASC p031120R1c.ASC | Type 3+ | Breakthrough | Laponite | 70 | 65 | 1.845 | 1.85 | N | synch ops | F |
| 11/20/2003 | UFP | Baseline 4 (8") + 2 (6") w/RH asynchronous | 1.21 | 8 | 80 | 6.2/3.3 | 3.2/2.5 | 20 | p031120R2a.ASC p031120R2b.ASC p031120R2c.ASC | Type 3 - | Breakthrough | Laponite | 70 | 65 | 1.845 | 1.85 | N | | F |
| 11/20/2003 | UFP | Baseline 4 (8") + 2 (6") w/RH synchronous | 1.21 | 10 | 80 | 4.9/2.6 | 2.5/1.6 | 20 | p031120R3a.ASC p031120R3b.ASC p031120R3c.ASC | Type 4- | Breakthrough | Laponite | 70 | 65 | 1.845 | 1.85 | N | synch ops | F |
| 11/20/2003 | UFP | Baseline 4 (8") + 2 (6") w/RH synchronous | 1.21 | 12 | 80 | 4.6/2.2 | 2.0/1.1 | 20 | p031120R4a.ASC p031120R4b.ASC p031120R4c.ASC | Type 4- | Breakthrough | Laponite | 70 | 65 | 1.845 | 1.85 | N | synch ops | F |
| 11/29/2003 | UFP | All-In Test - baseline 4 (6") + 2 (6") w/RH synchronous | 1.21 | 8 | 80 | 2.5 | 2.2 | 30 | p031129R1a.ASC p031129R1b.ASC p031129R1c.ASC | Determined by dye tracer | Breakthrough | Kaolin-Bentonite slurry | 30/30 yld/consist | 24/27 yld/consist | 1.845 | 1.85 | N | synch ops | F |
| 11/29/2003 | UFP | All-In Test - baseline 4 (6") + 2 (6") w/RH synchronous | 1.21 | 12 | 80 | 1.9 | 1.2 | 20 | p031129R2a.ASC p031129R2b.ASC p031129R2c.ASC | Determined by dye tracer | Breakthrough | Kaolin-Bentonite slurry | 30/30 yld/consist | 24/27 yld/consist | 1.845 | 1.85 | N | synch ops | F |
| 12/16/2003 | UFP | Mass transfer test - baseline 4 (6") +2 (6") w/RH air sparging ops only | 1.21 | 11 | 80 | 1.7 | 1.2 | 20 | p031216R1a.ASC p031216R1b.ASC p031216R1c.ASC | TBD by dye – tracer; results pending | | Kaolin-Bentonite slurry | 30/30 yld/consist | | 1.845 | 1.84 | N | synch ops | |

# 5.0 Discussion of Results

In general, the extent of mixing and cavern elevations was determined by observation, whether through the transparent simulant (Laponite) or by fluid movement at the simulant-tank wall interface, where the motion could be seen via entrained bubbles, miscellaneous particulate, or purposely introduced colored tracer beads of near neutral density (kaolin-bentonite opaque slurry simulants). The mixing pattern observations and cavern heights in Tables 4.1 and 4.2 for the LS vessel and Tables 4.3 and 4.4 for the UFP vessel were derived by direct observation unless other measurement methods were noted. Three separate methods were used to quantitatively (or at least semi-quantitatively) evaluate mixing/ mobilization results: 1) dye concentration, 2) bead distribution from core samples, and 3) radiofrequency (RF) tag distribution. These alternative techniques for assessing tank mixing performance are discussed in this section.

## 5.1 Dye Tracer Technique for Assessing Mixing

Mixing performance in the PJM test vessels was assessed using tracer chemicals. A summary of the technique used is shown in Figure 5.1. The chemical tracers used were Food Dye Color No. 1, or Brilliant Blue FCF (BB). A stock solution of these materials was prepared by dissolution in water. This solution was introduced through a sample tube near the bottom of the center PJM tube during operation. After the dye was injected, the system was operated continuously and samples drawn from multiple locations in each test vessel (five sample stations for LS, four for UFP). Schematic diagrams of the tracer sampling locations are shown in Figures 5.2 and 5.3 for the LS and UFP vessel, respectively.

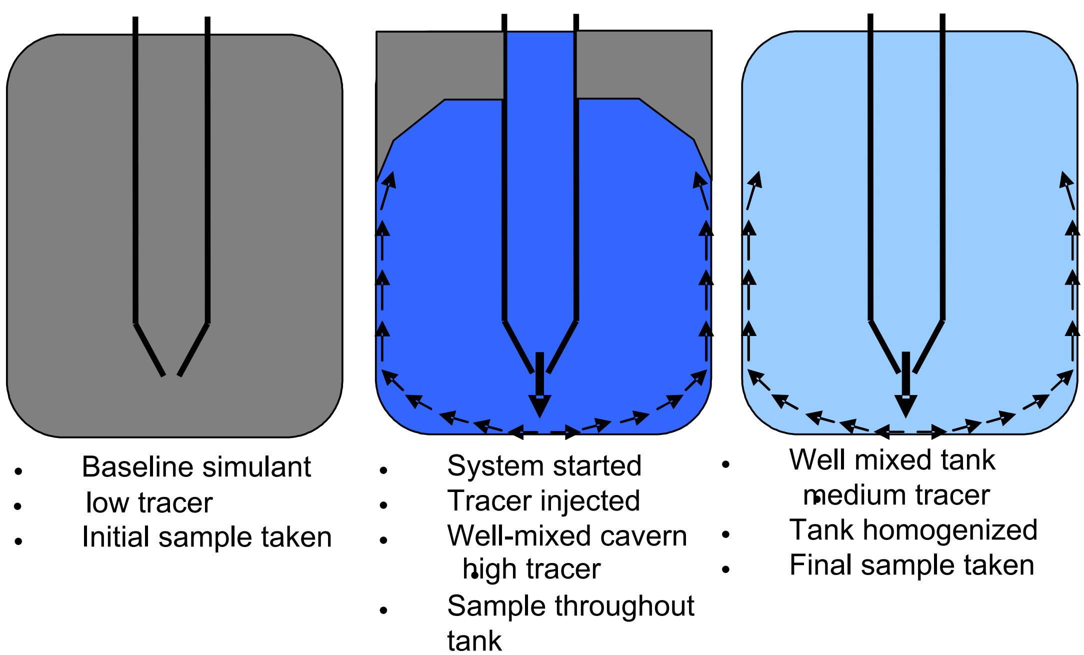


**Figure 5.1.** Summary of Tracer Dye Technique Steps

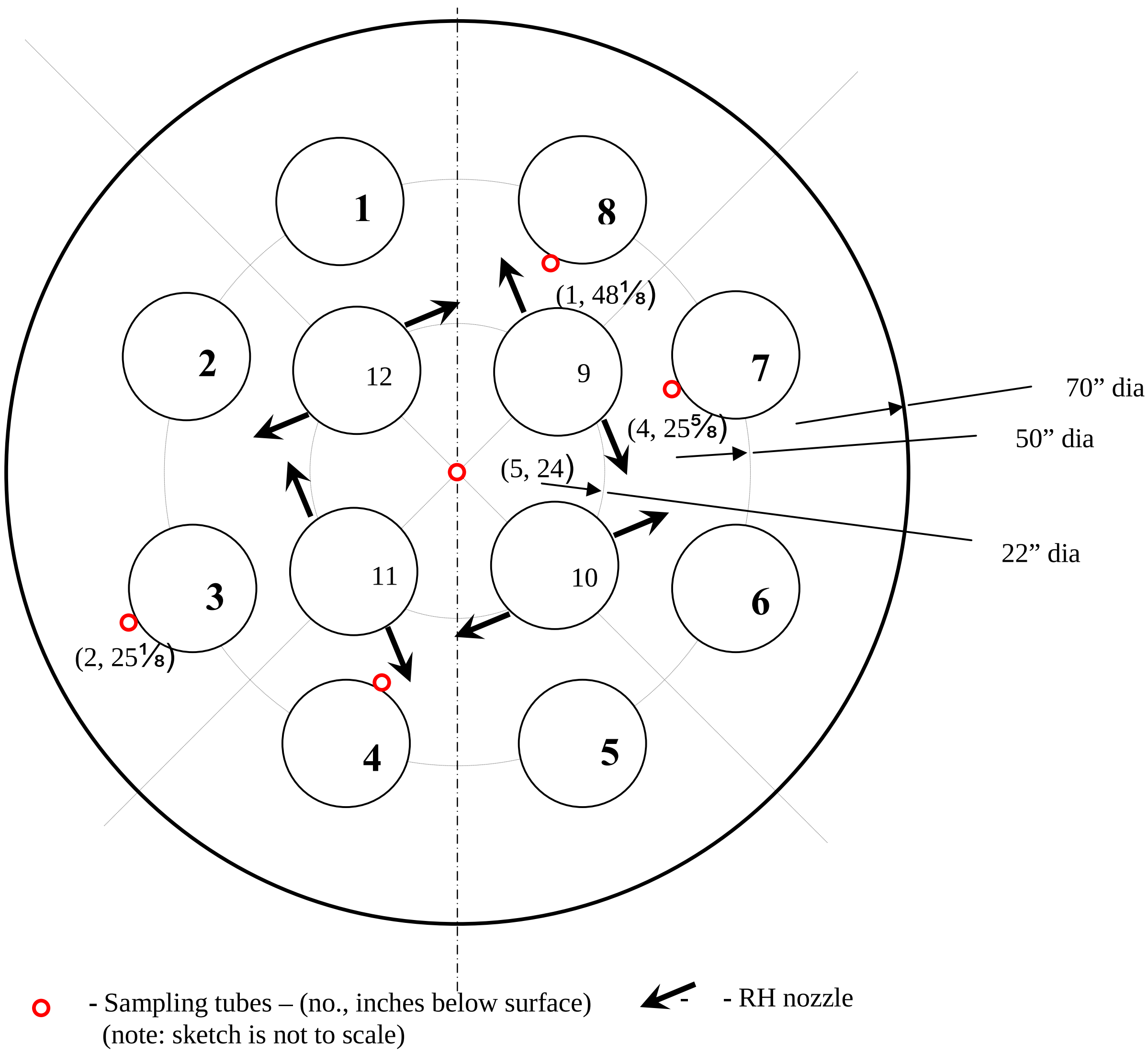


**Figure 5.2**. Schematic of Lag Storage Vessel Tracer Sampling Locations

Samples were drawn continuously over the testing period of approximately 60 minutes using a dedicated peristaltic pump for each sample location except for the line where the dye was initially injected. In several of the tests, the pump for a particular sample location failed and samples could not be obtained. Pump failure was generally related to pumping a viscous non-Newtonian fluid through several feet of small-diameter tubing. After the test period, the vessel was operated for an additional period of time (approximately 30 minutes) while the center sample tube, into which the dye was initially injected, was purged with clean simulant material to remove residual stock solution in the line. Finally, several samples were taken from the dye injection port. The samples were analyzed for dye concentration as described in WTP-RPT-121.[a] Results are shown in Figures 5.4, 5.5, and 5.6. The results of final

(a) WTP-RPT-121, *Chemical Tracer Techniques for Assessing Mixing Performance in Non-Newtonian Slurries for WTP Pulse Jet Mixer Systems*.

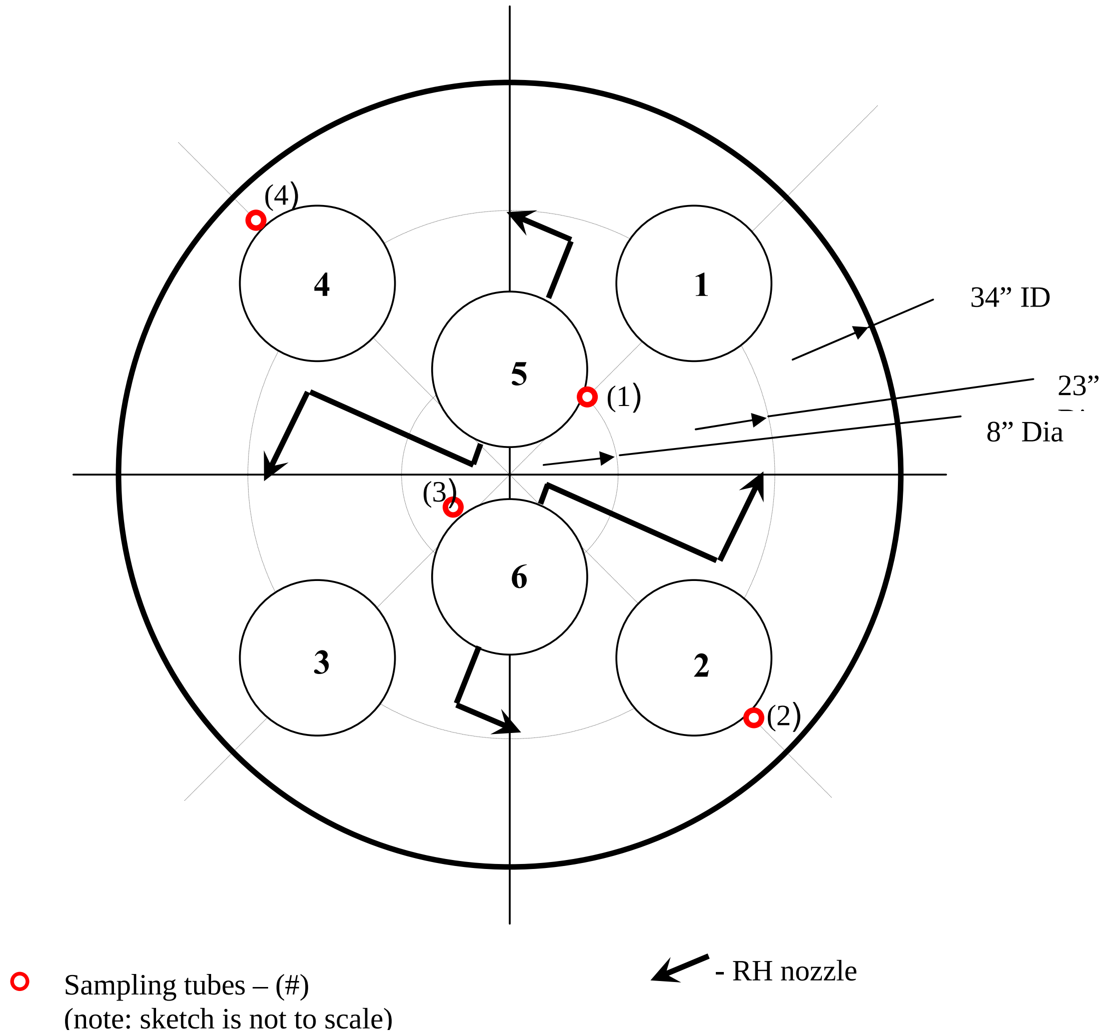


**Figure 5.3**. Schematic of UFP Vessel Tracer Sampling Locations

samples from the dye injection line were averaged and are labeled “steady state” in the figures. The standard deviation of these samples was used for the error bars on these lines. Because the vessel was operated for a longer period of time, the steady-state values should indicate the value toward which the other samples were trending. Because these samples were taken in several locations that are outside of the known or anticipated mixing cavern and the values converge to the steady state values, the results are consistent with a vessel that is homogeneously mixed. This observation is also consistent with the visual observations that the tank was homogenized during the testing. Outliers, such as the Station 1, sample 29 point in Figure 5.5, can appear while still mixing material in the vessel and sample lines extract a portion of undyed freshly mixed material. When mixing is in process, situations occur where noisy data indicate the presence of inhomogeneous dyed and undyed material. As the mixing proceeds, the concentrations come to steady state and the noise diminishes.

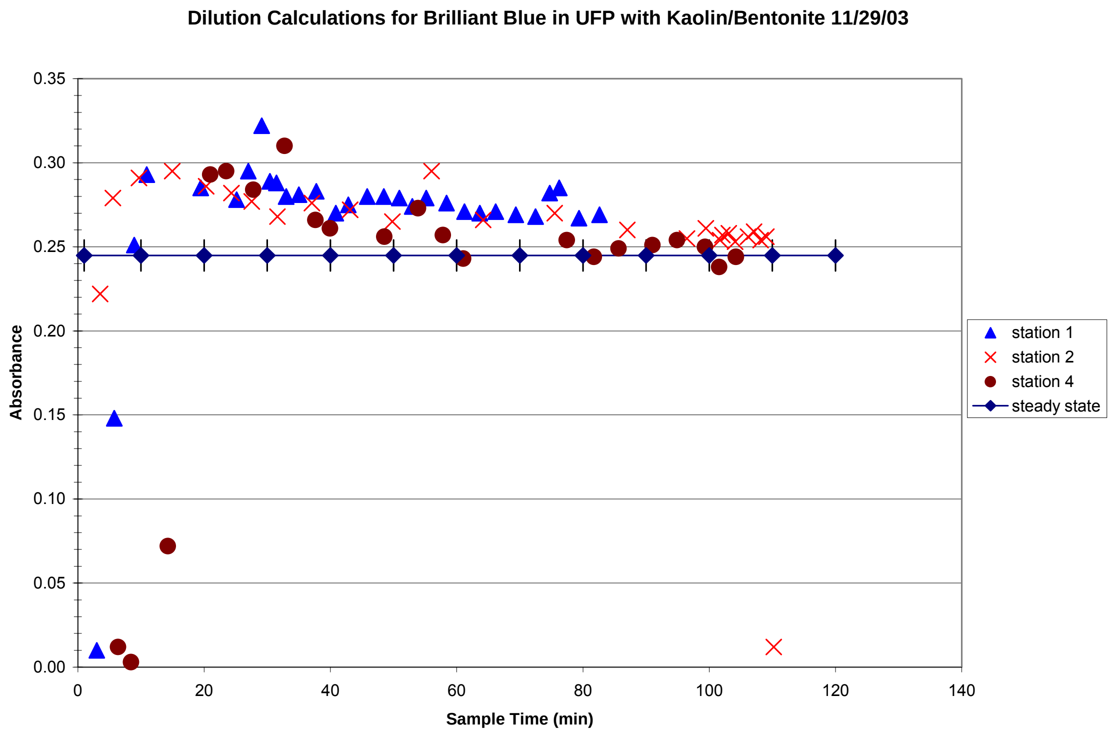


**Figure 5.4**. Dye Adsorption on Samples Taken from UFP All-in Test 11/29/03

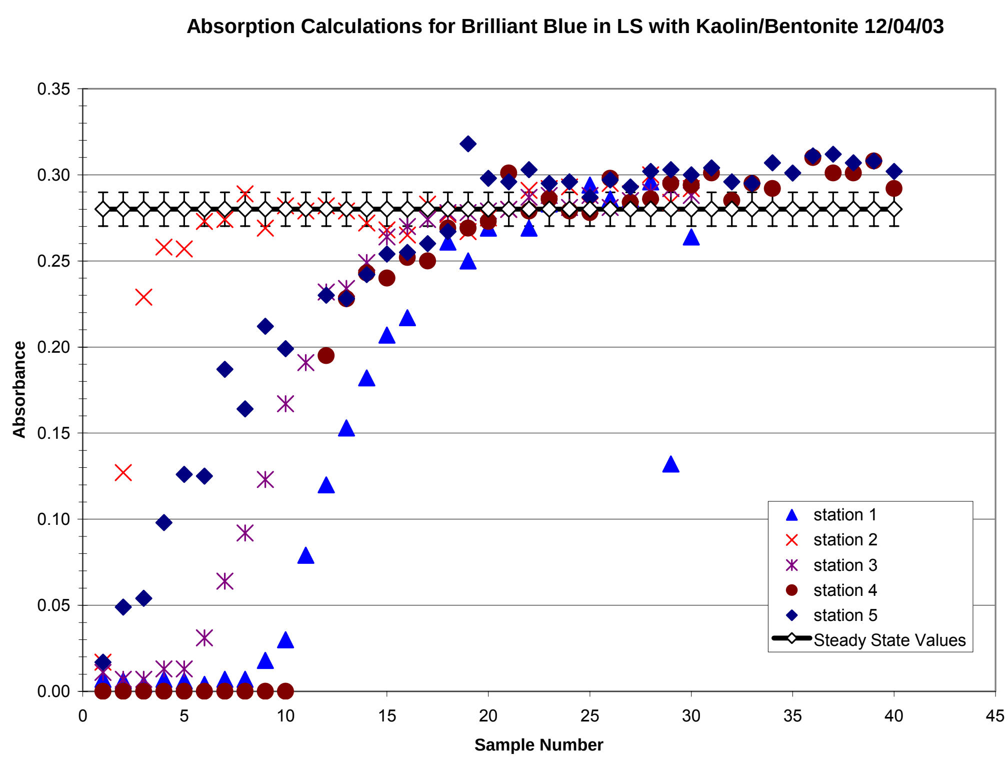


**Figure 5.5**. Dye Adsorption on Samples Taken from LS All-in Test 12/04/03

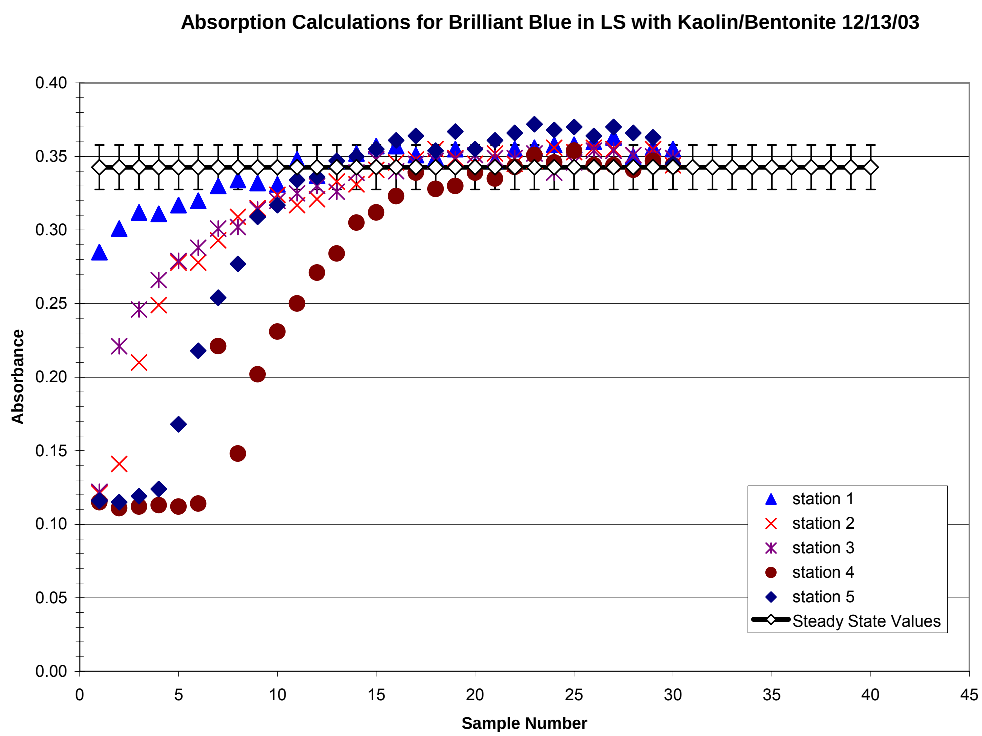


**Figure 5.6**. Dye Adsorption on Samples Taken from LS All-in Test 12/13/03

## 5.2 Other Mobilization Measurement Techniques

Bead distribution and RF tag tracking and distribution were applied to evaluate mobilization for selected pulse jet configurations and operating conditions. The procedures for applying these techniques are described in detail in Burgeson et al. (2004), which more fully presents the core sampling and RF tag techniques and results. The processes and results currently available that apply to the LS and UFP mobilization evaluations are summarized in this section.

### 5.2.1 Vibracore Sampling

Core sampling, which consists of inserting a hollow tube into the mixed slurry simulant to extract a sample for post-test analysis, was used to gather data on mixing performance in the PJM test vessels. A technique called vibracoring was used to sample the test vessels; vibracoring is commonly used by geologists to sample unconsolidated sediments under water (Morton and White 1997; Lanesky et al. 1979). To assess mixing in the PJM test vessels, core samples were taken, frozen after removal (or in-situ), and then analyzed for discreet counts of introduced tracer beads or dye concentration.

#### 5.2.1.1 Vibracoring and Freeze-Coring Equipment

Equipment for vibracoring consisted of concrete vibrators and core tubes. Additional equipment was needed for freeze-coring such as double-walled core tubes and an ice shaver. Two vibrators were used to insert the cores into the simulant depending on which tank was being sampled. A ViberMite[(a)] Model VME-2500 was used to insert the cores. The ViberMite operates on 120 volt AC/DC and has a speed of 13200 RPM (VPM) and a force of 180 lb. The core tubes were all pressure-rated 200 or 125 solvent weld PVC Pipe manufactured by PW Eagle.[(b)] The pipe specifications used in vibracoring and freezing the vibracores are listed in Table 5.1.

**Table 5.1.** Specifications for PVC Core Tubes Used in Vibracoring

| Pressure Rating | Nominal Pipe Size (in.) | Average Outside Diameter (in.) | Approximate Inside Diameter (in.) | Minimum Wall Thickness (in.) |
|---|---|---|---|---|
| 200 | 1 | 1.315 | 1.18 | 0.063 |
| 125 | 1¼ | 1.660 | 1.53 | 0.060 |
| 125 | 1½ | 1.900 | 1.77 | 0.060 |
| 125 | 2 | 2.375 | 2.21 | 0.073 |
| 125 | 2½ | 2.875 | 2.68 | 0.088 |
| 125 | 3 | 3.500 | 3.26 | 0.108 |

#### 5.2.1.2 Vibracoring Techniques

Prior to insertion, the inside of the core sampling tube was washed with water to help prevent core shortening (Morton and White 1997). The vibrator head is tightly attached parallel to the core tube using hose clamps. The core tube was held vertically above the tank by one person, and the vibrator power unit was held and activated by an assistant. The core tube was lowered slowly (see Morton and White 1997) into the sludge in one continuous motion. As soon as the tube touched the bottom of the tank, the vibrator was deactivated. The hose clamps were removed, and the vibrator head was detached from the core tube. The core tube was allowed to set up (simulants allowed to re-establish yield strength) for about 30 minutes and then capped with a mechanical test plug and removed. The bottom of the core was capped with another mechanical test plug immediately after removal. Cores were transported vertically to a large walk-in freezer and frozen (in a vertical position) for later analysis.

#### 5.2.1.3 Core Shortening

Core shortening can be caused by several different processes and results in compaction of the sample in the core tube or a loss of sample at or near the bottom of the core tube. Core shortening in the current application occurred due to plugging of the core barrel at the cutting edge and resulted in exclusion of samples from the lower portion of the tank (Morton and White 1997; Blomqvist 1991). To reduce core

---

(a) Global Manufacturing, Inc., 1102 W. Daisy Gaston Bates Dr., Little Rock, AR 72202, 1-800-551-3569; http://www.globalmanufacturing.com/products/internal_concrete/vibermite.asp.
(b) PW Eagle, Inc., 1550 Valley River Drive, Eugene, OR 97401, 541-343-0200; http://www.pweagleinc.com.

shortening, the inside of the core tube was washed with water prior to insertion, and insertion was controlled at a slow rate (Morton and White 1997; Blomqvist 1991).

To correct for core shortening, a measurement of the outer core height (OCH) was obtained by measuring from the top of the core tube (for freeze-coring measurement from the top of the outer core tube) to the surface of the simulant. The inner core height (ICH) was obtained by measuring from the top of the core tube (for freeze-coring from the top of the outer core tube) to the surface of the simulant inside the core tube. The amount of core shortening was obtained by subtracting the OCH from the ICH.

## 5.3 RF Tag Tracking

Individually numbered RF tags, interrogated by antennas, were used to evaluate the ability of the PJM to mix simulant. RF PIT[a] (passive integrated transponder) tags operating at 134.2 kHz and acting as passive flow followers were interrogated via antennas attached to the outside surface of the wall of the tank to track tag (and thus fluid) motion during PJM operation. The antenna dimensions and effective field of view are listed in Table 5.2, and antennas are shown attached to the tank perimeter in Figure 5.7 for tests conducted with Laponite simulant. The data loggers are shown in the foreground of the figure.

**Table 5.2.** Antenna Dimensions

| Inner Diameter | Outer Diameter | Scanned Volume |
|---|---|---|
| 7 in. | 9.75 in. | 296 cu. in. (9x9x7 half-ellipsoid) |

**Figure 5.7.** Antenna Placement for Laponite Test (similar to configuration used in slurry tests)

(a) Biomark, Inc., 7615 West Riverside Drive, Boise, ID 83714, (208) 275-0011; http://www.biomark.com.

The antennas record a tag when it enters the range of the antenna. When another tag enters the antenna field it is added to the list of interrogated tags. The tag replaced is not added to the list until it returns into the antenna field of view.

### 5.3.1 Tag Preparation

Before inserting them into the tank, the tags were coated with silicon sealant (Shoe Goo) to shield them from damage when they are ejected from the pulse tube nozzle and bump into the tank wall, each other, or internal tank hardware. Before use, each tag was weighed and characterized with a unique identification number. To ensure uniform initial placement of tags in the tank before mixing operations began, the tags were placed on the simulant surface in a square grid. The grid was designed based on the upper surface area (tank area-upper pulse tube area). Each tag's initial location on the grid was recorded.

## 5.4 Results from Other Mobilization Measurement Methods

Coring tests were conducted to support one UFP mobilization test and one LS mobilization test. The results of those tests are described in this section.

### 5.4.1 Vibracore Measurements on UFP

Before PJM operations began, the simulant was seeded with Lexan[a] (polycarbonate resin) beads, which were equally spaced in a grid on the simulant surface. Core samples using nominal 1-in.-diameter tubes were obtained December 3, 2003 following the final UFP final test completed on 11/29/03 and a repeat test on 12/1/03 (for applying the bead tracer and RF tag techniques). The three core sample locations, C1, C2, and C3, are shown in Figure 5.8.

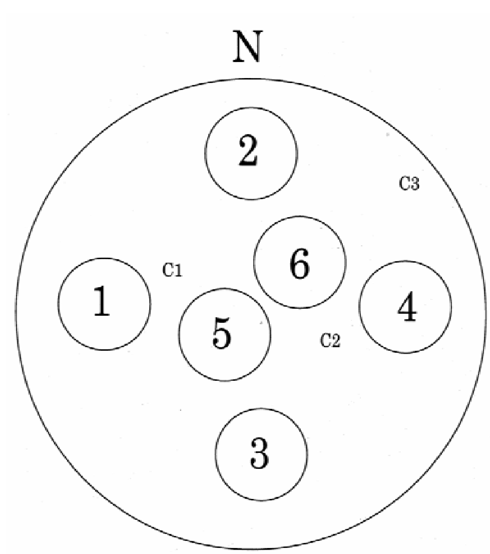


**Figure 5.8**. 031201 UFP Core Locations Sampled December 1, 2003

(a) GE Plastics, Lexan 123R-112, Lot No. L1902AA.

For analysis, each 60-in. core was divided into 15 4-in. segments. The number of beads in each segment was counted. The data for each core and the average are shown in Figure 5.9 and tabulated in Table 5.3. For the beads to be equally distributed throughout the slurry, each core would have eight beads. The bottom and top segments were not included in the analysis. Removing these cores from the analysis reduced the effects attributable to inserting the cores into the simulant.

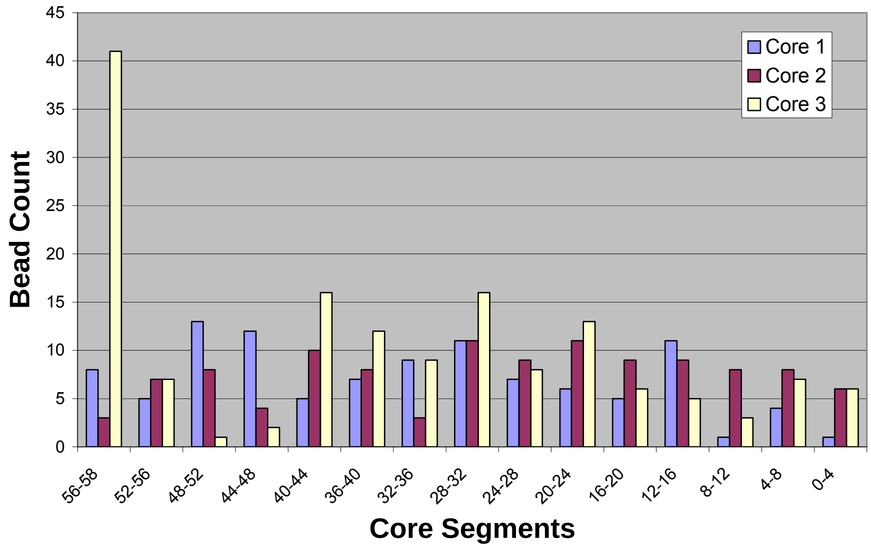


**Figure 5.9**. Core Segment Bead Distribution Obtained from UFP Cores Taken December 1, 2003

**Table 5.3.** UFP Core Data from December 1, 2003

| 031201 UFP Core Sampling Data[(a)] | | | | | | | | |
|---|---|---|---|---|---|---|---|---|
| **Core 1** | **Beads** | **Core 2** | **Beads** | **Core 3** | **Beads** | **Standard Core** | | **Average** |
| 56-59 | 8 | 56-58 | 3 | 56-58 | 41 | 56-58 | 8 | 17 |
| 52-56 | 5 | 52-56 | 7 | 52-56 | 7 | 52-56 | 8 | 6 |
| 48-52 | 13 | 48-52 | 8 | 48-52 | 1 | 48-52 | 8 | 7 |
| 44-48 | 12 | 44-48 | 4 | 44-48 | 2 | 44-48 | 8 | 6 |
| 40-44 | 5 | 40-44 | 10 | 40-44 | 16 | 40-44 | 8 | 10 |
| 36-40 | 7 | 36-40 | 8 | 36-40 | 12 | 36-40 | 8 | 9 |
| 32-36 | 9 | 32-36 | 3 | 32-36 | 9 | 32-36 | 8 | 7 |
| 28-32 | 11 | 28-32 | 11 | 28-32 | 16 | 28-32 | 8 | 13 |
| 24-28 | 7 | 24-28 | 9 | 24-28 | 8 | 24-28 | 8 | 8 |
| 20-24 | 6 | 20-24 | 11 | 20-24 | 13 | 20-24 | 8 | 10 |
| 16-20 | 5 | 16-20 | 9 | 16-20 | 6 | 16-20 | 8 | 7 |
| 12-16 | 11 | 12-16 | 9 | 12-16 | 5 | 12-16 | 8 | 8 |
| 8-12 | 1 | 8-12 | 8 | 8-12 | 3 | 8-12 | 8 | 4 |
| 4-8 | 4 | 4-8 | 8 | 4-8 | 7 | 4-8 | 8 | 6 |
| 0-4 | 1 | 0-4 | 6 | 0-4 | 6 | 0-4 | 8 | 4 |
| (a) Distance in inches from bottom of core sample tube. | | | | | | | | |

A Chi Square Test of goodness of fit, based on comparison of the three-segment average with the average core, yielded a p-value of 0.81. The Chi Square Test conclusion is “fail to reject homogeneity.” The same conclusion was obtained with the bottom and top segments included in the analysis.

### 5.4.2 Vibracore Measurements at LS Vessel

Core samples using nominal 1¼-in.-diameter tubes were obtained December 4, 2003 after UFP mobilization was completed. The seven core sample locations, C1 through C7, with duplicates at position C1, are shown in Figure 5.10.

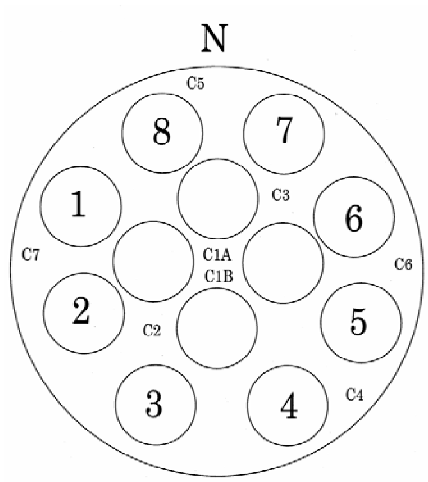


**Figure 5.10**. LS Core Locations Sampled December 4, 2003

For analysis, each 80 in. core was divided into 20 separate 4-in. segments. The number of beads was counted in each segment. The data for each core and the average are shown in Figure 5.11 and tabulated in Table 5.4. For the beads to be equally distributed throughout the slurry, each core would need to contain the same number of beads.

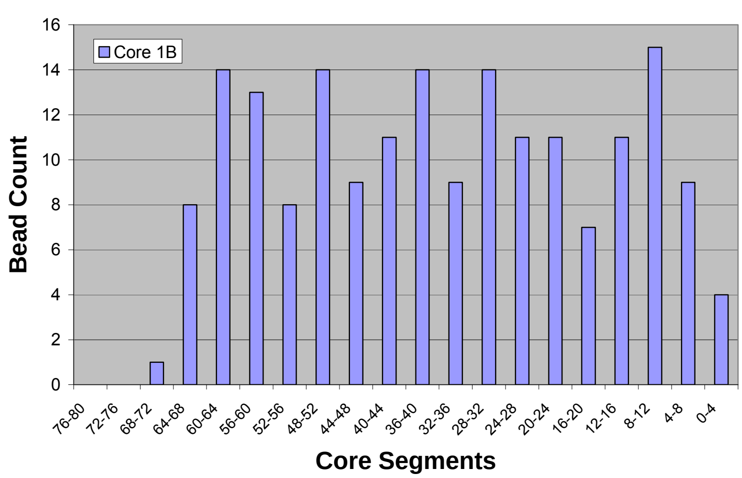


**Figure 5.11**. Core Segment Bead Distribution Obtained from LS Cores Taken December 4, 2003

**Table 5.4.** LS Core Data (031204) from December 4, 2003[a]

| Core 1A | | | Core 1B | | | Core 2 | | | Core 3 | | |
|---|---|---|---|---|---|---|---|---|---|---|---|
| | | | | | | 80-84 | 7 | | | | |
| 76-80 | 5 | Not full | 76-80 | | | 76-80 | 8 | 20% | 76-80 | | |
| 72-76 | 3 | Not full | 72-76 | | | 72-76 | 7 | 30% | 72-76 | 28 | ~20% |
| 68-72 | 1 | Not full | 68-72 | 1 | | 68-72 | 7 | 45% | 68-72 | | ~20% |
| 64-68 | 3 | Not full | 64-68 | 8 | | 64-68 | 5 | 50% | 64-68 | | ~20% |
| 60-64 | 17 | | 60-64 | 14 | | 60-64 | 10 | 50% | 60-64 | | ~20% |
| 56-60 | 19 | | 56-60 | 13 | | 56-60 | 10 | 50% | 56-60 | | ~20% |
| 52-56 | 18 | | 52-56 | 8 | | 52-56 | 3 | 60% | 52-56 | | ~20% |
| 48-52 | 16 | | 48-52 | 14 | | 48-52 | 8 | 60% | 48-52 | 3 | 60%full |
| 44-48 | 18 | | 44-48 | 9 | | 44-48 | 7 | 70% | 44-48 | 17 | |
| 40-44 | 11 | | 40-44 | 11 | | 40-44 | 9 | 90% | 40-44 | 10 | |
| 36-40 | 8 | | 36-40 | 14 | | 36-40 | 16 | 99% | 36-40 | 14 | 99%full |
| 32-36 | 18 | | 32-36 | 9 | | 32-36 | 18 | | 32-36 | 12 | 85%full |
| 28-32 | 12 | | 28-32 | 14 | | 28-32 | 10 | | 28-32 | 8 | 70%full |
| 24-28 | 11 | | 24-28 | 11 | | 24-28 | 11 | | 24-28 | 14 | 98%full |
| 20-24 | 6 | | 20-24 | 11 | | 20-24 | 16 | | 20-24 | 15 | |
| 16-20 | 12 | | 16-20 | 7 | | 16-20 | 9 | | 16-20 | 11 | |
| 12-16 | 10 | | 12-16 | 11 | | 12-16 | 12 | 85% | 12-16 | 13 | |
| 8-12 | 9 | | 8-12 | 15 | | 8-12 | 20 | 99% | 8-12 | 16 | |
| 4-8 | 15 | | 4-8 | 9 | | 4-8 | 13 | | 4-8 | 11 | |
| 0-4 | 16 | | 0-4 | 4 | | 0-4 | 15 | | 0-4 | 15 | |
| Mean | 13.5 | | Mean | 10.2 | | Mean | 14.9 | | Mean | 13.5 | |
| StdDev | 4.1 | | StdDev | 3.7 | | StdDev | 3.2 | | StdDev | 2.6 | |
| **Core 4** | | | **Core 5** | | | **Core 6** | | | **Core 7** | | |
| 76-80 | | | 76-80 | | | 76-80 | | | 76-80 | 4 | 20% |
| 72-76 | | | 72-76 | | | 72-76 | 24 | Not full | 72-76 | 14 | 30% |
| 68-72 | | | 68-72 | | | 68-72 | | Not full | 68-72 | 9 | Not full |
| 64-68 | | | 64-68 | 10 | 20% | 64-68 | | Not full | 64-68 | 12 | 70% |
| 60-64 | | | 60-64 | 10 | 20% | 60-64 | 8 | | 60-64 | 12 | 95% |
| 56-60 | | | 56-60 | 4 | 30% | 56-60 | 30 | | 56-60 | 15 | |
| 52-56 | | | 52-56 | 5 | 35% | 52-56 | 6 | | 52-56 | 24 | |
| 48-52 | | | 48-52 | 8 | 85% | 48-52 | 19 | | 48-52 | 16 | |
| 44-48 | | | 44-48 | 5 | 95% | 44-48 | 12 | | 44-48 | 21 | |
| 40-44 | | | 40-44 | 9 | 90% | 40-44 | 18 | | 40-44 | 13 | |
| 36-40 | | | 36-40 | 8 | 60% | 36-40 | 15 | | 36-40 | 23 | |
| 32-36 | | | 32-36 | 13 | 50% | 32-36 | 17 | | 32-36 | 24 | |
| 28-32 | | | 28-32 | 13 | 95% | 28-32 | 4 | Not full | 28-32 | 10 | 80% |
| 24-28 | | | 24-28 | 14 | | 24-28 | 10 | | 24-28 | 5 | 60% |
| 20-24 | | | 20-24 | 14 | | 20-24 | 4 | | 20-24 | 7 | 90% |
| 16-20 | | | 16-20 | 15 | | 16-20 | 15 | | 16-20 | 19 | 90% |
| 12-16 | | | 12-16 | 9 | | 12-16 | 17 | | 12-16 | 14 | |
| 8-12 | | | 8-12 | 14 | | 8-12 | 14 | | 8-12 | 4 | 75% |
| 4-8 | | | 4-8 | 18 | | 4-8 | 9 | | 4-8 | 11 | 75% |
| 0-4 | | | 0-4 | 14 | | 0-4 | 13 | | 0-4 | 18 | |
| | | | Mean[b] | 14.0 | | Mean | 13.8 | | Mean | 18.7 | |
| | | | StdDev[b] | 2.6 | | StdDev | 6.3 | | StdDev | 4.4 | |

(a) Distance in inches from bottom of core sample tube.

(yellow) Core not full; % full shown to right if available.

(pink) RF tag found with beads.

(b) Mean and standard deviation were calculated based on beads counted in full segments; 13.6 = mean of all full segments and 4.8 = standard deviation of all full segments.

These data were compromised because larger-diameter sample tubes were used and sample was lost from the bottom. Data from Core 4 were no good. The yellow areas indicate partially full core sections, indicating that clay had moved inside the sample core after the sample was taken. No formal statistics were obtained for these data, but the means of the number of tags per full segment are shown. These ranged from 10.2 + 3.7 to 18.7 + 4.4 beads per full segment. When all of the full segments were evaluated as one set, the mean was 13.6 + 4.8 tags per segment. This shows that the beads were relatively well distributed throughout the vessel where the core samples were taken. The locations were selected from central, potentially well-mixed and peripheral, potentially stagnant regions. The tag distribution among the cores did not show this tendency, supporting the conclusion that the tank was homogeneous.

### 5.4.3 RF Tag Measurements at UFP

RF tags were tracked during the UFP mixing test of December 1, 2003. The antenna grid was mounted over ~180 degrees of the tank periphery. The coverage in this grid was not 100% but provided information at three distinct elevations of the tank sidewall surface, with the exception of one low location at the 0 degree azimuthal position. The antenna location is shown superimposed on the 2-D roll-out drawing of UFP tube location in Figure 5.12. The tube location type is summarized in Table 5.5.

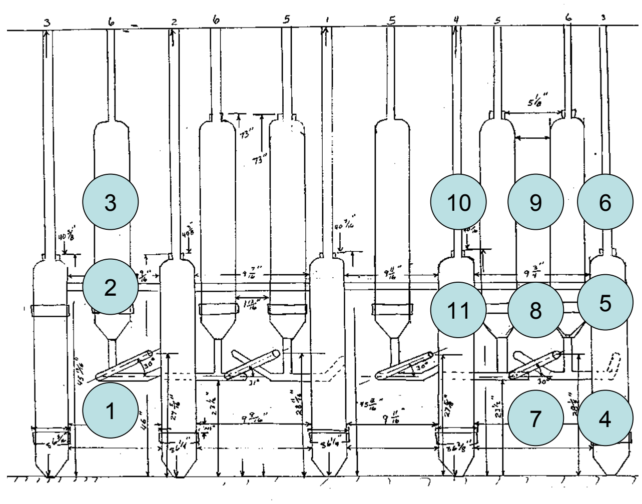


**Figure 5.12**. Approximate Antenna Position

#### 5.4.3.1 Transient Measurements

The objectives of the tag transient measurements is to track the RF tags as a function of time as they are entrained into the slurry and then move about the tank. After the PJM operation began, the tags were logged for ~ 80 minutes. During this time the 11 readers recorded 1628 hits. Of the 60 tags in the tank, 51 were identified as participating in the tag tracking. When the tag reader identifies a tag, its number remains in the reader until another tag comes into range and replaces it.

**Table 5.5.** Antenna Location Relative to PJM

| Antenna | Elevation | Close to PJM | At Gap |
|---|---|---|---|
| 1 | Low | | X |
| 2 | Mid | | X |
| 3 | High | | X |
| 4 | Low | X | |
| 5 | Mid | X | |
| 6 | High | X | |
| 7 | Low | | X |
| 8 | Mid | | X |
| 9 | High | | X |
| 10 | High | X | |
| 11 | Mid | X | |

In Figure 5.13, the transient data are plotted as a function of tags over time. The elapsed time during the test is plotted along the x axis. The tag number (sorted from the first-identified tag to last) is plotted along the y-axis. The numbers on the plot identify the antenna that observed the tag at the given time. The numbers are color coded, with darker colors denoting antennae at lower elevations. This plot shows some interesting details.

- **Two tags moving back and forth in the same antenna range**. Observe tags 10 and 16 at the start of the test. They both moved back and forth very locally in the range of antenna 3. This is also observed with tags 9 and 19 at antenna 10. Both of these antennas are at the top of the tank.
- **One stationary tag and many others moving in and out of view.** Observe tag 1 at the end of the test. This tag is parked at antenna 6 (also near the top). This tag alternates with quite a few different tags that move in and out from a variety of locations.
- **Timing.** The majority of tags (36 of 51 observed) came into view within the first 20 minutes of mixing. However the last tag, number 51, was observed only after 55 minutes of mixing.

#### 5.4.3.2 Post-Test Mapping of Tag Final Location

After mixing was stopped, the antennas were removed from the sides of the tank. A single antenna and a series of RF tags were used to scan the tank exterior horizontally and vertically.

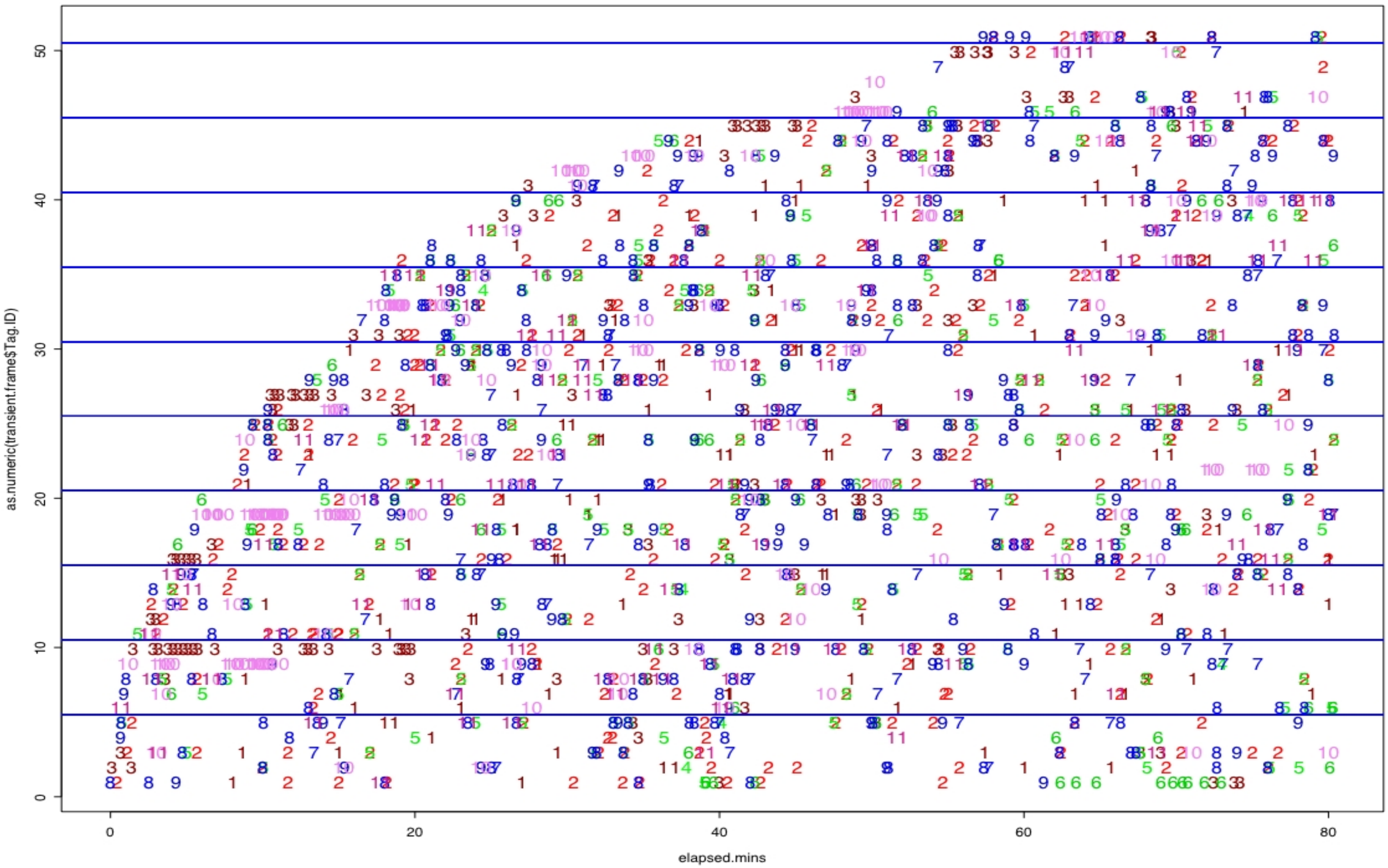


**Figure 5.13**. Transient Tag Frequency and Location of Observation Ordered by Time of First Observation

#### 5.4.3.3 Horizontal Characterization

To characterize the tank horizontally, measurements were made at seven elevations. The measurement location was tracked every 45 degrees using a known, externally mounted reference tag. Thus the tank external surface was divided into 56 cells, seven high by eight in circumference. These data are shown in Figure 5.14. The dark blue horizontal line at ~52 in. elevation represents the slurry surface. Some tags are seen above this level because some stuck to the side of the tank within adhered simulant deposited at some point during the transient mixing test. These tags can be correlated with the data shown in Figure 5.13 to determine when they were removed from the mixing process. The antenna range is ~8 in. deep and 8 in. wide. The grid pattern scanned provided some degree of overlap in measurement positions. This is shown by the multiple readings of certain tags. The large red numbers show the approximate location of the tag based on visual triangulation of the points shown.

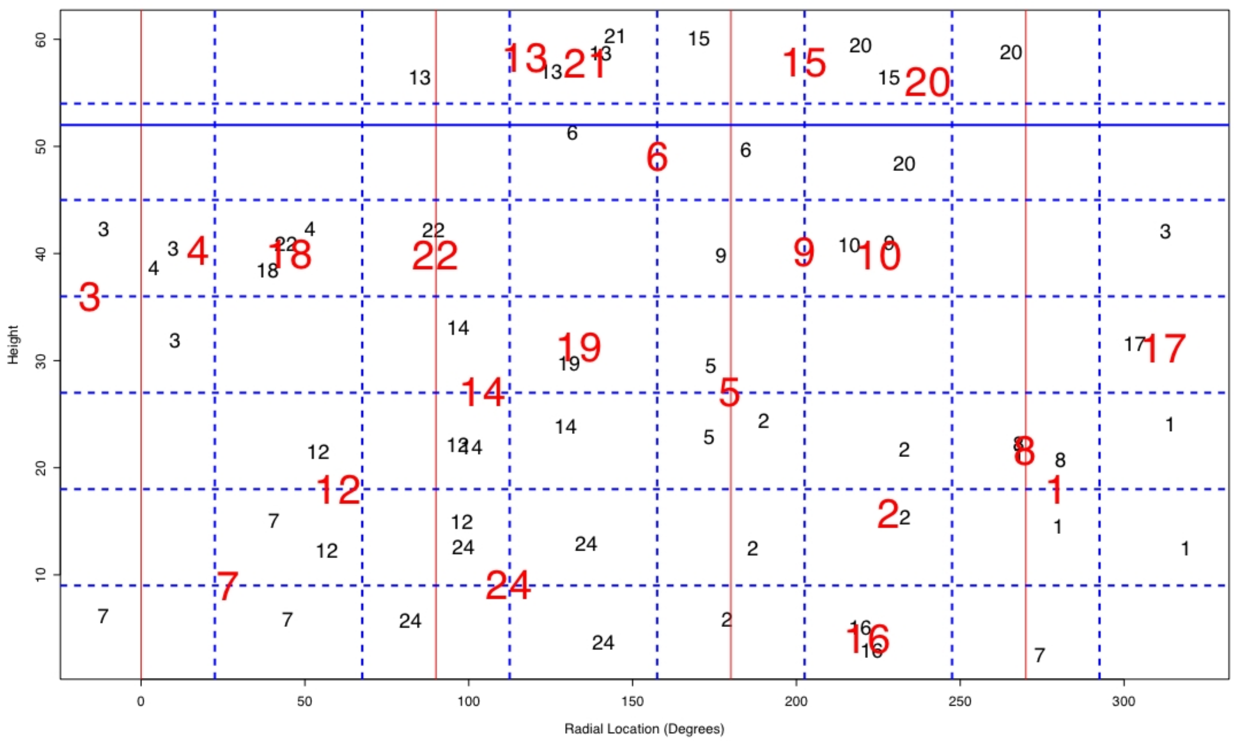


**Figure 5.14**. Tags Detected During Horizontal Scanning of the Static Mixture

#### 5.4.3.4 Vertical Characterization

Similar measurements were made during static condition vertical characterization. During these measurements, scans were made at 16 different locations around the tank. The additional eight locations are situated at 22.5-degree increments halfway vertically between the PJM tube and the gap. The histogram of the number of distinct tags observed at each vertical location is shown in Figure 5.15. These data were binned by location, as shown in Table 5.6.

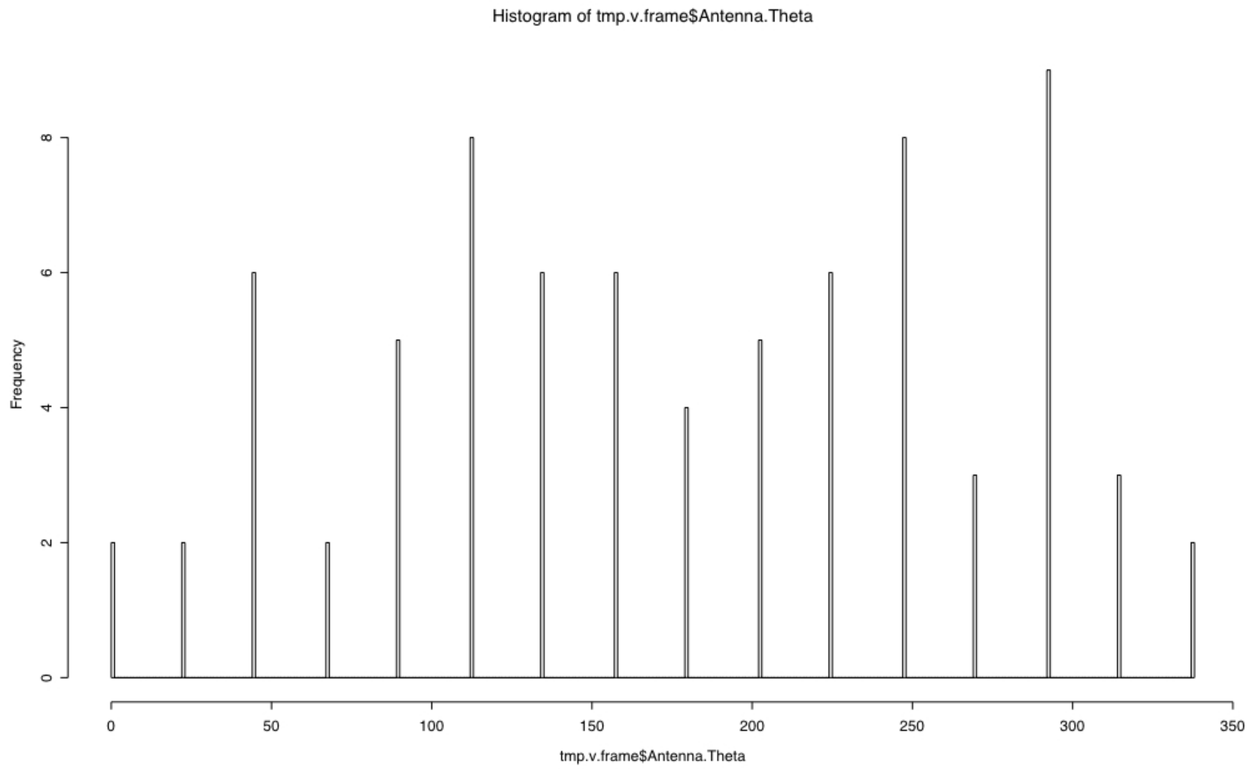


**Figure 5.15**. Unique Tags Detected During the Vertical Traverse

**Table 5.6.** Unique Tags Observed Based on Generic Location

| Location | Pulse Tube Gap | In Between | Space |
|---|---|---|---|
| Unique Tags | 8 | 26/2=13 | 12 |
| Angle | 0, 90, 180, 270 | 22.5, 67.5, 112.5, etc | 45, 135, 225, 315 |

At first observation, these data show that on average, 12 unique tags were observed in the spaces and 13 unique tags (26/2) in the "in-between" locations. Only eight unique tags were observed in the pulse tube gap. One possible explanation for this difference is that the width of the gap between the tube and the wall may limit the number of tags. Another explanation is that the antenna range is greater than the gap width, and the PJM wall inhibits comparison of equal volumes. This can be investigated further by evaluating the vertical traverses taken with the probe on edge. This orientation reduces the interrogation depth of the antenna. In addition to addressing the discrepancy shown above, these data can be used to determine which tags are located at a smaller radius (farther away from the antenna).

#### 5.4.3.5 Tag Identification Statistics

- 60 tags were seeded to the surface of the simulant in the UFP tank.
- 56 tags were eventually retrieved through normal pump-out of the simulant from the tank.

- 1628 hits were recorded during the transient test.
- 55 and 77 hits were recorded during the horizontal and vertical scanning, respectively.
- 57 unique tags were identified during the transient test, and horizontal and vertical scans.
- 51 unique tags were identified during the transient test.
- 26 unique tags (of approximately 43 expected) were identified during the vertical scans. The expected value is based on an estimate of the range of the antenna from the outside of the tank. The 43 count excludes the out of view volume in the central core of the tank.
- 22 unique tags were identified during the horizontal scans.
- 20 unique tags were identified in both the horizontal and vertical sets.
- 21 unique tags were identified in both the transient and vertical sets.
- 17 unique tags were identified in both the transient and horizontal sets.

The data from the horizontal scans were analyzed to determine if the spatial distribution of the 22 detected tags was homogeneous. The Pearson Chi-Squared statistic (Lindgren 1976, Section 9.1) was used after dividing the scanned volume up into different number of equi-volume cells and tabulating the number of tags in each. The small number of tags detected weakens our ability to assess homogeneity because the Pearson Chi-Squared statistic is most appropriate when expected cell counts (under the assumption of homogeneity) are at least 5, that is, when there are 4 cells. Unfortunately, the use of just 4 cells does not allow detection of any subtle non-homogeneous spatial patterns. Nonetheless, test statistics were computed using divisions of 4, 6, and 8 cells, with two arrangements of the latter, and shown in Table 5.7. No statistically significant results were found; that is, the assumption of homogeneity using the horizontal scan data could not be rejected. Visual examination of the spatial distribution suggests more tags are present in the center layer of the tank, but small number of tags does not allow for statistical confirmation of that observation.

**Table 5.7.** Chi-Squared Test Results

| Number of Cells | Test Statistic | Degrees of Freedom | Result |
|---|---|---|---|
| 8 | 3.45 | 7 | N.S. |
| 8 | 5.64 | 7 | N.S. |
| 6 | 0.91 | 5 | N.S. |
| 4 | 1.64 | 3 | N.S. |
| N.S. = Not statistically significant. | | | |

# 6.0 Conclusions

General observations:

- Asynchronous operations (between upper/lower or alternate PJMs) were generally not effective in improving the degree of mobilization. Synchronous operations tend to be more effective.
- Large nozzle diameters tend to be more effective than smaller ones. Total momentum, not just nozzle exit velocity is important to the degree of mobilization achieved.
- Ramsheads, or arrays of multiple nozzles pointing in directions other than straight down at the tank floor, can increase the effectiveness of mixing. Two-orifice, slightly upward pointing nozzle configurations for ramsheads were generally the most effective.
- Effectiveness of downward-pointing nozzles can be enhanced by aligning selected (and generally not all) discharge nozzles to impact the tank floor normally or at approximately 90 degrees to the local tank floor.
- Chandelier, or closely packed arrangements of PJMs, were generally not as effective at overall tank mobilization as were more distributed arrays of PJMs.

# 7.0 References

Battelle – Pacific Northwest Division. 2002. *River Protection Program – Waste Treatment Plant Technical Support Quality Assurance Project Plan.* RPP-WTP-QAPjP Rev. 1, Battelle – Pacific Northwest Division, Richland, WA.

Bechtel National, Inc. (BNI). 2003. *Test Specification: Development of Scaled Performance Data for PJM Mixers in the Ultrafiltration Feed and Lag Storage/Blend Tanks.* 24590-WTP-TSP-RT-03-008 Rev. 0, U.S. Department of Energy Office of River Protection, Richland, WA.

Bechtel National, Inc. (BNI). 2003. *Test Exception to Test Plan TP-RPP-WTP-296 Rev 0; title of work: "Revised UFP & LS Test Platforms Test Matrix to Facilitate WTP/DOE Decision on Alternative Mixing Trend."* 24590-WTP-TEF-RT-03-060, U.S. Department of Energy Office of River Protection, Richland, WA.

Bechtel National, Inc. (BNI). 2003 *Test Exception to Test Plan TP-RPP-WTP-296 Rev 0; title of work: "Revised Test Matrix and Direction to Reconfigure and Test in Final Down Selected 'Best' Mixing Configuration for Both UFP & LS Test Platforms."* 24590-WTP-TEF-RT-03-081, U.S. Department of Energy Office of River Protection, Richland, WA.

Bechtel National, Inc. (BNI). 2002. *Guidelines for Performing Chemical, Physical, and Rheological Properties Measurements*. 2450-WTP-GPG RTD-001 Rev. 0, Bechtel International Inc., Richland, WA.

Blomqvist S. June 1991. *Quantitative Sampling of Soft-Bottom Sediments - Problems and Solutions*. Marine Ecology-Progress Series, 72(3):295-304.

Lanesky DE, BW Logan, RG Brown, and AC Hine. 1979. A *new approach to portable vibracoring underwater and on land: Journal of Sedimentary Petrology*, v. 49, p. 654-657.

Lindgren BW. 1976. *Statistical Theory,* Third Edition. Macmillan, New York.

Morton RA and WA White. 1997. "Characteristics of and Corrections for Core Shortening in Unconsolidated Sediments." *Journal of Coastal Research* 13(3):761-769.

Poloski AP, PA Meyer, LK Jagoda, and PR Hrma. August 2004. *Non-Newtonian Slurry Simulant Development and Selection for Pulse Jet Mixer Testing.* PNWD-3495, Battelle – Pacific Northwest Division, Richland, WA.

# Appendix A

# Technical Basis for Scaled Testing of Waste Treatment Plant Mixing Vessels with Non-Newtonian Slurries

# Appendix A

# Technical Basis for Scaled Testing of Waste Treatment Plant Mixing Vessels with Non-Newtonian Slurries

## A.1 Introduction

Small-scale testing is a common approach used successfully in the many varied fields of applied fluid dynamics. The success of the approach depends greatly on the fact that system performance depends on certain nondimensional groupings of physical parameters. If these parameter groupings can be preserved at different geometric scales (i.e., large and small), the essential behavior of the system will be the same at both scales. This principle is referred to as *similarity* in the theory of fluid dynamics engineering. Limitations of scaled testing are attributed to the inability to match important nondimensional parameter groupings at both scales. In complex fluid dynamics problems, there can be many nondimensional parameter groups; however, often the essential behavior of the phenomenon is dominated by only a few key groups. In this situation small-scale testing can produce results that are very close to large-scale behavior.

This appendix presents the approach used to establish the scalability of the scaled prototypic mixing tests. Section A.2 gives a brief introduction to the basics of pulse jet mixer (PJM) operation. Section A.3 gives a summary of the important properties and parameters involved in PJM mixing of non-Newtonian materials. Section A.4 explains the geometric scaling approach and how velocities and time are scaled. Section A.5 discusses the important nondimensional parameters which, ideally, are to be preserved during scaled testing. Finally, Section A.6 summarizes the basis for scaled-testing.

## A.2 Principles of PJM Operation

A schematic of a typical PJM system in a vessel is shown in Figure A.1. The tank has diameter $D_T$, volume $V_T$, and an operating level $H$. There are $N$ PJMs in the tank, each with diameter $D_{PT}$ and volume $V_{PT}$. Each PJM has a conical nozzle with diameter $d_0$. For the baseline design, the total volume of the pulse tubes $N\,V_{PT}$ is approximately 10% the operating volume of the vessel.

There are three phases to the operation of the PJM. During the drive phase, the tube is pressurized and a volume of slurry is discharged. The level change in the tube during discharge is $\Delta L$. The corresponding increase in waste level is $\Delta H$ where

$$\Delta H = N\Delta L\left(\frac{D_{PT}^2}{D_T^2 - N D_{PT}^2}\right) \quad \text{(partially submerged PJMs)} \tag{A.1}$$

or

$$\Delta H = N\Delta L\frac{D_{PT}^2}{D_T^2} \quad \text{(fully submerged PJMs)} \tag{A.2}$$

Typical values of $\Delta H$ are about 10% of the operating level $H$. The average velocity $u_0$ discharged during the drive phase is given by

$$u_0 = \frac{D_{PT}^2}{d_0^2} \frac{\Delta L}{t_D} \tag{A.3}$$

where $t_D$ is the drive time.

The drive pressure, $p_D$, required to produce the discharge velocity is given by

$$p_D = p_e + \frac{C_L}{2} \rho u_0^2 \tag{A.4}$$

where $p_e$ is the pressure head at the exit of the nozzle, $C_L$ is the nozzle loss coefficient, and $\rho$ is the slurry density. The other two phases of PJM operation are the vent phase and suction phase.

Immediately after the drive phase, a vent is opened and excess pressure is allowed to vent to the atmosphere. During the suction phase, vacuum is applied to the pulse tube. The tube fills due to a combination of the applied vacuum and the difference in hydrostatic head between the waste level and the level in the tube. The vent time and suction time are given by $t_V$ and $t_S$, respectively. The total cycle time for PJM operation is given by

$$t_C = t_D + t_V + t_S \tag{A.5}$$

It is important to emphasize that the average drive velocity given by Eq. (A.3) is both spatially and temporally averaged. Spatially, the velocity will vary over the cross section of the nozzle. Temporally, the velocity varies due to inertial effects. When the drive phase is over, some fluid continues to discharge due to the inertia of the moving column of fluid. These inertial effects are dependent on the physical size of the system. The actual velocity varies somewhat over the operating cycle, as shown in Figure A.2.

For comparing PJM operation at different scales, various average velocities can be considered. One is the area-averaged velocity, given by

$$\bar{u}_{area} = \frac{1}{t_P - t_m} \int_{t_m}^{t_D} u \, dt \tag{A.6}$$

Another is the true average velocity given by

$$\bar{u}_{disch} = \frac{D_{PT}^2}{d_0^2} \frac{\Delta L_A}{t_{DA}} \tag{A.7}$$

where $\Delta L_A$ and $t_{DA}$ are the actual measured level change and drive times in the pulse tube. Generally, Eq. (A.6) will produce higher velocities than Eq. (A.7).

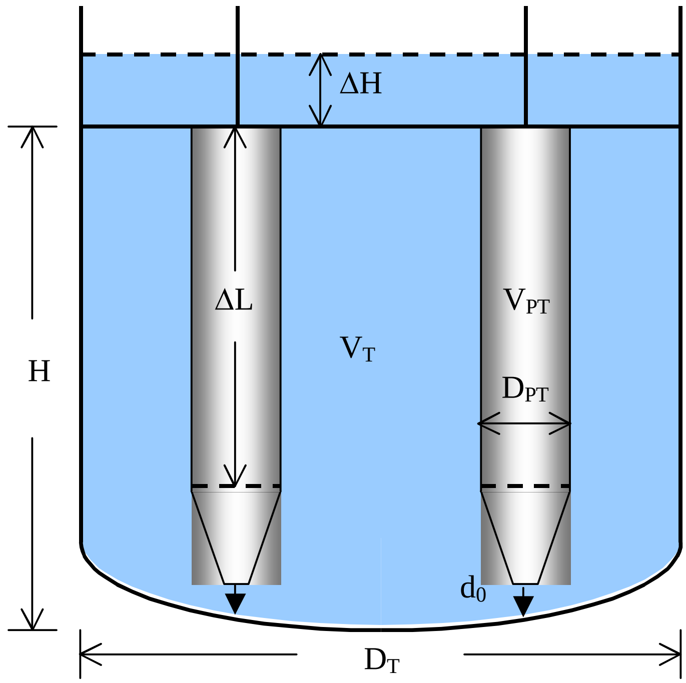


**Figure A.1**. Illustration of a Typical PJM System in a Waste Treatment Plant Vessel

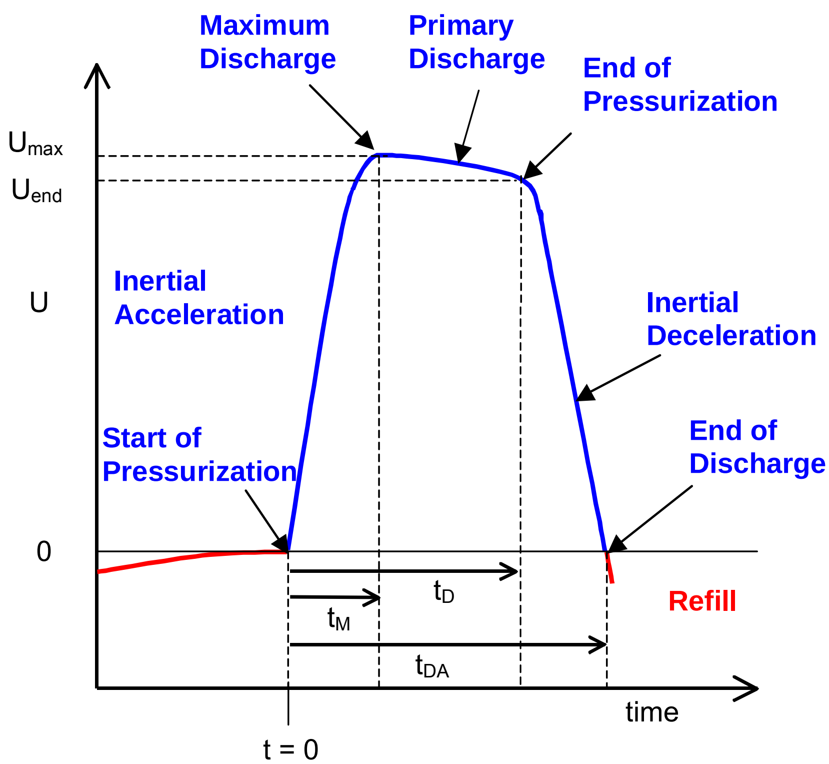


**Figure A.2**. Illustration of Temporal Variation of Velocity During PJM Operation

## A.3 Important Properties, Parameters, and Nondimensional Groups

The following is a list of pertinent waste properties and system parameters to be used in forming non-dimensional parameter groups:

- Waste properties
  - $\rho$ slurry density (kg/m$^3$) (assumes well-mixed slurry with no settling)
  - $\tau_s$ slurry shear strength (Pa)
  - $\tau_0$ laminar flow yield stress (Pa) (from Bingham plastic fit of waste rheogram)
  - $K$ laminar flow consistency (mPa-s) (assumed to be effective Newtonian viscosity ($\mu$) in turbulent region)
  - $t_{rel}$ slurry relaxation time (s) (characteristic response time of gelled slurry to an impulse)

- Physical parameters
  - $u_0$ nominal PJM jet velocity (m/s) (may be replaced with an averaged velocity)
  - $d_0$ PJM nozzle diameter (m)
  - $t_D$ PJM nominal drive time (s) (or actual drive time)
  - $t_c$ cycle time (s)
  - $H$ waste fill level (m)
  - $V$ vessel volume (m$^3$)
  - $V_{PT}$ pulse tube volume (m$^3$)
  - $p$ average hydrostatic pressure $\rho g H/2$ (Pa)
  - $Q_0$ PJM flow rate (per pulse) $(\pi/4)u_0 d_0^2$ (m$^3$/s)
  - $P_0$ PJM hydraulic power (per pulse) $(\pi/8)\rho u_0^3 d_0^2$ (W)

The relevant nondimensional parameter groups for the physical system are as follows:

Yield Reynolds number: $$\mathrm{Re}_\tau = \frac{\rho u_0^2}{\tau_s}$$

This is the ratio of dynamic stress to slurry strength, which directly affects size of the mixing cavern. It is considered a dominant nondimensional parameter.

Jet Reynolds number: $$\mathrm{Re}_0 = \frac{\rho u_0 d_0}{\mu}$$

This is the ratio of dynamic stress to viscous stress. It affects the degree of turbulence in the mixed region as well as weakly affecting stresses at the cavern and boundary layers. It is considered a secondary non-dimensional parameter.

Non-Newtonian stress ratio: $$N_\tau = \frac{\tau_s}{\tau_0}$$

This is the ratio of shear strength to Bingham yield stress. It may affect boundary layer structure and possibly the friction coefficient at the cavern boundary. The importance of this parameter is considered low.

Strouhal number: $$S_0 = \frac{t_D u_0}{d_0}$$

This is the ratio of pulse time to flow time scale. It affects the degree to which flow approaches steady jet behavior and is considered a primary nondimensional parameter. In the limit of steady jet flows, the Strouhal number become infinite, and the effects of pulsation are no longer present. For small Strouhal numbers, the mixing behavior will be highly dominated by pulsation effects.

Deborah number: $$D_0 = \frac{t_D}{T_s}$$

This is the ratio of pulse time to material response time. It affects how well non-steady flow at cavern mobilizes gelled slurry and is considered a secondary nondimensional parameter.

Pressure ratio: $$\frac{p_a}{\rho g H}$$

This is the ratio of ambient pressure to static head. It affects the scaling of gravity refill of a PJM but should not affect the discharge flow.

Densimetric Froude number: $$F_0 = \frac{\rho u_0^2}{\Delta\rho g H}$$

This is the ratio of the potential energy to kinetic energy of flow. It requires density stratification and affects the ability of a jet to transport material upward. The importance of this parameter is considered low due to minimal solids settling in the turbulent region.

## A.4 Geometric Scaling Approach

The non-Newtonian test program uses geometric scaling. We define the geometric scale factor s as

$$s = \frac{L_L}{L_S} \tag{A.8}$$

where $L_L$ is any characteristic linear dimension of the large-scale system (such as tank diameter, nozzle diameter, waste level, etc.). At small scale, every linear dimension, $L_S$, is reduced or *scaled* by $s$ (i.e., $d_{0_S} = d_{0_L}/s$, $D_{T_S} = D_{T_L}/s$, $H_S = H_L/s$). Hence the ideal small-scale test is an exact geometric miniature of the large system, with all areas scaled according to

$$A_s = \frac{1}{s^2} A_L \tag{A.9}$$

and all volumes scaled according to

$$V_s = \frac{1}{s^3} V_L \tag{A.10}$$

Typically in scaled fluid mixing tests, scale factors up to about 10 are considered acceptable; that is, much of the important physics can be captured at small scale. For the non-Newtonian test program, conservative scale factors in the range of 4 to 5 were selected due to the relatively new nature of the tests and the importance of the outcome.

When testing at small scale, one must determine how to scale velocity (i.e., PJM drive velocity $u_0$). One choice is to scale velocity by the scale factor. This is problematic, however, because it tends to reduce the Reynolds number by $1/s^2$ and introduce further difficulties with the scaling of time. A better choice is to keep jet velocity constant at both scales:

$$u_{0_S} = u_{0_L} \tag{A.11}$$

With geometric scaling and constant velocity scaling, nozzle flow rates per pulse scale according to

$$Q_{0_S} = Q_{0_L} / s^2 \tag{A.12}$$

Jet hydraulic power also scales similarly. However, power per unit volume scales according to

$$\left.\frac{P_0}{V}\right)_S = s \left.\frac{P_0}{V}\right)_L \tag{A.13}$$

For steady jet mixing, time does not come into play. However, PJM operation is a periodic process. Therefore, the scaling of time must be addressed.

If velocity is held constant and the geometry is scaled, then it follows that all imposed time scales must be reduced at small scale. Similarly, to keep the jet discharge velocity the same while scaling pulse volume geometrically, the pulse time will be reduced by the scale factor according to

$$t_{DS} = \frac{1}{s} t_{DL} \tag{A.14}$$

Hence the PJM drive time (as well as refill time and cycle time) are all reduced by $s$ at small scale.

## A.5 Scaling Nondimensional Parameters

In general, for a given non-Newtonian PJM mixing test, the nondimensional cavern position should depend on all of the nondimensional parameter groups:

$$\frac{H_C}{D_T} = f\left(Re_\tau, Re_0, N_\tau, S_0, D_0, F_0\right) \tag{A.15}$$

Similarly, nondimensional mixing time (time to steady cavern formation, time to break through, or time to full mobilization) should depend on the same parameters:

$$\frac{t_M}{t_D} = g\left(Re_\tau, Re_0, N_\tau, S_0, D_0, F_0\right) \tag{A.16}$$

The ideal small-scale test is one where the measured nondimensional cavern height and mixing time are the same as those at full scale. Hence, the extent to which the nondimensional parameters scale will determine the success of the small scale test approach. To this end, we consider how each of the non-dimensional parameters scale with the geometric scale factor $s$:

Yield Reynolds Number: $Re_{\tau_S} = Re_{\tau_L}$

The yield Reynolds number will be the same at both scales so long as the simulant used has the same shear strength $\tau_s$:

Jet Reynolds Number: $Re_{0_S} = \frac{1}{s} Re_{0_L}$

The Reynolds number at small scale is reduced by the geometric scale factor. This should introduce only minor differences in test results since the Reynolds numbers in both tests are quite large. Whether the reduction in Reynolds number produces conservative results (i.e., lower caverns) at small scale is not clear due to the competing effects of Reynolds number on jet structure and friction coefficients. The potential need for a minor Reynolds number correction to small-scale results should be evident from the scaling tests. If necessary, the Reynolds number can be matched at small scale by reducing the consistency or viscosity by the factor $1/s$.

Non-Newtonian stress ratio: $N_{\tau_S} = N_{\tau_L}$

The non-Newtonian stress ratio will be the same at both scales if the same simulant is used.

Strouhal number: $S_{0S} = S_{0L}$

The Strouhal number will be the same at both scales.

Deborah number: $D_{0S} = \frac{1}{s} D_{0L}$

The Deborah number will be smaller in the small-scale tests. If the Deborah number is large overall, the effect will be negligible. If the Deborah number is close to unity, then the small-scale results will be conservative.

Densimetric Froude number: $F_{0S} = sF_{0S}$

The densimetric Froude number will be larger at small scale. This would produce nonconservative results at small scale should the effect be important. So long as simulants with very slow particle settling are used, this effect should be negligible.

## A.6 Summary of Scaled Test Approach

The primary nondimensional parameters required for small-scale testing are the yield Reynolds number $Re_\tau$, and the Strouhal number $S_0$. If these are matched at large and small scale, then we expect, to first order, nondimensional cavern heights and mixing times to be the same:

$$\left.\frac{H_C}{D_T}\right)_S \approx \left.\frac{H_C}{D_T}\right)_L \tag{A.17}$$

and

$$\left.\frac{t_M}{t_D}\right)_S \approx \left.\frac{t_M}{t_D}\right)_L \tag{A.18}$$

Given that full-scale cavern heights are adequately predicted by reduced-scale testing, it follows that specification of PJM operation parameters sufficient to achieve complete mixing (no stagnant regions) at reduced scale will produce designs that also provide complete mixing at full-scale. Further, testing at reduced scale will provide a degree of conservatism so long as the consistency, k, of the simulant is the same as the full-scale bounding value. This is true since the jet Reynolds number will be smaller in the scaled-test than in the full-scale system:

$$Re_{0S} = \frac{1}{s} Re_{0L} \tag{A.19}$$

If adequate mixing is achieved in a reduced-scale test, then it can be expected that the degree of turbulence will be greater in the full-scale vessel due the associated effect of increased jet Reynolds number.

# Appendix B

# Test Exceptions

# Appendix B

# Test Exception

**24590-WTP-TEF-RT-03-060**

# R&T Test Exception Form



| | | |
|---|---|---|
| Test Exception Number: 24590-WTP-TEF-RT-03-060 | Title: | Test Exception to Test Plan TP-RPP-WTP-296 Rev 0; title of work: "Revised UFP & LS Test Platforms Test Matrix to Facilitate WTP/DOE ORP Decision on Alternative Mixing Trend" |

RPP-WTP Facility Name: Pretreatment / High-Level Waste Vitrification

Test Document Number(s) and Title(s): Test Plan TP-RPP-WTP-296 Rev 0; titled "Test Plan for Determination of Scaled Performance Data for Pulse Jet Mixers in Prototypic Ultrafiltration Feed Process (UFP) and HLW Lag Storage (LS) Vessels"

| | |
|---|---|
| Originator: Gary L. Smith | Originating Date: 09/24/03 |

Impacting Test Exception: ☐ Yes ☒ No (If No, approval by Cognizant R&T Manager Only)

If Impacting, Identify Impact:

| | | |
|---|---|---|
| Increase in scope, or significant change in cost or schedule | ☐ Yes | ☐ No |
| Decrease in Safety Margin or Increase in Environmental impact | ☐ Yes | ☐ No |
| Significant change in test parameters or sequence from the spec. or plan | ☐ Yes | ☐ No |
| Decrease in data quality | ☐ Yes | ☐ No |

**Required Approval Signatures**

| | Print/Type Name | Signature | Date |
|---|---|---|---|
| Cognizant R&T Functional Manager: | Steve Barnes | [signature] | 10/1/2003 |

**Other Required Approvals if Impacting**

| | Print/Type Name | Signature | Date |
|---|---|---|---|
| ☐ R&T Manager: | | | |
| ☐ QA: | | | |
| ☐ Design Engineering: | | | |
| ☐ ES&H: | | | |
| ☐ Other: | | | |
| ☐ Other: | | | |

**Description of Problem**: (Describe reason for change.)

The current Test Plan testing matrix, Table 6.1, needs to be reordered to garner enough test data to determine if an adequate design solution is possible to eventually provide design information on the operating parameters critical for the uniform movement (total mobilization) of the UFP and LS tank contents by mid October. This information will be used to facilitate a WTP/DOE ORP decision on whether or not an Alternative Mixing Trend is required.

# R&T Test Exception Form



| Test Exception Number: 24590-WTP-TEF-RT-03-060 | Title: | Test Exception to Test Plan TP-RPP-WTP-296 Rev 0; title of work: "Revised UFP & LS Test Platforms Test Matrix to Facilitate WTP/DOE ORP Decision on Alternative Mixing Trend" |
|---|---|---|

**Resolutions**:

Justification for change: Data is needed to help make an early decision by WTP/DOE ORP as to whether an Alternative Mixing test program needs to be initiated for the WTP non-Newtonian vessels.

Revised Test Matrix attached:

| Test Series | LS Prototypic Vessel | Test Series | UFP Prototypic Vessel |
|---|---|---|---|
| LS1 | Constant Drive Volume Test - Baseline PJM Configuration<br>Laponite - ≈ 70 Pa $\tau_{ss}$<br>• Nominal $d_0$<br>• Find $H_C$ @ 8 m/s<br>• Find $H_C$ @ 12 m/s<br>• Determine $U_{BT}$<br>• If break-thru, observe mixing<br>• Measure breakthrough* – evaluate mobilized diameter as a function of U<br>• Determine maximum U for test system | UFP1 | Constant Drive Volume Test - Baseline PJM Configuration<br>Laponite - ≈ 100 Pa $\tau_{ss}$<br>No Recirculation<br>• Nominal $d_0$<br>• Find $H_C$ @ 8 m/s<br>• Find $H_C$ @ 12 m/s<br>• Determine $U_{BT}$<br>• If break-thru, observe mixing<br>• Measure breakthrough* – evaluate mobilized diameter as a function of U<br>• Determine maximum U for test system |
| LS2 | Constant Drive Volume Test - Maximum Alternative PJM Configuration (see Figure 1.1)<br>Laponite - ≈ 70 Pa $\tau_{ss}$<br>• Nominal $d_0$<br>• Find $H_C$ @ 8 m/s<br>• Find $H_C$ @ 12 m/s<br>• Determine $U_{BT}$<br>• If break-thru, observe mixing<br>• Measure breakthrough* – evaluate mobilized diameter as a function of U | UFP2 | Constant Drive Volume Test - Baseline PJM Configuration<br>Laponite - ≈ 100 Pa $\tau_{ss}$<br>30 ft/s Recirculation<br>• Nominal $d_0$<br>• Find $H_C$ @ 8 m/s<br>• Find $H_C$ @ 12 m/s<br>• Determine $U_{BT}$<br>• If break-thru, observe mixing<br>• Measure breakthrough* – evaluate mobilized diameter as a function of U |

# R&T Test Exception Form



| | | |
|---|---|---|
| Test Exception Number: 24590-WTP-TEF-RT-03-060 | Title: | Test Exception to Test Plan TP-RPP-WTP-296 Rev 0; title of work: "Revised UFP & LS Test Platforms Test Matrix to Facilitate WTP/DOE ORP Decision on Alternative Mixing Trend" |

**Resolutions**:

| | | | |
|---|---|---|---|
| Evaluate LS mixing data using Laponite at ≈ 70 Pa $\tau_{ss}$; if complete mobilization of tank contents achieved do not continue. Use of particulate simulant in LS prototypic tank will be determined by WTP PJM Steering Committee. If complete mobilization of tank contents has not been achieved, continue to LS3. | | UFP3 | Constant Drive Volume Test - Maximum Alternative PJM Configuration (see Figure 1.2)<br>Laponite - ≈ 100 Pa $\tau_{ss}$<br>No Recirculation<br>• Nominal $d_0$<br>• Find $H_C$ @ 8 m/s<br>• Find $H_C$ @ 12 m/s<br>• Determine $U_{BT}$<br>• If break-thru, observe mixing<br>• Measure breakthrough* – evaluate mobilized diameter as a function of U |
| LS3 | Constant Drive Volume Test - Maximum Alternative PJM Configuration (see Figure 1.1)<br>Laponite - ≈ 30 Pa $\tau_{ss}$<br>• Nominal $d_0$<br>• Find $H_C$ @ 8 m/s<br>• Find $H_C$ @ 12 m/s<br>• Determine $U_{BT}$<br>• If break-thru, observe mixing<br>Measure breakthrough* – evaluate mobilized diameter as a function of U | UFP4 | Constant Drive Volume Test - Maximum Alternative PJM Configuration (see Figure 1.2)<br>Laponite - ≈ 70 Pa $\tau_{ss}$<br>No Recirculation<br>• Nominal $d_0$<br>• Find $H_C$ @ 8 m/s<br>• Find $H_C$ @ 12 m/s<br>• Determine $U_{BT}$<br>• If break-thru, observe mixing<br>Measure breakthrough* – evaluate mobilized diameter as a function of U |
| LS4 | Constant Drive Volume Test - Baseline PJM Configuration<br>Laponite - ≈ 30 Pa $\tau_{ss}$<br>• Nominal $d_0$<br>• Find $H_C$ @ 8 m/s<br>• Find $H_C$ @ 12 m/s<br>• Determine $U_{BT}$<br>• If break-thru, observe mixing<br>• Measure breakthrough* – evaluate mobilized diameter as a function of U | UFP5 | Constant Drive Volume Test - Maximum Alternative PJM Configuration (see Figure 1.2)<br>Laponite - ≈ 70 Pa $\tau_{ss}$<br>30 ft/s Recirculation<br>• Nominal $d_0$<br>• Find $H_C$ @ 8 m/s<br>• Find $H_C$ @ 12 m/s<br>• Determine $U_{BT}$<br>• If break-thru, observe mixing<br>Measure breakthrough* – evaluate mobilized diameter as a function of U |
| LS5 | TBD | UFP6 | Constant Drive Volume Test - Baseline PJM Configuration<br>Laponite - ≈ 70 Pa $\tau_{ss}$<br>No Recirculation<br>• Nominal $d_0$ |

# R&T Test Exception Form



| Test Exception Number: 24590-WTP-TEF-RT-03-060 | Title: | Test Exception to Test Plan TP-RPP-WTP-296 Rev 0; title of work: "Revised UFP & LS Test Platforms Test Matrix to Facilitate WTP/DOE ORP Decision on Alternative Mixing Trend" |
|---|---|---|

**Resolutions**:

| | | | |
|---|---|---|---|
| | | | • Find $H_C$ @ 8 m/s<br>• Find $H_C$ @ 12 m/s<br>• Determine $U_{BT}$<br>• If break-thru, observe mixing<br>• Measure breakthrough* – evaluate mobilized diameter as a function of U |
| | | UFP7 | Constant Drive Volume Test - Baseline PJM Configuration<br>Laponite - ≈ 70 Pa $\tau_{ss}$<br>30 ft/s Recirculation<br>• Nominal $d_0$<br>• Find $H_C$ @ 8 m/s<br>• Find $H_C$ @ 12 m/s<br>• Determine $U_{BT}$<br>• If break-thru, observe mixing<br>• Measure breakthrough* – evaluate mobilized diameter as a function of U |
| | | Evaluate UFP mixing data using Laponite at ≈ 100 and 70 Pa $\tau_{ss}$; if complete mobilization of tank contents achieved to not continue. Use of particulate simulant in UFP prototypic tank will be determined by WTP PJM Steering Committee. If complete mobilization of tank contents has not been achieved continue to UFP8. | |
| | | UFP8 | Constant Drive Volume Test - Maximum Alternative PJM Configuration (see Figure 1.2)<br>Laponite - ≈ 30 Pa $\tau_{ss}$<br>No Recirculation<br>• Nominal $d_0$<br>• Find $H_C$ @ 8 m/s<br>• Find $H_C$ @ 12 m/s<br>• Determine $U_{BT}$<br>• If break-thru, observe mixing<br>Measure breakthrough* – evaluate mobilized diameter as a function of U |

# R&T Test Exception Form



| Test Exception Number: 24590-WTP-TEF-RT-03-060 | Title: | Test Exception to Test Plan TP-RPP-WTP-296 Rev 0; title of work: "Revised UFP & LS Test Platforms Test Matrix to Facilitate WTP/DOE ORP Decision on Alternative Mixing Trend" |
|---|---|---|

**Resolutions**:

| | | | |
|---|---|---|---|
| | | UFP9 | Constant Drive Volume Test - Maximum Alternative PJM Configuration (see Figure 1.2)<br>Laponite - ≈ 30 Pa $\tau_{ss}$<br>30 ft/s Recirculation<br>• Nominal $d_0$<br>• Find $H_C$ @ 8 m/s<br>• Find $H_C$ @ 12 m/s<br>• Determine $U_{BT}$<br>• If break-thru, observe mixing<br>Measure breakthrough* – evaluate mobilized diameter as a function of U |
| | | UFP10 | Constant Drive Volume Test - Baseline PJM Configuration (see Figure 1.2)<br>Laponite - ≈ 30 Pa $\tau_{ss}$<br>No Recirculation<br>• Nominal $d_0$<br>• Find $H_C$ @ 8 m/s<br>• Find $H_C$ @ 12 m/s<br>• Determine $U_{BT}$<br>• If break-thru, observe mixing<br>Measure breakthrough* – evaluate mobilized diameter as a function of U |
| | | UFP11 | TBD |

* Breakthrough is noted when the mobilized simulant fraction reaches the surface of the stagnant region of the simulant. Observation and notes will be documented on the size of the opening, as a function of time through which the mobilized simulant reaches the surface will be noted along with the effects on the stagnant region.

Retest or Inspection Required: ☐ Yes ☒ No

**Reference Additional Documents:**

1.

2.

3.

# Test Exception

## 24590-WTP-TEF-RT-03-081

# R&T Test Exception Form

GLS 11/26/03



| | | |
|---|---|---|
| Test Exception Number: 24590-WTP-TEF-RT-03-081 | Title: | Test Exception to Test Plan TP-RPP-WTP-296 Rev 0; title of work: "Revised Test Matrix and Direction to Reconfigure and Test in Final Down Selected 'Best' Mixing Configuration for both UFP & LS Test Platfors" |

RPP-WTP Facility Name: Pretreatment / High-Level Waste Vitrification

Test Document Number(s) and Title(s): Test Plan TP-RPP-WTP-296 Rev 0; titled "Test Plan for Determination of Scaled Performance Data for Pulse Jet Mixers in Prototypic Ultrafiltration Feed Process (UFP) and HLW Lag Storage (LS) Vessels"

Originator: Gary L. Smith | Originating Date: 11/26/03

Impacting Test Exception: ☒ Yes ☐ No (If No, approval by Cognizant R&T Manager Only)

If Impacting, Identify Impact:

| | | |
|---|---|---|
| Increase in scope, or significant change in cost or schedule | ☒ Yes | ☐ No |
| Decrease in Safety Margin or Increase in Environmental impact | ☐ Yes | ☒ No |
| Significant change in test parameters or sequence from the spec. or plan | ☐ Yes | ☒ No |
| Decrease in data quality | ☐ Yes | ☒ No |

**Required Approval Signatures**

| | Print/Type Name | Signature | Date |
|---|---|---|---|
| Cognizant R&T Functional Manager: | Steve Barnes | [signature] | 11/24/2003 |

**Other Required Approvals if Impacting**

| | Print/Type Name | Signature | Date |
|---|---|---|---|
| ☒ R&T Manager: | Walt Tamosaitis | [signature] | 11/26/03 |
| ☐ QA: | | | |
| ☐ Design Engineering: | | | |
| ☐ ES&H: | | | |
| ☐ Other: | | | |
| ☐ Other: | | | |

**Description of Problem**: (Describe reason for change.)

The testing matrix within Test Plan TP-RPP-WTP-296 Rev 0; titled "Test Plan for Determination of Scaled Performance Data for Pulse Jet Mixers in Prototypic Ultrafiltration Feed Process (UFP) and HLW Lag Storage (LS) Vessels" has led to a final 'best design' configuration was chosen for both the UFP and LS Prototypic Test Platforms on which to finish testing to demonstrate mixing using a particulate simulant that has rheologcial properties deemed to be closer to actual waste.

# R&T Test Exception Form



| Test Exception Number: 24590-WTP-TEF-RT-03-081 | Title: | Test Exception to Test Plan TP-RPP-WTP-296 Rev 0; title of work: "Revised Test Matrix and Direction to Reconfigure and Test in Final Down Selected 'Best' Mixing Configuration for both UFP & LS Test Platfors" |
|---|---|---|

**Resolutions:**

Justification for change: Test data is needed to demonstrate adequate mixing in the UFP & LS prototypic test configurations deemed to be the best mixing design for the WTP non-Newtonian vessels using a particulate clay simulant which more closely matches actual waste rheological properties.

UFP and LS Prototypic Test Configuration:

See attached drawings and figures.

Simulant:

Simulant will be a kaoline:bentonite clay mixture with rheological properties approximating a Bingham Plastic with a Yield Stress of 30 Pa and Consistency of 30 cP.

Nozzle Velocity:

Testing will begin at 8 m/s and progress to 12 m/s gathering mixing data, etc. as the nozzle velocity is increased. If turbulent, Type 4, mixing is not observed at or below 12 m/s then the nozzle velocity is to be increased until Type 4 mixing is observed and data collected at the appropriate velocity.

Cycle Time Information:

UFP Prototypic Vessel: Actual Drive Time (sec.) = 2.5; Total Cycle Time (sec.) = 20

LS Prototypic Vessel: Actual Drive Time (sec.) = 3.2; Total Cycle Time (sec.) = 25

Measurement Methods:

1. Colorimetric dye method for determining mixing volume and uniformity
2. Radio Frequency (RF) tags to help determine mixing volume and uniformity
3. Polycarbonate beads to help determine mixing volume and uniformity; may be for indication only depending on testing results.

Retest or Inspection Required: ☐ Yes ☒ No

**Reference Additional Documents:**

1.

2.

3.

4/8

# UFP *ALL IN*

Dimensions in Inches, Full scale shown in ()

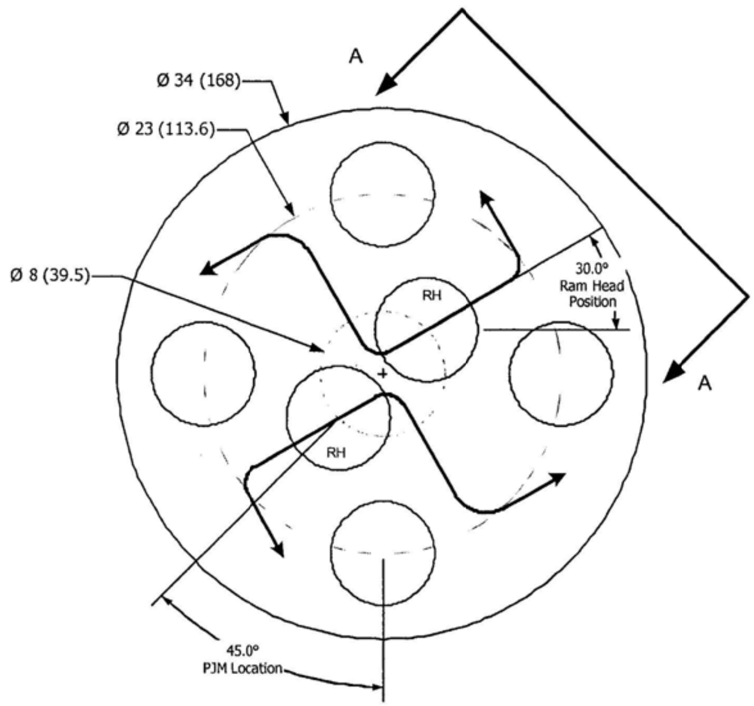


Outer PJMs
- 6" standard Pipe
- 1.214" ID
- 2" off bottom
- Downward

Ram's Head PJMs
- 6" standard Pipe
- 0.824" ID
- Same Height as last 6x3 test
- Nozzle end angles up 30 deg

PAGE 3 of 13

# 5/8

## UFP *ALL IN*

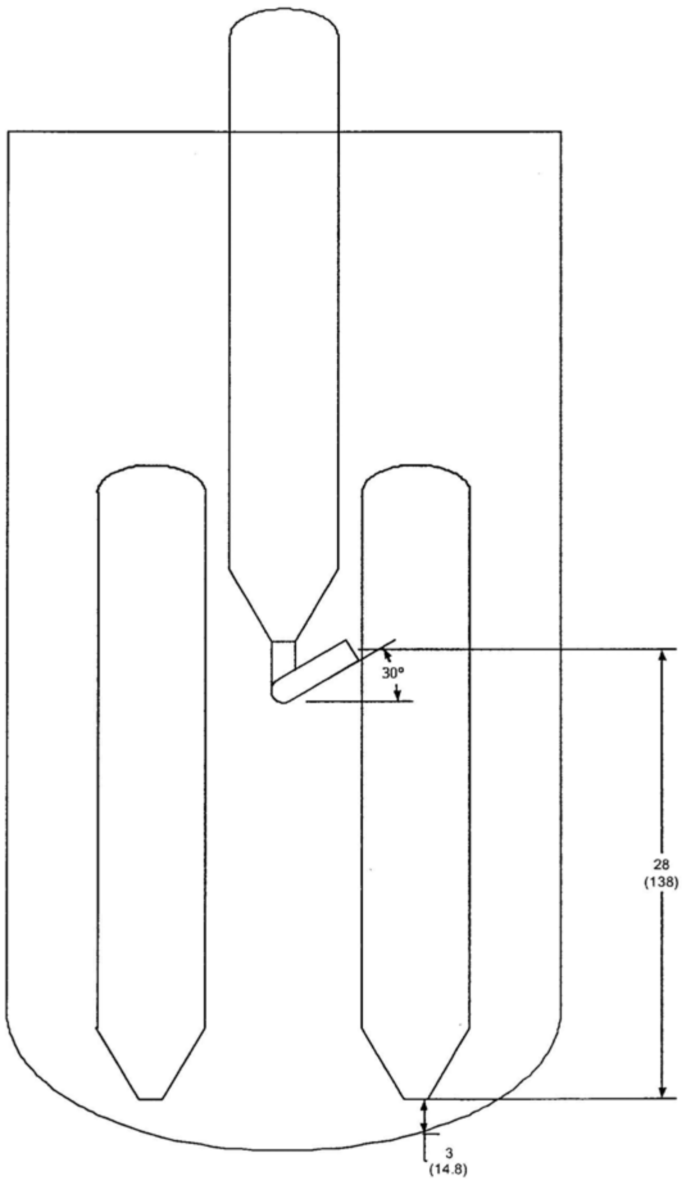


A-A

6/8

# UFP *ALL IN*

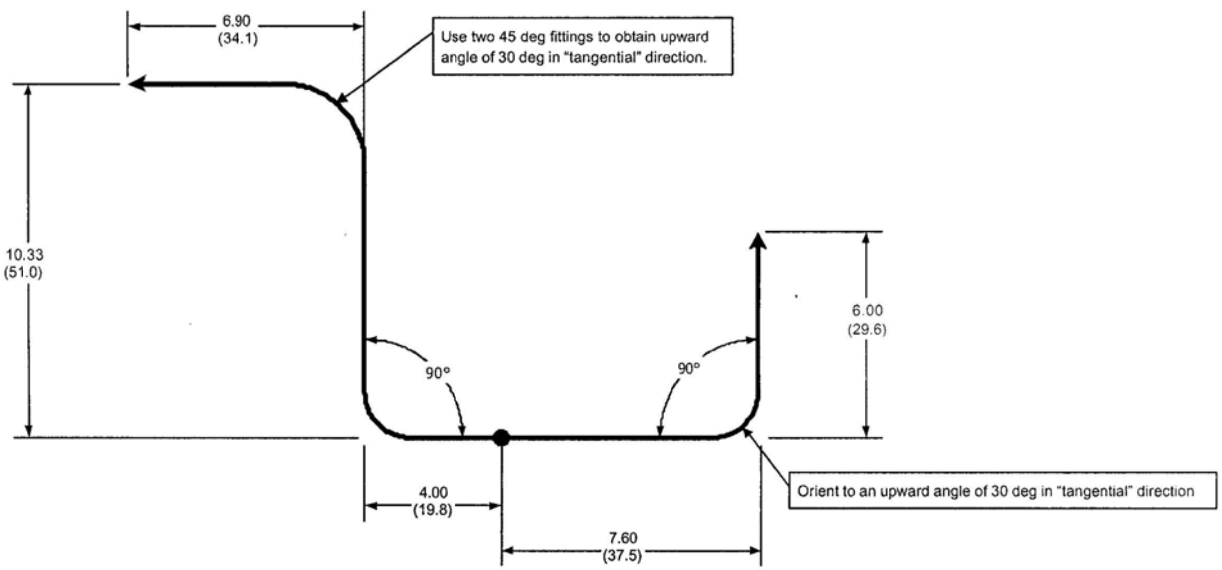


**Looking down on Ram's Head with all pipe in same plane**

# 1/8

## Lag Storage ***ALL IN***

Dimensions in Inches, Full scale shown in ()

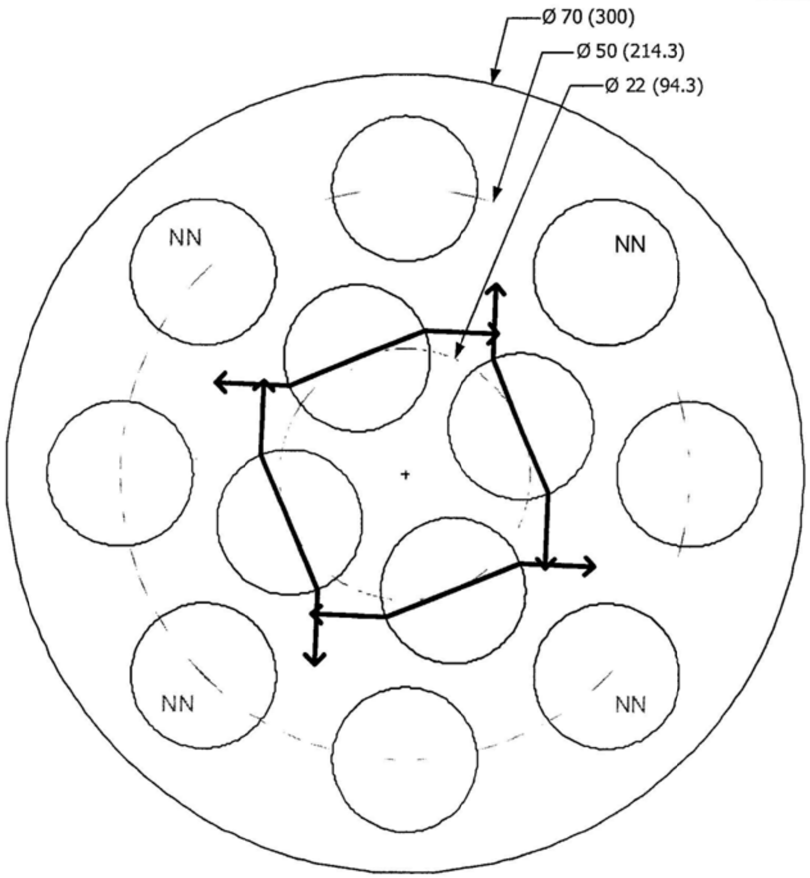


Outer PJMs
- 12" standard Pipe
- 2.067" Pipe Nozzles
    - 3 normal to tank bottom
    - 3 straight down
    - 3" off bottom

Ram's Head PJMs
- 12" standard Pipe
- 1.38" Nozzles, 30 deg up
- elevated such that jet impacts ~half way up

**2/8**

# Lag Storage ***ALL IN***

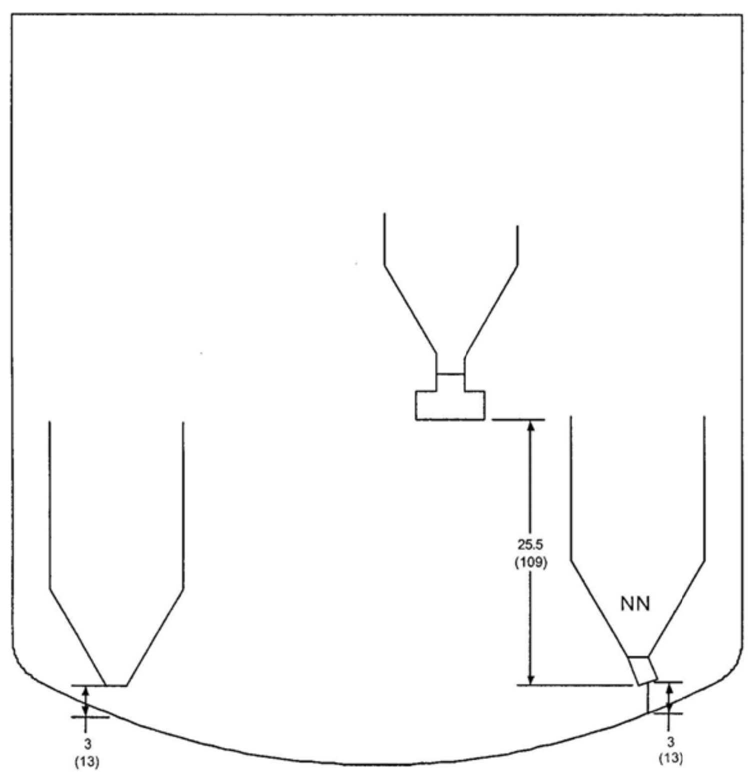


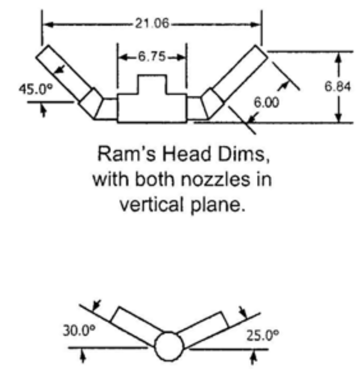


Ram's Head Dims, with both nozzles in vertical plane.

Side View after orientation of nozzles

# 3/8

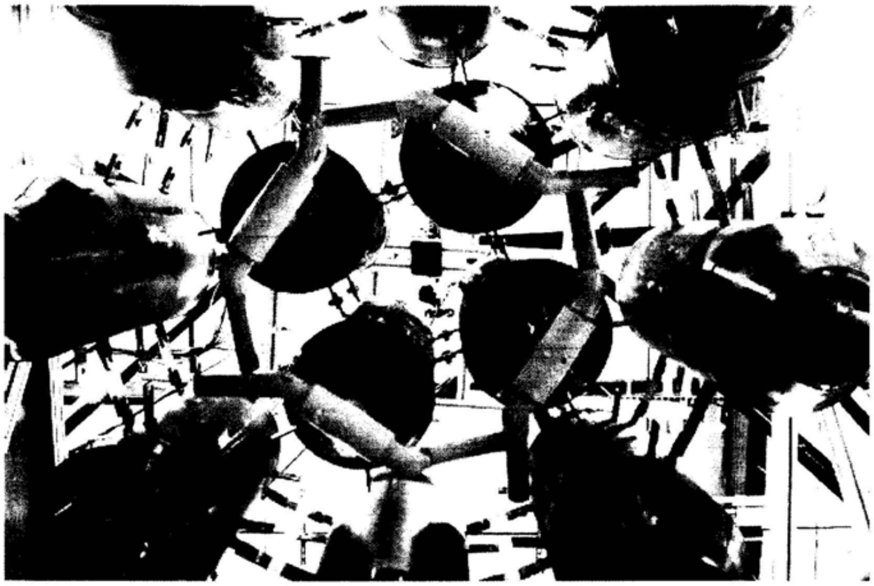

*Lag Storage Assembly - ALL IN*

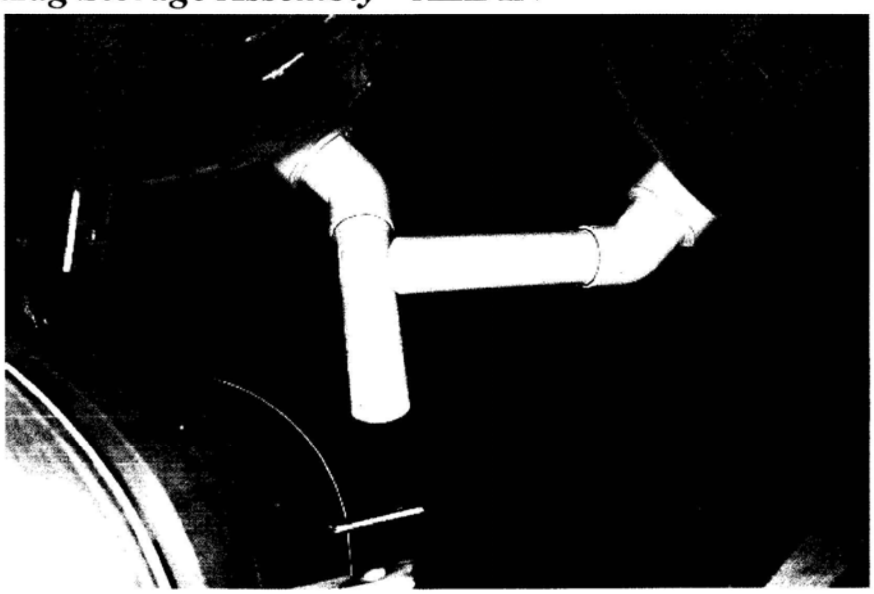

| | | ALL IN | | |
|---|---|---|---|---|
| | | UFP | LS | CRV |
| Full Scale | Vessel ID | 168 | 300 | 162 |
| | PJM PCD (in) | 113.6 | 214.3 | 72.0 |
| | PJM ID (in) | 32 | 52 | 32 |
| | PJM OD (in) | 32.75 | 52.75 | 32.75 |
| | PJM Vol (gal) | 610 | 1451 | 448 |
| | RH PJM PCD (in) | 39.5 | 94.3 | 69.6 |
| | RH PJM ID (in) | 32 | 48 | 32 |
| | RH PJM OD (in) | 32.75 | 48.75 | 32.75 |
| | RH PJM Vol (gal) | 610 | 1451 | 448 |
| | Nozzle ID (in) | 6.00 | 8.86 | 6.00 |
| | RH Nozzle ID (in) | 4.07 | 5.91 | 6.00 |
| | Operating Level (in) | 306 | 329 | 144 |
| | H/D (operating) | 1.82 | 1.10 | 0.89 |
| Small Scale | Vessel ID (in) | 34 | 70 | 40.5 |
| | Scale Factor | 4.94 | 4.29 | 4.00 |
| | PJM PCD (in) | 23 | 50 | 18 |
| | PJM Pipe Size | 6" S40 | 12" S40 | 8" S5 |
| | PJM ID (in) | 6.065 | 11.94 | 8.407 |
| | PJM OD (in) | 6.625 | 12.75 | 8.625 |
| | PJM Length (in) | 43.39 | 43.6 | 39.3 |
| | PJM Vol (gal) | 5.055 | 18.43 | 7 |
| | RH PCD (in) | 8 | 22 | 17.4 |
| | RH Pipe Size | 6" S40 | 12" S40 | 8" S10 |
| | RH PJM ID (in) | 6.065 | 11.94 | 8.329 |
| | RH PJM OD (in) | 6.625 | 12.75 | 8.625 |
| | RH PJM Vol (gal) | 5.055 | 18.43 | 7 |
| | Nozzle ID (in) | 1.214 | 2.067 | 1.500 |
| | RH Nozzle ID (in) | 0.824 | 1.38 | 1.500 |
| | Operating Level (in) | 61.9 | 76.8 | 36.0 |
| | H/D (operating) | 1.82 | 1.10 | 0.89 |

# Scaled UFP

**Title: Pulse Jet Mixer Sizing**

| Inputs | | |
|---|---|---|
| Inside Diameter= | 6.065 | in |
| Total Volume= | 5.055 | gal |
| NozzleDia= | 1.214 | in |

| | | |
|---|---|---|
| Head Volume= | 29.20 | $in^3$ |
| | 0.13 | gal |
| Head Height= | 1.52 | in |
| $h+h_b$= | 5.25 | in |
| h= | 4.20 | in |
| Volume of frustum= | 50.18 | $in^3$ |
| | 0.22 | gal |
| Cylindrical Volume= | 1,088.33 | $in^3$ |
| | 4.71 | gal |
| Cross. Area= | 28.89 | $in^2$ |
| Cylindrical Height= | 37.67 | in |
| Total Height = | 43.39 | in |

**Notes:**
Head is 2:1 SE
Angle of the cone is 60 deg

Height to Tan Line= 41.87 in

Overall Height= 43.39 in

Height of Cone= 4.20 in

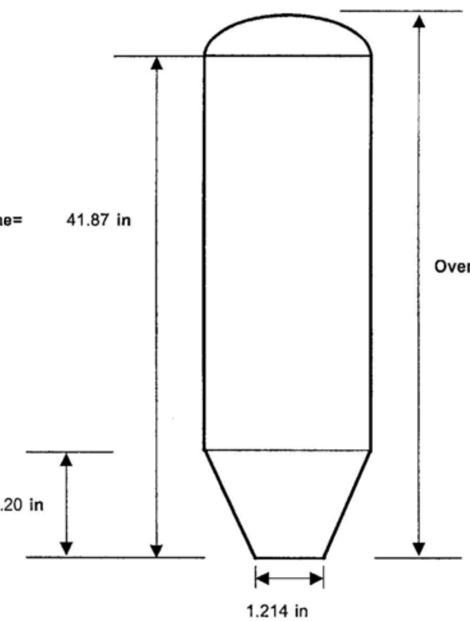

# UFP

**Title: Pulse Jet Mixer Sizing**

| Inputs | | |
|---|---|---|
| Inside Diameter= | 32.000 | in |
| Total Volume= | 610 | gal |
| NozzleDia= | 6.000 | in |

| | | |
|---|---|---|
| **Head Volume=** | 4,289.32 | $in^3$ |
| | 18.57 | gal |
| **Head Height=** | 8.00 | in |
| **$h+h_b$=** | 27.71 | in |
| **h=** | 22.52 | in |
| **Volume of frustum=** | 7,380.35 | $in^3$ |
| | 31.95 | gal |
| Cylindrical Volume= | 129,240.33 | $in^3$ |
| | 559.48 | gal |
| **Cross. Area=** | 804.25 | $in^2$ |
| **Cylindrical Height=** | 160.70 | in |
| **Total Height =** | 191.21 | in |

**Notes:**
Head is 2:1 SE
Angle of the cone is 60 deg

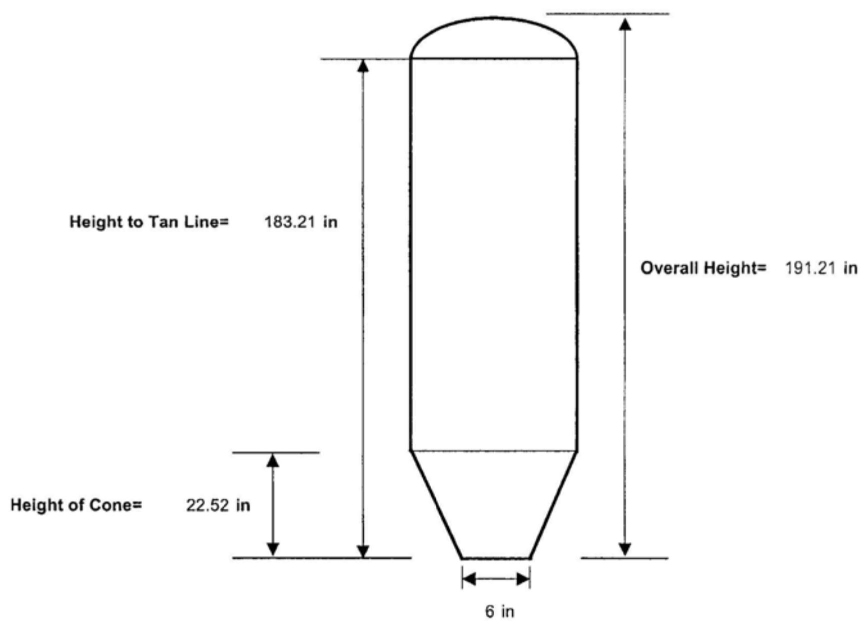

# Scaled HLP (LS)

**Title: Pulse Jet Mixer Sizing**

| Inputs | | |
|---|---|---|
| Inside Diameter= | 11.940 | in |
| Total Volume= | 18.430 | gal |
| NozzleDia= | 2.065 | in |

| | | |
|---|---|---|
| **Head Volume=** | 222.82 | $in^3$ |
| | 0.96 | gal |
| **Head Height=** | 2.99 | in |
| **$h+h_b$=** | 10.34 | in |
| **h=** | 8.55 | in |
| **Volume of frustum=** | 383.94 | $in^3$ |
| | 1.66 | gal |
| **Cylindrical Volume=** | 3,650.57 | $in^3$ |
| | 15.80 | gal |
| **Cross. Area=** | 111.97 | $in^2$ |
| **Cylindrical Height=** | 32.60 | in |
| **Total Height =** | 44.14 | in |

**Notes:**
Head is 2:1 SE
Angle of the cone is 60 deg

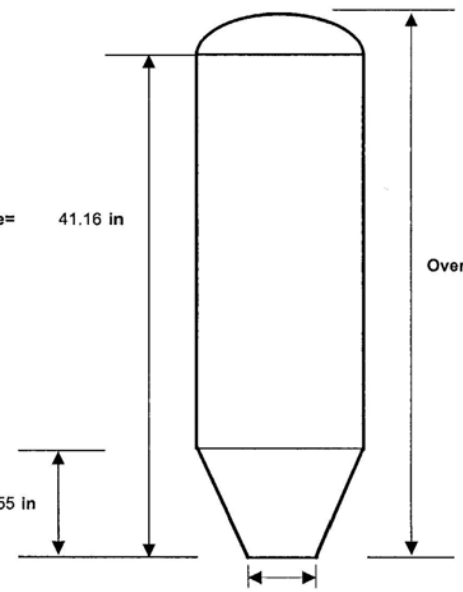

# HLP (LS)

**Title: Pulse Jet Mixer Sizing**

| Inputs | | |
|---|---|---|
| Inside Diameter= | 52 | in |
| Total Volume= | 1451 | gal |
| NozzleDia= | 8.860 | in |

| | | |
|---|---|---|
| **Head Volume=** | 18,405.54 | $in^3$ |
| | 79.68 | gal |
| **Head Height=** | 13.00 | in |
| **$h+h_b$=** | 45.03 | in |
| **h=** | 37.36 | in |
| **Volume of frustum=** | 31,721.65 | $in^3$ |
| | 137.32 | gal |
| **Cylindrical Volume=** | 285,053.81 | $in^3$ |
| | 1,234.00 | gal |
| **Cross. Area=** | 2,123.72 | $in^2$ |
| **Cylindrical Height=** | 134.22 | in |
| **Total Height =** | 184.58 | in |

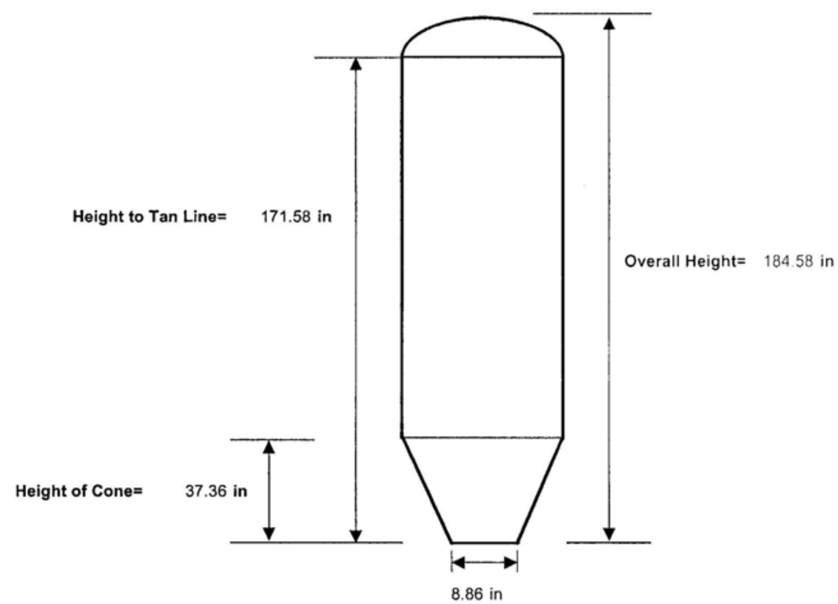


**Notes:**
Head is 2:1 SE
Angle of the cone is 60 deg

# Appendix C

# Vendor Specifications of Instruments Used

# Appendix C

# Vendor Specifications of Instruments Used

Pulse Jet Mixer liquid level probes:

Drexelbrook Model 508-45, with 408-82 electronics

Pressure transducers:

Cerabar T PMP 135, 150 psia range, +0.5% of full-scale accuracy

Thermocouples:

Type K thermocouples, stainless steel sheath, standard ASTM limits of error, ±2.2 C or ±0.75% whichever is larger

# Appendix D

# Nomenclature Used to Describe Data

# in Tables 4.2 and 4.4

# Appendix D

# Nomenclature Used to Describe Data in Tables 4.2 and 4.4

Information in Table 4.1 includes:

Column 1 – Test date = date testing was conducted

Column 2 – Test type = vessel under test (UFP or LS)

Column 3 – PJM config = brief description of PJM geometry and sequencing

Column 4 – Nozzle diameter (in.) = inside diameter of discharge nozzle of PJMs installed for testing

Column 5 – Nozzle vel (m/s) = target PJM nozzle discharge velocity in m/s

Column 6 – PJM $\Delta$H (cm) = fluid level change inside any single PJM during a discharge cycle in cm

Column 7 – Nom. drive time, sec = calculated drive time to achieve target nozzle velocity given nozzle diameter, PJM ID, and PJM $\Delta$H.

Column 8 – Actual drive time, sec = drive time set on DACS to achieve target velocity. Different from nominal due to system pressure drop, inertial effects, drive pressure variations, etc.

Column 9 – Cycle time, sec = cumulative duration of PJM drive, vent, and refill times; in effect, the time between consecutive start of PJM pressurization events.

Column 10 – DACS files = names of files where test data captured by DACS system are stored

Column 11 – Mixing pattern observed – observed mobilization state, as defined in Figure S.1.

Column 12 – Cavern height if appropriate (in.) = where a mixing cavern can be discerned (see Type 1 mobilization state in Figure S.1), the maximum height above the tank bottom where mobilization (defined as at least intermittent turbulent flow) was observed.

Column 13– Simulant – the type of simulant used for the designated test. Two simulants were used during Phase 1 prototype testing: 1) Laponite, an optically transparent mixture of water and hydrated synthetic particulate of 25-nm average particle size exhibiting non-Newtonian fluid properties including yield strength and 2) kaolin-Bentonite slurry, a mixture of water and two natural clay materials, optically opaque and possessing both yield strength and consistency index approximating actual Hanford waste properties.

Column 14 – Yield, nominal – target shear strength of the simulant used for the current test in Pascals.

Column 15 – Yield, actual – measured shear strength of the simulant used in the current test in Pascals (note: where both shear strength and a consistency index are important [kaolin-bentonite slurry simulants], both quantities are shown as y/k, where y = shear strength in Pascals and k = consistency index in centipoise)

Column 16 – Target H/D – tank fill height to inside diameter ratio selected as test condition for the current test.

Column 17 – Actual H/D – measured tank fill divided by the test tank inside diameter (inside diameter for the LS is 70 inches, for the UFP 34 inches).

Column 18 – Recirc, Y/N – indicates within pump induced recirculation was used to enhance mixing during the test.

Column 19 – Recirc flow, gpm – if recirculation was used during the test, flow rate measured in gallons per minute (note: also includes notations related to synchronous or asynchronous operations of arrays of PJMs).

Column 20 – Scoping (S) or Final (F) – designation as to whether the test was classed as a scoping test or final test, implying differences in QA requirements.

The data files containing the DACS collected test data are included in Column 10 of Table 4.1. The data file nomenclature is as follows:

xxmmddyyns.ASC where:

| | | |
|---|---|---|
| xx | = | P for prototype UFP data files |
| | = | LS for prototype Lag Storage data files |
| mm | = | month |
| dd | = | day of month |
| yy | = | year |
| n | = | sequential test number for the particular day of testing (e.g., 2 = second test of given day) |
| s | = | section number of data files. Data files stored in separate sections due to nature of DACS software. Typically a, b, and c sections for prototype test data files. |

# Distribution

**No. of Copies**

**OFFSITE**

1 Savannah River National Laboratory
Richard Edwards
Westinghouse SA
Aiken, South Carolina 29808-0001

**No. of Copies**

**ONSITE**

15 Battelle – Pacific Northwest Division

| | |
|---|---|
| J. M. Alzheimer | K7-15 |
| J. M. Bates (2) | K7-15 |
| J. R. Bontha | K6-24 |
| P. A. Meyer | K7-15 |
| J. W. Brothers | K7-15 |
| C. W. Enderlin | K7-15 |
| M. D. Johnson | K6-96 |
| D. E. Kurath | P7-28 |
| T. E. Michener | K7-15 |
| D. E. Wallace | P7-27 |
| Project File (2) | P7-28 |
| Information Release (2) | K1-06 |

5 Bechtel National, Inc.

| | |
|---|---|
| H. A. Abodishish | H4-02 |
| S. M. Barnes | H4-02 |
| D. E. Larson | H4-02 |
| J. F. Doyle (2) | H4-02 |